CAPITAL UNIVERSITY OF SCIENCE AND TECHNOLOGY, ISLAMABAD


# Numerical Analysis of MHD Heat Transfer and Nanofluid Flow over a Porous Plate with Radiation and Joule Heating Effects

by

Nimra Shanakhat

A thesis submitted in partial fulfillment for the degree of Master of Philosophy

in the

Faculty of Computing
Department of Mathematics

2020

**I dedicate this work to my family and my grandparents.**


# CERTIFICATE OF APPROVAL

## Numerical Analysis of MHD Heat Transfer and Nanofluid Flow over a Porous Plate with Radiation and Joule Heating Effects

by

Nimra Shanakhat

(MMT183003)

### THESIS EXAMINING COMMITTEE

| S. No. | Examiner | Name | Organization |
|---|---|---|---|
| (a) | External Examiner | Dr. Mehmood ul Hassan | COMSATS University, Islamabad |
| (b) | Internal Examiner | Dr. Rashid Ali | CUST, Islamabad |
| (c) | Supervisor | Dr. Shafqat Hussain | CUST, Islamabad |

Dr. Shafqat Hussain
Thesis Supervisor
December, 2020

Dr. Muhammad Sagheer
Head
Dept. of Mathematics
December, 2020

Dr. Muhammad Abdul Qadir
Dean
Faculty of Computing
December, 2020

# *Author's Declaration*

I, **Nimra Shanakhat** hereby state that my M.Phil thesis titled "**Numerical Analysis of MHD Heat Transfer and Nanofluid Flow over a Porous Plate with Radiation and Joule Heating Effects**" is my own work and has not been submitted previously by me for taking any degree from Capital University of Science and Technology, Islamabad or anywhere else in the country/abroad.

At any time if my statement is found to be incorrect even after my graduation, the University has the right to withdraw my M.Phil Degree.

**(Nimra Shanakhat)**

Registration No: MMT183003

# *Plagiarism Undertaking*

I solemnly declare that research work presented in this thesis titled "**Numerical Analysis of MHD Heat Transfer and Nanofluid Flow over a Porous Plate with Radiation and Joule Heating Effects**" is solely my research work with no significant contribution from any other person. Small contribution/help wherever taken has been duly acknowledged and that complete thesis has been written by me.

I understand the zero tolerance policy of the HEC and Capital University of Science and Technology towards plagiarism. Therefore, I as an author of the above titled thesis declare that no portion of my thesis has been plagiarized and any material used as reference is properly referred/cited.

I undertake that if I am found guilty of any formal plagiarism in the above titled thesis even after award of M.Phil Degree, the University reserves the right to withdraw/revoke my M.Phil degree and that HEC and the University have the right to publish my name on the HEC/University website on which names of students are placed who submitted plagiarized work.

**(Nimra Shanakhat)**
Registration No: MMT183003

# *Acknowledgements*

First and formest, I would like to thank Almighty **Allah** for bringing me this far in my academic career and helping me surpass all kinds of road blocks that I experienced. It is all by his blessings that I would have been able to complete this work to the best of my ability.

I would like to express my deepest gratitude to my supervisor, **Dr. Shafqat Hussain**, for the valuable guidance, encouragement and motivation. His guidance helped me in all the time of research and writing of this thesis. May Allah bless you sir with his blessings.

Besides my supervisor, I would like to thank all my other **teachers** who taught me during my coursework. I learnt alot from them.

I would like to pay great tribute to my **parents**, for their prayers, moral support, encouragement and appreciation. I would not have made it this far without them.

I would like to thank my siblings (**Iqra and Hamza**) for their constant support and unconditional love.

Last but not the least, I want to express my gratitude to my **friend**s who helped me throughout in my M.Phil degree. Thank you for every little help.

**Nimra Shanakhat**

# *Abstract*

This thesis investigates the numerical analysis of Magnetohydrodynamics nanofluid flow of multi-wall carbon nantubes with water over a porous plate with radiation and slip boundary condition. Effect of joule heating has also been incorporated. Appropriate similarity transformations are used to convert the modeled partial differential equations into a system of nonlinear ordinary differential equations. The resulting system of ordinary differential equations are solved numerically by using a well known shooting method, using the computational software package MATLAB. Moreover we studied the influence of nanoparticles volume fraction, suction or injection, the heat generation or absorption, the Eckert number, thermal and velocity slip parameters, Magnetic parameter and radiation on the velocity and temperature over a porous flat plate. Numerical values of the skin friction coefficient and Nusselt number are also discussed.

# Contents

# Symbols

| | |
|---|---|
| $\alpha$ | Thermal diffusivity, $m^2/s$ |
| $\eta$ | Similarity variable |
| $\theta$ | Dimensionless temperature |
| $\lambda$ | Velocity slip parameter |
| $\beta$ | Thermal slip parameter |
| $\mu$ | Dynamic viscocity, $kg/(m.s)$ |
| $\nu$ | Kinematic viscocity, $m^2/s$ |
| $\rho$ | Fluid density $kg/m^3$ |
| $\sigma$ | Stephan-Boltzmann constant, $W/(m^2.K^4)$ |
| $\tau_w$ | Surface shear stress, $kg/(m.s^2)$ |
| $\phi$ | Nanoparticles volume fraction |
| $\gamma$ | Local heat generation/absorption parameter |
| $\psi$ | Stream function |
| $Nu_x$ | Local Nusselt number |
| $Nu$ | Nusselt number |
| $Cp$ | Specific heat at constant pressure, $J/(kg.K)$ |
| $C_{fx}$ | Local skin-friction cofficent |
| $Ec$ | Eckert number |
| $k$ | Thermal conductivity, $W/(m.K)$ |
| $k^*$ | Mean absorption cofficent, $m^{-1}$ |
| $N$ | Radiation parameter |
| $B_0$ | Applied magnetic field |
| $M$ | Magnetic parameter |

| | |
|---|---|
| $Re_x$ | Local Reynolds number |
| $Re$ | Reynolds number |
| $Pr$ | Prandtl number |
| $Q_0$ | Heat generation/absorption cofficient, $J/m^3.K.s$ |
| $q_r$ | Radiative haet flux, $W/m^2$ |
| $q_w$ | Surface heat flux, $W/m^2$ |
| $T$ | Fluid temperature, $K$ |
| $u, v$ | Velocity components along $x$ and $y$ direction, $m/s$ |
| $x$ | Coordinate along the plate |
| $y$ | Coordinate normal to the plate |

**Subscripts**

| | |
|---|---|
| $f$ | fluid |
| $w$ | Condition at the surface |
| $\infty$ | Ambient condition |
| $nf$ | Nanofluid |
| $s$ | Solid |

# List of Figures

# List of Tables

# Abbreviations

| | |
|---|---|
| **BVP** | Boundary value problem |
| **CNTs** | Carbon nanotubes |
| **IVP** | Initial value problem |
| **MHD** | Magnetohydrodynamics |
| **MWCNTs** | Multi-wall carbon nanotubes |
| **ODEs** | Ordinary differential equations |
| **PDEs** | Partial differential equations |
| **RK** | Runge-Kutta |
| **SWCNTs** | Sigle-wall carbon nanotubes |

# Chapter 1

# Introduction

Fluid is a material that can not maintain its shape and deforms continuously when exposed to shear forces. A substance as a liquid, or gas phase material referred as fluid [1]. Fluid is the essential requirement of daily life and due to its role in many natural processes, many scientists have been trying to discover different facts about fluid flow. Fluid dynamics is a subbranch of fluid mechanics which characterizes the flow of fluids and how forces influence them. It illustrates the methodology of understanding the evolution of stars, meteorological phenomena, blood circulation, etc. Archimedes was a Greek mathematician, who first examined the fluid statics and buoyancy, and formulated his famous law known as the Archimedes principle. In early fifteenth century, the actual study of fluid mechanics had begun. Leonardo da Vinci (1452 - 1519) gave the equation of mass for 1D steady-state flow. He played with waves, jets, etc. Isaac Newton (1642 -1727) stated the law of viscosity and the laws of motion. Leonhard Euler (1707-1783) postulated integral and differential form of equations of motion, known as Bernoulli equation. Navier (1785 - 1836) and Stokes (1819 - 1903) added viscous term in equation of motion. Ludwig Prandtl (1875 - 1953) noted that fluid flows with limited viscosity, such as water flows and airflows can be divided into thin viscous/boundary layers close to the solid surfaces. In engineering and human activities fluid mechanics has a wide variety of applications, e.g. hydrology [2], energy generations [3] and medical

experiment on breathing and blood flow [4]. Some engineering applications of fluid flow includes rocket engine,oil pipeline and wind turbines [3].

Nanofluid is the combination of nano-sized particles and the base fluid. These particles are termed as nanoparticles with dimension less than 100nm. Choi was the first who introduced the concept of nanofluids in 1995 [5]. Afterward, Buongiorno studied the thermal conductivity of nanofluid [6]. There is wide variety of nanoparticles which are categorised according to their size, shape, thermal and electrical conductivity and heat transfer abilities. They are made up of metal, carbides and oxides. Some are named as nanofibers, nanowires, nanotubes and nanosheets [7]. Nanofluid has various applications in industrial devices, heat exchanger [8], drug delivery, medicines, car radiators, cooling of heat exchanging equipments, transformer oil cooling, electronic cooling [9, 10]. Nanofluids are synthesised in order to achieve better thermal conductivity as compared to any other base fluids. Nanofluids have high potential to enhance heat transfer rate as they have more thermal conductivity [11]. Thermal conductivity of nanofluid can be increased by using nanoparticles of gold, copper, silver etc., into the base fluid. The combined effect of viscous-Ohmic dissipation and thermal radiation on hydromagnetic flow of nanofluid over a stretching/shrinking sheet in the presence of slip and porous medium was studied by Ganesh et al. [12]. Zeeshan et al. [13] studied the effect of MHD on transportation of titanium dioxides and they analyzed that suspended nanoparticles in base fluid induces a decrease in nanofluid velocity. The effects of different parameters such as suction, Joule heating, thermal radiation, heat generation and absorption in the MHD flow of Casson nanofluid using a porous non-linear sheet was investigated by Ghadikolaei et al. [14]. Xuan and Li [15] used pure copper particles in the study of convective heat transfer and flow features of nanofluid. They found that not only the volume fraction but also the particle dimensions and material properties are important in order to achieve a substantial rise in heat transfer coefficient.

The phenomenon in which amount of heat transfers from high to low temperature region are known as heat transfer. It occurs when a body has different temperature with respect to its surroundings. Immense region of industry and engineering

deals with the problem of heat transfer. Various industrial appliances utilize water, refrigerants, ethylene glycol and engine oil, etc., as the convectional heat transfer fluids. Low thermal conductivity of such fluids hampers high efficiency and compactness of heat exchangers. Thermal conductivity of these fluids can be boosted by adding nanometer size particles called nanoparticles. The comparative analysis on thermophysical properties was studied by Hwang et al. [16–18], their study revealed that physical nature of nanoparticles with base fuids has significant impacts on maximum heat transfer process. Research has demonstrated that the thermal properties, boundary conditions and physical flow geometry are used to increase the process of heat convection in fluid flow. Over a flat plate heat transfer and fluid flow of nanofluid were studied by Hajmohammadi et al. [19] and the study concluded that heat transfer rate increased by varying the nanoparticles volume fraction in case of injection and impermeable plate. In many other applications heat transfer plays the major role e.g., food industry [20], building designing [21] and air compressor [22]. Fast heat transfer ability of nanofluids has been used in solar heating of water and solar collector. These devices absorb sunlight in the form of radiations and transfer it to the fluid running through the solar panels for water heating which can be stored for further uses [23]. Radiation is the process of heat transfer which has wide use in various applications [24]. Heat transfer and nanofluid flow were examined by Sadri and Babealahi [25] over a permeable flat plate. They used smilirity transformation for the conversion of PDEs into ODEs and then solved these equations by using appropriate numerical method.

Carbon nanotubes (CNTs) have a long cylindrical profile, such as frames of carbon atoms with a diameter ranging from 0.7nm - 50nm. Carbon nanotubes have a specific importance in nanotechnology, conductive plastics, hardwater, air purification mechanisms, structural composite materials, sensors, display of flat panels, storage of gas, biosensors, extra-long fibers, and many other areas of science and engineering. The idea of CNTs was first discovered in 1991 by Lijima [26]. Carbon nanotubes are further classified as single-wall carbonnanotubes (SWCNTs) and multi-wall carbonnanotubes (MWCNTs). Haq et al. [27] investigated the impact of the thermal conductivity and viscosity of CNTs nanoparticles within

different base fluids. Nandeppanvar et al. [28] investigated the effects of carbon nanotubes on heat transfer over flat surface. It was concluded through their study that SWCNTs has better heat convection than MWCNTs, usually CNTs have more thermal conductivity [29].

The layer in which viscous effects are more dominant is known as boundary layer around which the fluid is flowing. Ludwing Prandtl gave the idea of boundary layer in 1904. Skiadis [30] was the first who discussed the fluid flow problem related to boundary layer over stretching sheet. Many researchers have gained attention towards the investigation of boundary layer flow. Blasius [31] was the first who investigated the boundary layer flow on flat plate. Further different forms of Blasius flat plate problem were studied by Hawart [32]. It has important applications over stretching sheet such as hot rolling, wire drawing etc. [33]. Crane [34] was the one who established the steady flow across the stretching sheet. For 2D steady flow he analytically solved the flow pass across the linear stretching plate. Further for 3D case, this problem was extended by Wang [35]. The impact of slip boundary condition on heat transfer rate were investigated by Das et al [36]. Through their study, they found that in the presence of thermal slip condition or hydrodynamic suction, injection parameter has large impact on surface temperature of plate.

The thermal radiation effect becomes intensified at high absolute temperature levels due to basic difference between radiation , convection and conduction energy-exchange mechanisms. It has an important effect on heat transport properties in the dynamics and manufacturing area, interstellar technology, high temperature developments. In the context of space technology, some devices for space applications are designed to operate at high temperature levels in order to achieve high thermal efficiency. Hence, the effects of radiation are of vital importance when calculating thermal effects in the processes involving high temperatures. Akbar et al. [37] studied the radiation effects on MHD stagnation point flow of nanofluid towards a stretching surface with convective boundary condition.

Porous medium is a material having pores (voids), which means that the pores are fully connected and filled with the fluid, and fluid may flow through the voids. It

can be examined that, thermal systems become more efficient by using porous media and nanofluid, because nanoparticle increases the thermal conductivity while contact surface area increases by porous media [11]. Properties of porosity are discussed by Sumirat et al. [38]. The heat transfer and nanofluid flow through porous media reviewed by Mahdi et al [39]. First they collected information about porous media like porosity, thermal conductivity, permeability. Then, they described the works of thermophysical properties with fluid flow and the convection heat transfer process. Khanafer and Chamkha [40] studied the fluid flow thorough porous medium using Brinkman-extended Darcy model. They observed that boosting Darcy number, the $Nu$ enhances. Many industrial, engineering and biological fields are using porous medium for thermal energy management [41].

Magnetohydrodynamics has gained the attention of investigators due to its numerous applications in various fields of sciences and engineering like aerodynamics, fuid dynamics, [42], biomedical engineering, [43] the fluid flow in microelectronic devices, and the flow of liquid metals., etc [44]. The idea of MHD fluid flow was first introduced by Alfven [45]. MHD is the branch of mechanics which deals with magnetic behavior and properties of electrically conducting fluid. When a conducting fluid moves through a magnetic field, it induces current, as a result Lorentz force is produced which changes the movement of the fluid. The MHD factor has a fundamental role in controlling the cooling rate and for achieving the desired quality of the product. The effects of viscoelastic fluid on MHD boundary layer flow over a permeable surface were studied by Rita et al. [46]. MHD flow and heat transfer over permeable plate were studied numerically by Yasin et al. [47]. They studied the effects of different parameters (e.g., radiation, heat generation/absorption, suction/injection). Hayat et al. [48] explored the impact of chemical reaction in MHD flow through a nonlinear over stretching surface. They analyzed that the Nusselt number is an increasing function of power-law index. The effects of unsteady MHD flow over a permeable plate were investigated by Muhammad et al. [49] and considered the effects of temperature, velocity slip parameter, Joule heating, viscous dissipation and magnetic field. Aman et al. [50] investigated the flow of 2D incompressible viscous fluid using a shrinking surface

in the existence of an external magnetic filed. Kabir et al. [51] investigated the impact of viscous dissipation on MHD natural convectional flow with a vertical wavy surface. They concluded that the velocity and temperature profiles increases by increasing the Eckert number.

## 1.1 Thesis Contribution

In this thesis, we provide a detailed review of Maleki et al. [52]. The objective of their work is to study the heat transfer and nanofluid flow over a porous plate with radiation and slip boundary conditions. Numerical results are obtained using Runge-Kutta-Fehlberg forth-fifth order (RKF45) technique, using Maple software. By considering various effects such as radiation, heat generation/absorption, viscous dissipation and nanoparticles volume fraction on temperature and velocity profiles through graphs and tables. Futher more, the leading motivation of extended work is to investigate the impact of magnetic field and Joule heating on MHD nanofluid flow of MWCNTs-water nanofluid over a porous plate. For numerical analysis we convert a system of PDEs into nonlinear ODEs using similarity transformations. A well known shooting technique with fourth order Runge-Kutta method is used to obtain the numerical results using MATLAB software. Moreover behavior of velocity and temperature profile are analyzed by studying different parameters like nanoparticle volume fraction, magnetic parameter, Eckert number etc, through tables and graphs.

## 1.2 Thesis Outline

This thesis is further composed of four chapters:

**Chapter 2** demonstrates some important definitions, concept and laws that are helpful in understanding the present work.

**Chapter 3** interprets a review analysis of the study performed in [52]. This work has covered the scope related to heat transfer nanofluid flow over a porous plate by considering the radiation and heat/generation absorption effects over a porous plate. An appropriate similarity transformation is used for the conversion of PDEs into ODEs and obtained the numerical results by solving the system of ODEs with the help of shooting method.

**Chapter 4** extends the work of Maleki et al [52]. In this work the effect of magnetic and Joule heating is inspected by adding MHD effects to the preceding problem. The governing equations have been dealt in same manner as aforementioned in Chapter 3.

**Chapter 5** summarizes the whole study and includes the conclusion arising from the entire discussion.

# Chapter 2

# Basic Definitions and Governing Equations

Some basic definitions, governing laws, terminologies and and dimensionless numbers will be discussed in this chapter, which will be used in next chapters. Furthermore, shooting method has been discussed at the end of this chapter which is used to find the numerical results..

## 2.1 Important Definitions

**Definition 2.1.1. (Fluid)**

"A substance exists in three primary phases. solid, liquid and gas. (At very high temperatures, it also exists as plasma) A substance in the liquid or gas phase is referred to as a fluid. Distinction between a solid and fluid is made on the basis of substances ability to resist an applied shear or (tangential) stress that tends to change its shape." [53]

**Definition 2.1.2. (Fluid Mechanics)**

"Fluid mechanics is defined as the science that deals with the behavior of fluids at rest (fluid statics) or in motion (fluid dynamics) and the interaction of fluids with

solid or other fluids at the boundaries." [53]

**Definition 2.1.3. (Magnetohydrodynamics)**

"Magnetohydrodynamics (MHD) is concerned with the flow of electrically conducting fluids in the presence of magnetic fields, either externally applied or generated within the fluid by inductive action." [54]

**Definition 2.1.4. (Fluid Dynamics)**

"The study of the motion of gases, liquids and plasmas from one place to another. It has many useful applications which are use in our daily life such as, mass flow rate of petroleum passing through pipelines, prediction of weather, etc." [53]

**Definition 2.1.5. (Nanofluids)**

"Nanofluids are engineered by suspending nanoparticles with average sizes below 100 nm in traditional heat transfer fluids such as water, oil, and ethylene glycol. A very small amount of guest nanoparticles, when dispersed uniformly and suspended stably in host fluids, can provide dramatic improvements in the thermal properties of host fluids." [55]

## 2.2 Types of Flow

**Definition 2.2.1. (Steady vs Unsteady Flow)**

" The term steady implies no change of properties, velocity, temperature, etc., at a point with time. The opposite of steady is unsteady." [53]

**Definition 2.2.2. (Laminar vs Turbulent Flow)**

"Some flows are smooth and orderly while others are rather chaotic. The highly ordered fluid motion characterized by smooth layers of fluid is called laminar. The

highly disordered fluid motion that typically occurs at high velocities and is characterized by velocity fluctuations is called turbulent." [53]

**Definition 2.2.3. (Uniform Flow)**

"The simplest plane flow is one for which the streamlines are all straight and parallel, and the magnitude of the velocity is constant. This type of flow is called a uniform flow." [56]

**Definition 2.2.4. (Natural vs Forced Flow)**

"A fluid flow is said to be natural or forced, depending on how the fluid motion is initiated. In forced flow, a fluid is forced to flow over a surface or in a pipe by external means. Whereas In natural flows, fluid motion is due to natural means such as the buoyancy effect." [53]

**Definition 2.2.5. (External vs Internal Flow)**

"The flow of an unbounded fluid over a surface such as a plate, a wire, or a pipe is external flow. The flow in a pipe or duct is internal flow if the fluid is completely bounded by solid surfaces. For example, flow of water in a pipe is internal flow." [57]

**Definition 2.2.6. (Viscous vs Inviscous Flow)**

"When two fluid layers move relative to each other, a friction force develops between them and the slower layer tries to slow down the faster layer. This internal resistance to flow is quantified by the fluid property viscosity, which is a measure of internal stickiness of the fluid. Viscosity is caused by cohesive forces between the molecules in liquids and by molecular collisions in gases. There is no fluid with zero viscosity, and thus all fluid flows involve viscous effects to some degree. Flows in which the frictional effects are significant are called viscous flows. However, in many flows of practical interest, there are regions (typically regions not close to solid surfaces) where viscous forces are negligibly small compared to inertial or

pressure forces. Neglecting the viscous terms in such inviscid flow regions greatly simplifies the analysis without much loss in accuracy." [53]

## 2.3 Classifications and Properties of Fluid

**Definition 2.3.1. (Compressible vs Incompressible Flow)**
"A flow is classified as being compressible or incompressible, depending on the level of variation of density during flow. Incompressibility is an approximation, and a flow is said to be incompressible if the density remains nearly constant throughout. Therefore, the volume of every portion of fluid remains unchanged over the course of its motion when the flow (or the fluid) is incompressible. The densities of liquids are essentially constant, and thus the flow of liquids is typically incompressible. Therefore, liquids are usually referred to as incompressible substances. A pressure of 210 atm, for example, causes the density of liquid water at 1 atm to change by just 1 percent. Gases, on the other hand, are highly compressible. A pressure change of just 0.01 atm, for example, causes a change of 1 percent in the density of atmospheric air." [53]

**Definition 2.3.2. (Newtonian Fluids vs non-Newtonian Fluids)**
"Fluids for which the rate of deformation is linearly proportional to the shear stress are called Newtonian fluids. In one-dimensional shear flow of Newtonian fuids, shear stress can be expressed by the linear relationship as

$$\tau_{xy} = \mu \left( \frac{du}{dy} \right)^n , \tag{2.1}$$

where the constant of proportionality $\mu$ is called the coefficient of viscosity or the dynamic (or absolute) viscosity of the fluid." Examples are air, water, kerosene and gasoline. "Fluids for which the shear stress is not linearly related to the shear strain rate are called non-Newtonian fluids." [53]

**Definition 2.3.3. (Ideal vs Real Fluid)**
"An ideal fluid is defined as a non-viscous and incompressible fluid. That is the

fluid has zero viscosity and a constant density ($\rho$= constant, $\mu = 0$). Although no ideal fluid exists, many real fluid have small viscosity and the effects of compressibility are negligible." [58]

**Definition 2.3.4. (Newton's Law of Viscosity)**

"This law states that for a fluid, tangential stress is proportional to rate of deformation. It is mathematically written as:

$$\tau_{xy} = \mu \left( \frac{du}{dy} \right). \tag{2.2}$$

where $\tau_{xy}$ represents shear stress, $\mu$ represents dynamic viscosity and $\frac{du}{dy}$ shows deformation rate, respectively." [59]

**Definition 2.3.5. (Density)**

"Density is defined as mass per unit volume. That is

$$\rho = \frac{m}{\mathbf{V}},$$

where, $\mathbf{V}$ is the volume." [53]

**Definition 2.3.6. (Pressure)**

"Pressure is defined as a normal force exerted by a fluid per unit area. We speak of pressure only when we deal with a gas or a liquid. It is formulated as" [53]

$$p = \frac{F}{A}.$$

**Definition 2.3.7. (Boundary Layer)**

"The region where viscous effects are dominate are known as boundary layer region around which fluid is flowing. The concept of boundary layer, implies that flow at high Reynold numbers can be divided into two unequally large regions. In the bulk of flow region, the viscosity can be neglected, and the flow corresponds to the inviscid limiting solution. This is called the inviscid outer flow. The second

region is the very thin boundary layer at wall where the viscosity must be taken into account. Within the boundary layer the two different flow forms, that is, the flow can be laminar or turbulent." [60]

**Definition 2.3.8. (Heat Transfer)**
"Due to temperature difference it is the energy transfer. Heat transfer is directed to:

1. The estimation of rate of flow energy as heat through the boundary of a system both under steady and transient conditions.

2. The determination of temperature field under steady and transient conditions, which also will provide the information about the gradient and time rate of change of temperature at various location and time." [61]

## 2.4 Modes of Heat Transfer

There are three modes of heat transfer:

**Definition 2.4.1. (Conduction)**
"Conduction is the transfer of heat from one part of a body at a higher temperature to another part of the same body at a lower temperature." [62]

**Definition 2.4.2. (Convection)**
"Convection, relates to the transfer of heat from a bounding surface to a fluid in motion, or to the heat transfer across a ow plane within the interior of the flowing fluid." [62]

**Definition 2.4.3. (Forced Convection)**
"If the fluid motion is induced by a pump, a blower, a fan, or some similar device,

the process is called forced convection."[62]

**Definition 2.4.4. (Natural Convection)**

"If the fluid motion occurs as a result of the density difference produced by the temperature difference, the process is called free or natural convection.". [62]

**Definition 2.4.5. (Mixed Convection)**

"Mixed convection occurs when both natural convection and forced convection play significant roles in the transfer of heat. Mixed convection occurs when the heat transfer is significantly different from that for either pure natural convection or pure forced convection." [62]

**Definition 2.4.6. (Radiation)**

"Radiation, or more correctly thermal radiation, is electromagnetic radiation emitted by a body by virtue of its temperature and at the expense of its internal energy. All heated solids and liquids, as well as some gases, emit thermal radiation. The transfer of energy by conduction requires the presence of a material medium, while radiation does not." [62]

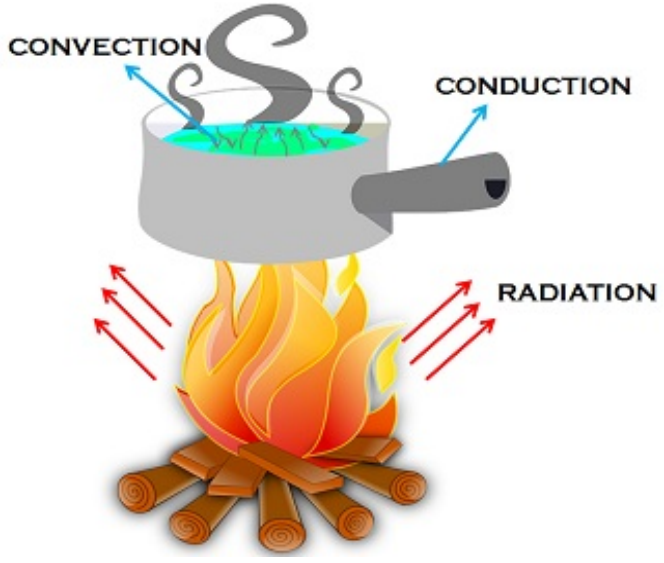


FIGURE 2.1: Modes of heat transfer.

## 2.5 Fundamental Laws

In this section governing equations and fundamental laws are described which are important in the study of different flow problems.

### 2.5.1 Conservation of Mass

"The principle of conservation of mass can be stated as the time rate of change of mass is fixed volume is equal to the net rate of flow of mass across the surface. For unsteady and compressible flow the mathematical form of continuity equation is given as:

$$\frac{\partial \rho}{\partial t} + \bigtriangledown.\,(\rho V) = 0, \tag{2.3}$$

here $\rho$, $t$ and $V$ represent the fluid's density, time and the velocity vector respectively. For steady-state conditions, the continuity equation becomes

$$\nabla.(\rho V) = 0.$$

When the density changes following a fluid particle are negligible, the continum is termed incompressible. The continuity equation then becomes

$$\nabla.V = 0, \tag{2.4}$$

which is often referred to as the incompressibility condition or incompressibility constraint." [63]

### 2.5.2 Law of Conservation of Momentum

"The momentum equation states that the time rate of change of linear momentum of a given set of particles is equal to the vector sum of all the external forces acting on the particles of the set, provided Newton's Third Law action and reaction

governs the internal forces. Newton's second law can be written as

$$\frac{\partial(\rho V)}{\partial t} + \nabla.[(\rho V)V] - \nabla.(\sigma) + (\rho g) = 0, \tag{2.5}$$

where, $\sigma$ is the caushy stress tensor and $g$ is the body force vector, measured per unit mass and normally taken to be the gravity vector. The form of the momentum equation shown in Eq. (2.5) is the conservation form that is most often utilize as compressible flows. This equation may be simplified to a form more commonly used with incompressible flows. Expanding the first two derivatives and collecting terms

$$\rho\left(\frac{\partial V}{\partial t} + V.\nabla V\right) + V\left(\frac{\partial \rho}{\partial t} + \nabla.\rho V\right) = \nabla.\sigma - \rho g. \tag{2.6}$$

The second term in parentheses is the continuity equation and neglecting this term allows (2.6) to reduce to the non-conservation form

$$\rho\frac{DV}{Dt} = \nabla.\sigma + \rho g,$$

where, $\frac{DV}{Dt}$ is the material derivative." [63]

### 2.5.3 Law of Conservation of Energy

"The law of conservation of energy (or the First Law of Thermodynamics) states that the time rate of change of the total energy is equal to the sum of the rate of work done by applied forces and the change of heat content per unit time. The resulting form of energy equation can be written as

$$\rho\frac{DT}{Dt} = -\nabla.q + Q + \phi, \tag{2.7}$$

Where $\phi$ is the dissipation function which is defined by

$$\phi = \sigma : \nabla.V$$

which is the standard form used for incompressible flows." [63]

## 2.6 Dimensionless Numbers

**Definition 2.6.1. (Reynolds Number)**

"This number expresses the ratio of the fluid inertia force to that of molecular friction (viscosity). It determines the character of the flow (laminar, turbulent and transient flows). For a laminar flow $Re < 200$ is valid, for a transient flow $200 < Re < 400$ , and for a turbulent flow it is $Re > 400$. Mathematically:

$$Re = \frac{VL}{\nu},$$

where $V$, $L$, and $\nu$ are used to denote the flow velocity, characteristics length and kinematic viscosity, respectively." [64]

**Definition 2.6.2. (Eckert Number)**

"It express the ratio of kinetic energy to a thermal energy change. It is mathematically written as:

$$Ec = \frac{V_\infty^2}{C_p \Delta T}.$$

Here $V_\infty^2$ is the fluid flow velocity far from body, $C_p$ denotes specific heat and $\Delta T$ is the temperature difference." [64]

**Definition 2.6.3. (Prandtl Number)**

"This number expresses the ratio of the momentum diffusivity (viscosity) to the thermal diffusivity. Mathematical expression for prandtl number is:

$$Pr = \frac{\nu}{\alpha} = \frac{C_p \mu}{k}.$$

Here $C_p$, $\mu$ and $k$ is written for specific heat, dynamic viscosity and thermal conductivity respectively.

With small $Pr$ numbers ($Pr < 1$), the molecular heat transfer by conduction predominates over that by convection.

With ($Pr > 1$), it is the opposite case." [64]

**Definition 2.6.4. (Skin friction)**

"It expresses the dynamic friction resistance originating in viscous fluid flow around a fixed wall. The skin friction coefficient can be defined as

$$C_f = \frac{\tau_w}{\rho U_\infty^2},$$

where $\tau_w$ denotes the shear stress on the wall, $\rho$ the density and $U_\infty$ the free-stream velocity." [64]

**Definition 2.6.5. (Nusselt Number)**

"It expresses the ratio of the total heat transfer in a system to the heat transfer by conduction.. Mathematically,

$$Nu = \frac{hL}{k},$$

where $h$ stands for heat transfer coefficient, $L$ for the characteristics length and $k$ stands for the thermal conductivity." [64]

**Definition 2.6.6. (Hartmann Number)**

"It expresses the ratio of the induced electrodynamic (magnetic) force to the hydrodynamic force of the viscosity.

$$Ha = BL\sqrt{\frac{\sigma}{\mu}},$$

where $\sigma$, $B$, $\mu$ and $L$ stand for electrical conductivity, magnetic field, dynamic viscosity and characteristic length scale respectively." [64]

## 2.7 Solution Methodology

"In a shooting method, the missing initial condition at the initial point of the interval is assumed, and the differential equation is then integrated numerically

as an initial value problem to the terminal point. The accuracy of the assumed missing initial condition is then checked by comparing the calculated value of the dependent variable at the terminal point with its given value there. If a difference exists, another value of the missing initial condition must be assumed and the process is repeated. This process is continued until the agreement between the calculated and the given condition at the terminal point is within the specified degree of accuracy. For this type of iterative approach, one naturally inquires whether or not there is a systematic way of finding each succeeding (assumed) value of the missing initial condition."

### 2.7.1 Newton's Method

"In this method, the differential equation is kept in its nonlinear form and the missing slope is found systematically by Newton's method. This method provides quadratic convergence of the iteration and is far better than the usual cut-and-tr methods. Consider the second-order differential equation

$$\frac{d^2y}{dx^2} = f(x, y, dy/dx) \tag{2.8}$$

subject to the boundary conditions

$$y(0) = 0, \quad y(L) = A \tag{2.9}$$

First, Eq. (2.8) is written in terms of a system of two first-order differential equations:

$$\frac{dy}{dx} = u, \quad \frac{du}{dx} = f(x, y, u) \tag{2.10}$$

We denote the missing initial slope by

$$\frac{dy(0)}{dx} = s \quad \text{or} \quad u(0) = s \tag{2.11}$$

The problem is to find $s$ such that the solution of Eq. (2.10), subject to the initial conditions (2.9) and (2.11), satisfies the boundary condition at the second point, (2.9). In other words, if the solutions of the initial value problem are denoted by $y(x, s)$ and $u(x, s)$, one searches for the value of $s$ such that

$$y(L, s) - A = \phi(s) = 0 \tag{2.12}$$

For Newton's method, the iteration formula for $s$ is given by

$$s^{(n+1)} = s^{(n)} - \frac{\phi(s^{(n)})}{d\phi(s^{(n)})/ds}$$

or

$$s^{(n+1)} = s^{(n)} - \frac{y(L, s^{(n)}) - A}{\partial y(L, s^{(n)})/\partial s} \tag{2.13}$$

To find the derivative of $y$ with respect to $s$, Eqs. (2.10), (2.9), and (2.11) are differentiated with respect to $s$, and we get

$$\frac{dY}{dx} = U, \quad \frac{dU}{dx} = \frac{\partial f}{\partial y}Y + \frac{\partial f}{\partial u}U \tag{2.14}$$

and

$$Y(0) = 0, \quad U(0) = 1 \tag{2.15}$$

where

$$Y = \frac{\partial y}{\partial s}, \quad U = \frac{\partial u}{\partial s} \tag{2.16}$$

The solution of Eq. (2.10), subject to the boundary conditions (2.9), can therefore be obtained by the following steps.

1. Assume a value of $s$ for the missing initial slope, (2.11). Let us denote this approximate value of $s$ by $s(I)$.

2. Integrate Eq. (2.10), subject to the boundary conditions (2.9) and (2.11), as an initial value problem from $x = 0$ to $x = L$.

3. Integrate Eq. (2.14), subject to the boundary conditions (2.15), as an initial value problem, from $x = 0$ to $x = L$.

4. Substituting the values of $y(L, s^{(1)})$ and $Y(L, s^{(1)})$ into Eq. (2.13), we get

$$s^{(2)} = s^{(1)} - \left[y(L, s^{(1)}) - A\right] / Y(L, s^{(1)}).$$

the next approximation of the missing initial slope $s^{(2)}$ is obtained.

5. Repeat steps $2 - 4$ until the value of $s$ is within the specified degree of accuracy." [65]

# Chapter 3

# Flow of Heat Transfer and Nanofluid with Radiation and Slip Boundary Conditions over a Porous Plate

The main objective of this chapter is to analyze the heat transfer and nanofluid flow using slip boundary condition with radiation effects over a porous plate. Viscous effects and heat generation/absorption are also taken into account. Similarity transformation has been used for the conversion of nonlinear PDEs to the system of ODEs. The numerical solution of ordinary differential equations is found by using shooting method. Lastly, the results are analyzed through graphs by taking different physical parameters effects on temperature and velocity profile. This chapter provide the review study of Maleki et al. [52].

## 3.1 Mathematical Modeling

In this model we consider the $2D$ steady, incompressible flow along with slip boundary condition and radiation effects. Moreover the model also investigates

the water based nanofluid containing MWCNTs nanomaterial over a flat porous plate. The plate is placed in such a way that $y$-axis is normal to the plate and fluid is flowing along $x$-axis. It has been assumed that the velocity of plate along $x$-axis is $u = \lambda_1 \left(\frac{\partial u}{\partial x}\right)$ and the free stream velocity is $U_\infty$. Here $T$ and $T_\infty$ are the temperature of nanofluid in the boundary layer and away from the plate. While $T_w$ is the temperature at the surface oh plate.

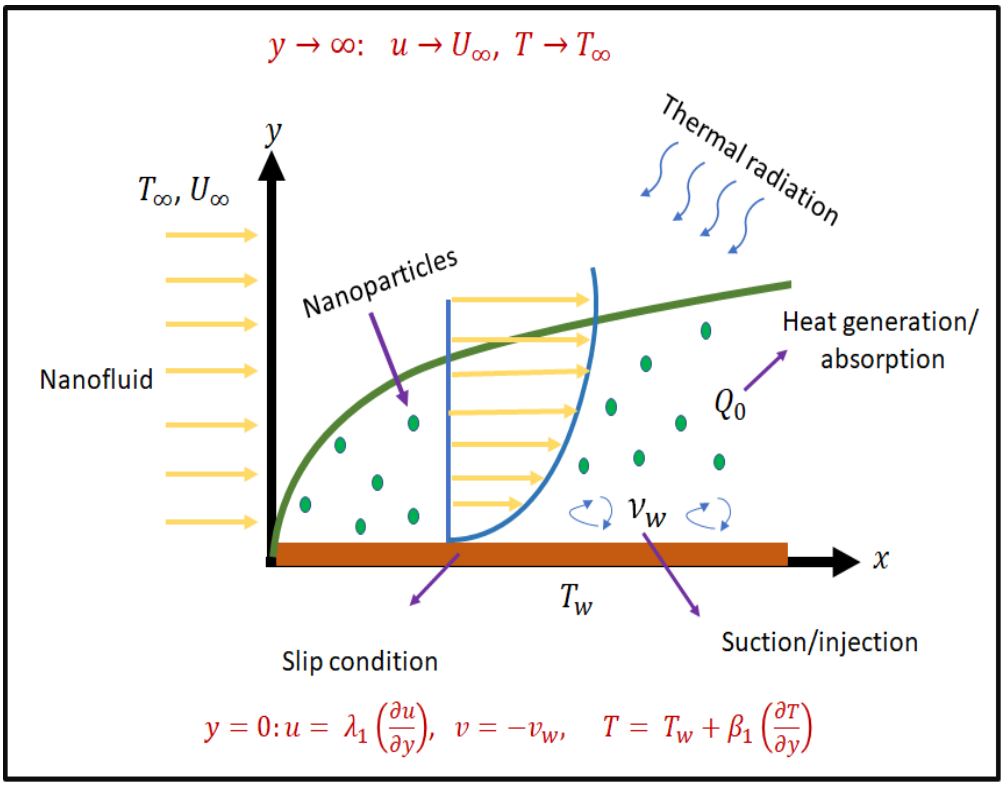


FIGURE 3.1: Flow model geometry.

The governing equations for the boundary layer flow are mentioned below:

$$\frac{\partial u}{\partial x} + \frac{\partial v}{\partial y} = 0, \tag{3.1}$$

$$u\frac{\partial u}{\partial x} + v\frac{\partial u}{\partial y} = \frac{\mu_{nf}}{\rho_{nf}}\frac{\partial^2 u}{\partial y^2}, \tag{3.2}$$

$$u\frac{\partial T}{\partial x} + v\frac{\partial T}{\partial y} = \alpha_{nf}\frac{\partial^2 T}{\partial y^2} + \frac{\mu_{nf}}{(\rho C_p)_{nf}}\left(\frac{\partial u}{\partial y}\right)^2 + \frac{Q_0(T - T_\infty)}{(\rho C_p)_{nf}} - \frac{1}{(\rho C_p)_{nf}}\left(\frac{\partial q_r}{\partial y}\right). \tag{3.3}$$

The corresponding boundary conditions are:

$$\left.\begin{aligned} &u = \lambda_1 \left(\frac{\partial u}{\partial y}\right), \quad v = -v_w, \quad T = T_w + \beta_1 \left(\frac{\partial T}{\partial y}\right) \quad \text{at} \quad y = 0, \\ &u \to U_\infty, T \to T_\infty \quad \text{as} \quad y \to \infty, \end{aligned}\right\} \tag{3.4}$$

here $v$ and $u$ are the velocity components in $y$ and $x$ direction, respectively. $(\rho C_p)_{nf}$, $\rho_{nf}$ $\alpha_{nf}$ and $\mu_{nf}$ are the heat capacity, density, thermal diffusivity and viscosity of nanofluid, where $U_\infty$, $T$, $T_\infty$, $T_w$, $\lambda_1$, $\beta_1$ and $v_w$ indicate free stream velocity, nanofluid temperature in the boundary layer, temperature of free stream, temperature of plate, velocity slip parameter, thermal slip parameter and mass velocity normal to the wall.

By using Roseland model the radiative heat flux is calculated as:

$$q_r = -\frac{4\sigma}{3k^*}\frac{\partial T^4}{\partial y}, \tag{3.5}$$

where $T^4$, $k^*$ and $\sigma$ represent the fluid temperature, mean absorption factor and Stefan-Boltzmann coefficient. By applying Taylor series, temperature difference $T^4$ can be expended about $T_\infty$ which is ambient temperature, as follows:

$$T^4 = T_\infty^4 + \frac{4T_\infty^3}{1!}(T - T_\infty)^1 + \frac{12T_\infty^2}{2!}(T - T_\infty)^2 + \frac{24T_\infty}{3!}(T - T_\infty)^3 + \dots$$

By ignoring the higher order terms, we have

$$\begin{aligned} T^4 =& T_\infty^4 + 4T_\infty^3(T - T_\infty), \\ \Rightarrow T^4 =& T_\infty^4 + 4T_\infty^3 T - 4T_\infty^4), \\ \Rightarrow T^4 =& 4T_\infty^3 T - 3T_\infty^4. \end{aligned}$$

$$\Rightarrow \frac{\partial T^4}{\partial y} = 4T_\infty^3 \frac{\partial T}{\partial y}. \tag{3.6}$$

Using Eq. (3.6) in Eq. (3.5) and then differentiating w.r.t $y$, we get

$$\frac{\partial q_r}{\partial y} = -\frac{16\sigma T_\infty^3}{3k^*}\frac{\partial^2 T}{\partial y^2}. \tag{3.7}$$

## 3.2 Thermophysical Properties

The different thermophysical properties of water and multi-wall carbon nanotubes (MWCNTs) particles are given below in Table 3.1. [52]

TABLE 3.1: Thermophysical properties of base fluid and nanomaterials

| **Material** | $C_p(J.kg^{-1}K^{-1})$ | $\rho/(kg.m^{-3})$ | $k/(W.m^{-1}.K^{-1})$ |
|---|---|---|---|
| **Water** | 4179 | 997.1 | 0.613 |
| ***MWCNTs*** | 796 | 1600 | 3000 |

Thermophysical properties are formulated as follow [52].

$$\alpha_{nf} = \frac{k_{nf}}{(\rho C_p)_{nf}} \tag{3.8}$$

$$\mu_{nf} = \frac{\mu_f}{(1-\phi)^{2.5}}, \tag{3.9}$$

$$\rho_{nf} = (1-\phi)\,\rho_f + \phi\rho_s, \tag{3.10}$$

$$(\rho C_p)_{nf} = (1-\phi)\,(\rho C_p)_f + \phi\,(\rho C_p)_s\,, \tag{3.11}$$

where $\rho_s$, $\rho_f$ are densities of solid particles and base-fluid and $\phi$ is the nanoparticles volume fraction, respectively.

There are many theoretical models available in the literature for measuring the thermal conductivity of carbon nanotubes.

(e.g., Maxwell's, Jeffery's, Davis's, Hamilton's, and crosser models).

But only the model of Xue's employs key models that are efficient for nanotubes. We use Xue's model [29] to calculate thermal conductivity of nanofluid (MWCNTs) .

$$\frac{k_{nf}}{k_f} = \frac{1-\phi+2\phi\frac{k_s}{k_s-k_f}ln\left(\frac{k_s+k_f}{2k_f}\right)}{1-\phi+2\phi\frac{k_f}{k_s-k_f}ln\left(\frac{k_s+k_f}{2k_f}\right)}. \tag{3.12}$$

### 3.2.1 Similarity Transformation

Following transformation has been used to convert PDEs Eqs. (3.1)-(3.3) into system of ODEs [52].

$$\left.\begin{aligned} \eta &= y\left(\frac{U_\infty}{\nu_f x}\right)^{\frac{1}{2}}, & \psi(\eta) &= (U_\infty \nu_f x)^{\frac{1}{2}} f(\eta), \\ \theta(\eta) &= \frac{T - T_\infty}{T_w - T_\infty}, & T &= \theta(T_w - T_\infty) + T_\infty. \end{aligned}\right\} \tag{3.13}$$

The continuity equation Eq. (3.1) is satisfied directly stream function in the following sense,

$$u = \frac{\partial \psi}{\partial y}, v = -\frac{\partial \psi}{\partial x}. \tag{3.14}$$

The calculation of velocity component along $x$ and $y$ direction as

$$\begin{aligned} u &= \frac{\partial \psi}{\partial y}, \\ &= \frac{\partial}{\partial y}(U_\infty \nu_f x)^{\frac{1}{2}} f(\eta), \\ &= (U_\infty \nu_f x)^{\frac{1}{2}} \frac{\partial}{\partial y} f(\eta), \\ &= (U_\infty \nu_f x)^{\frac{1}{2}} \left(\frac{\partial f}{\partial \eta}\right)\left(\frac{\partial \eta}{\partial y}\right), \\ &= (U_\infty \nu_f x)^{\frac{1}{2}} f' \left(\frac{U_\infty}{\nu_f x}\right)^{\frac{1}{2}}, \\ u &= U_\infty f'(\eta). \end{aligned} \tag{3.15}$$

similarly, we can find

$$\begin{aligned} v &= -\frac{\partial \psi}{\partial x}, \\ &= -\frac{\partial}{\partial x}[(U_\infty \nu_f x)^{\frac{1}{2}} f(\eta)], \\ &= -(U_\infty \nu_f)^{\frac{1}{2}} \frac{\partial}{\partial x}\left(x^{\frac{1}{2}} f(\eta)\right), \\ &= -(U_\infty \nu_f)^{\frac{1}{2}} \left[\frac{1}{2} x^{\frac{-1}{2}} f + f' \left(-\frac{1}{2} y \left(\frac{U_\infty}{\nu_f}\right)^{\frac{1}{2}} x^{\frac{-3}{2}} . x^{\frac{1}{2}}\right)\right], \\ v &= \frac{-1}{2}\left(\frac{U_\infty \nu_f}{x}\right)^{\frac{1}{2}} f + \frac{1}{2} y \frac{U_\infty}{x} f'. \end{aligned} \tag{3.16}$$

Further we can write,

$$\begin{aligned}
\frac{\partial u}{\partial x} &= \frac{\partial}{\partial x}\left(U_\infty f'(\eta)\right), \\
&= U_\infty \left(\frac{\partial f'}{\partial \eta}\right)\left(\frac{\partial \eta}{\partial x}\right), \\
&= U_\infty f'' \left(-\frac{1}{2} y \left(\frac{U_\infty}{\nu_f}\right)^{\frac{1}{2}} x^{\frac{-3}{2}}\right), \\
&= -\frac{1}{2} y \left(\frac{U_\infty^{\frac{3}{2}}}{\nu_f^{\frac{1}{2}}}\right) x^{\frac{-3}{2}} f'', \qquad (3.17) \\
\frac{\partial v}{\partial y} &= -\frac{1}{2}\left(\frac{U_\infty \nu_f}{x}\right)^{\frac{1}{2}} f' \left(\frac{U_\infty}{\nu_f x}\right)^{\frac{1}{2}} + \frac{U_\infty}{2x}\left(f' + f'' \left(\frac{U_\infty}{\nu_f x}\right)^{\frac{1}{2}} y\right), \\
&= -\frac{1}{2}\frac{U_\infty}{x} f' + \frac{1}{2}\frac{U_\infty}{x} f' + \frac{1}{2}\frac{U_\infty^{\frac{3}{2}}}{x^{\frac{3}{2}}\nu_f^{\frac{1}{2}}} y f'', \\
&= \frac{1}{2}\frac{U_\infty^{\frac{3}{2}}}{x^{\frac{3}{2}}\nu_f^{\frac{1}{2}}} y f''. \qquad (3.18)
\end{aligned}$$

Adding Eqs. (3.17) and (3.18) we get the following result

$$\frac{\partial u}{\partial x} + \frac{\partial v}{\partial y} = 0.$$

Conversion of momentum and energy PDEs Eq. (3.2) or Eq. (3.3) into ODEs has discussed below,

$$\begin{aligned}
\frac{\partial u}{\partial x} &= \frac{\partial}{\partial x}\left(U_\infty f'(\eta)\right), \\
&= U_\infty \left(\frac{\partial f'}{\partial \eta}\right)\left(\frac{\partial \eta}{\partial x}\right), \\
&= U_\infty f'' \left(-\frac{1}{2} y \left(\frac{U_\infty}{\nu_f}\right)^{\frac{1}{2}} x^{\frac{-3}{2}}\right), \\
&= -\frac{1}{2} y \left(\frac{U_\infty^{\frac{3}{2}}}{\nu_f^{\frac{1}{2}}}\right) x^{\frac{-3}{2}} f'', \\
\frac{\partial u}{\partial y} &= \frac{\partial}{\partial y}\left(U_\infty f'(\eta)\right), \\
&= U_\infty^{\frac{3}{2}} \left(\frac{1}{x\nu_f}\right)^{\frac{1}{2}} f''.
\end{aligned}$$

$$u\frac{\partial u}{\partial x} = -\frac{1}{2}y\frac{U_\infty^{\frac{5}{2}}}{\nu_f^{\frac{1}{2}}x^{\frac{3}{2}}}f''f'. \tag{3.19}$$

$$v\frac{\partial u}{\partial y} = -\frac{1}{2}\frac{U_\infty^2}{x}ff'' + \frac{1}{2}y\frac{U_\infty^{\frac{5}{2}}}{x^{\frac{3}{2}}\nu_f^{\frac{1}{2}}}f'f''. \tag{3.20}$$

Now

$$\frac{\partial^2 u}{\partial y^2} = \frac{\partial}{\partial y}\left(\frac{\partial u}{\partial y}\right),$$

using $\frac{\partial u}{\partial y}$ we get

$$\frac{\partial^2 u}{\partial y^2} = \frac{U_\infty^{\frac{3}{2}}}{x^{\frac{1}{2}}\nu_f^{\frac{1}{2}}}\left(\frac{\partial f''}{\partial \eta}\frac{\partial \eta}{\partial y}\right),$$

$$\frac{\partial^2 u}{\partial y^2} = \frac{U_\infty^2}{x\nu_f}f'''. \tag{3.21}$$

Using Eq. (3.19) to Eq. (3.21) in Eq. (3.2) we get

$$-\frac{1}{2}y\frac{U_\infty^{\frac{5}{2}}}{\nu_f^{\frac{1}{2}}x^{\frac{3}{2}}}f''f' - \frac{1}{2}\frac{U_\infty^2}{x}ff'' + \frac{1}{2}y\frac{U_\infty^{\frac{5}{2}}}{x^{\frac{3}{2}}\nu_f^{\frac{1}{2}}}f'f'' = \frac{\mu_f}{(1-\phi)^{2.5}\left[(1-\phi)\rho_f + \phi\rho_s\right]}\left[\frac{U_\infty^2}{x\nu_f}f'''\right],$$

$$\begin{aligned}
-\frac{1}{2}\frac{U_\infty^2}{x}ff'' &= \frac{\mu_f}{(1-\phi)^{2.5}\left[\rho_f[(1-\phi)+\phi\frac{\rho_s}{\rho_f}]\right]}\left[\frac{U_\infty^2}{x\nu_f}f'''\right], \\
\implies \frac{\mu_f}{\rho_f}.\frac{1}{(1-\phi)^{2.5}\left[(1-\phi)+\phi\frac{\rho_s}{\rho_f}\right]}\frac{U_\infty^2}{x\nu_f}f''' + \frac{1}{2}\frac{U_\infty^2}{x}ff'' &= 0, \\
\implies \frac{U_\infty^2}{x}\left[\frac{\mu_f}{\rho_f}m_0\frac{f'''}{\nu_f} + \frac{1}{2}ff''\right] &= 0, \\
\implies \frac{\mu_f}{\rho_f}\frac{\rho_f}{\mu_f}m_0 f''' + \frac{1}{2}ff'' &= 0.
\end{aligned}$$

The dimensionless form of Eq. (3.2) is:

$$m_0 f''' + \frac{1}{2}ff'' = 0. \tag{3.22}$$

The conversion of Eq. (3.3) into dimensionless form has been described, below using similarity variables,

$$\theta(\eta) = \frac{T - T_\infty}{T_w - T_\infty},$$

and

$$T = \theta(T_w - T_\infty) + T_\infty.$$

$$\begin{aligned}
\frac{\partial T}{\partial x} &= \frac{\partial}{\partial x}\left(\theta(\eta)(T_w - T_\infty) + T_\infty\right), \\
&= (T_w - T_\infty)\frac{\partial \theta}{\partial \eta}\frac{\partial \eta}{\partial x}, \\
&= (T_w - T_\infty)\theta' - \frac{1}{2}y\left(\frac{U_\infty}{\nu_f}\right)^{\frac{1}{2}} x^{\frac{-3}{2}}.
\end{aligned}$$

$$u\frac{\partial T}{\partial x} = -\frac{1}{2}y\frac{U_\infty^{\frac{3}{2}}}{\nu_f^{\frac{1}{2}}}x^{\frac{-3}{2}}(T_w - T_\infty)f'\theta'. \tag{3.23}$$

Next, differentiating $'T'$ with respect to $'y'$

$$\begin{aligned}
\frac{\partial T}{\partial y} &= \frac{\partial}{\partial y}\left(\theta(\eta)(T_w - T_\infty) + T_\infty\right), \\
&= (T_w - T_\infty)\frac{\partial \theta}{\partial \eta}\frac{\partial \eta}{\partial y}, \\
\frac{\partial T}{\partial y} &= (T_w - T_\infty)\theta'\left(\frac{U_\infty}{x\nu_f}\right)^{\frac{1}{2}}. \\
v\frac{\partial T}{\partial y} &= -\frac{1}{2}(T_w - T_\infty)\frac{U_\infty}{x}f\theta' + \frac{1}{2}y\frac{U_\infty^{\frac{3}{2}}(T_w - T_\infty)}{x^{\frac{3}{2}}\nu_f^{\frac{1}{2}}}\theta' f'. \qquad (3.24) \\
\frac{\partial^2 T}{\partial y^2} &= \frac{\partial}{\partial y}\left(\frac{\partial T}{\partial y}\right), \\
&= (T_w - T_\infty)\left(\frac{U_\infty}{x\nu_f}\right)^{\frac{1}{2}}\frac{\partial \theta'}{\partial \eta}\frac{\partial \eta}{\partial y}, \\
\frac{\partial^2 T}{\partial y^2} &= (T_w - T_\infty)\left(\frac{U_\infty}{x\nu_f}\right)\theta' \qquad (3.25) \\
\left(\frac{\partial u}{\partial y}\right)^2 &= \left(U_\infty^{\frac{3}{2}}\left(\frac{1}{x\nu_f}\right)^{\frac{1}{2}} f''\right)^2 \\
\left(\frac{\partial u}{\partial y}\right)^2 &= \frac{U_\infty^3}{x\nu_f}f''^2. \qquad (3.26) \\
T - T_\infty &= \theta(T_w - T_\infty). \qquad (3.27)
\end{aligned}$$

Radiative heat flux $q_r$ is given as:

$$q_r = -\frac{4\sigma}{3k^*}\frac{\partial T^4}{\partial y}$$

$$\frac{\partial q_r}{\partial y} = \frac{\partial}{\partial y}\left(-\frac{4\sigma}{3k^*}\frac{\partial T^4}{\partial y}\right). \tag{3.28}$$

$$T^4 \approx 4T_\infty^3 T - 3T_\infty^4,$$

$$T^4 \approx 4T_\infty^3 \left(\theta(T_w - T_\infty)\right) - 3T_\infty^4.$$

$$\begin{aligned}\frac{\partial T^4}{\partial y} &= 4T_\infty^3(T_w - T_\infty)\frac{\partial \theta}{\partial \eta}\frac{\partial \eta}{\partial y},\\ \frac{\partial T^4}{\partial y} &= 4T_\infty^3(T_w - T_\infty)\theta'\left(\frac{U_\infty}{x\nu_f}\right)^{\frac{1}{2}}.\end{aligned} \tag{3.29}$$

Putting the value of $\frac{\partial T^4}{\partial y}$ in Eq. (3.28)

$$\begin{aligned}\frac{\partial q_r}{\partial y} &= -\frac{4\sigma}{3k^*}\frac{\partial}{\partial y}\left[4T_\infty^3(T_w - T_\infty)\theta'\left(\frac{U_\infty}{x\nu_f}\right)^{\frac{1}{2}}\right],\\ &= -\frac{16\sigma T_\infty^3(T_w - T_\infty)}{3k^*}\left(\frac{U_\infty}{x\nu_f}\right)^{\frac{1}{2}}\frac{\partial \theta'}{\partial \eta}\frac{\partial \eta}{\partial y},\\ \frac{\partial q_r}{\partial y} &= -\frac{16\sigma T_\infty^3(T_w - T_\infty)}{3k^*}\left(\frac{U_\infty}{x\nu_f}\right)\theta''.\end{aligned} \tag{3.30}$$

Using above Eq. (3.23) to Eq. (3.30) in Eq.(3.3), we get

$$\begin{aligned}-\frac{1}{2}(T_w - T_\infty)\frac{U_\infty}{x}f\theta' = \alpha_{nf}(T_w - T_\infty)\frac{U_\infty}{x\nu_f}\theta'' + \frac{\mu_{nf}}{(\rho C_p)_{nf}}\left(\frac{U_\infty^3}{x\nu_f}f''^2\right) +\\ \frac{Q_0\theta(T_w - T_\infty)}{\rho C_p)_{nf}} + \frac{16\sigma T_\infty^3(T_w - T_\infty)}{3(\rho C_p)_{nf}k^*}\frac{U_\infty}{x\nu_f}\theta''.\end{aligned}$$

Multiplying the above equation with $\frac{x\nu_f}{U_\infty(T_w - T_\infty)}$

$$\frac{\nu_f}{2}f\theta' + \alpha_{nf}\theta'' + \frac{16\sigma T_\infty^3}{3k^*(\rho C_p)_{nf}}\theta'' + \frac{\mu_{nf}U_\infty^2}{(\rho C_p)_{nf}(T_w - T_\infty)}f''^2 + \frac{xQ_0\theta\nu_f}{U_\infty(\rho C_p)_{nf}} = 0.$$

Putting values of $\alpha_{nf}$, $\mu_{nf}$ and $(\rho C_p)_{nf}$ (3.8)-(3.11), we get

$$\begin{aligned}&\frac{k_{nf}}{(\rho C_p)_f\left[(1-\phi) + \phi\frac{(\rho C_p)_s}{(\rho C_p)_f}\right]}\theta'' + \frac{16\sigma T_\infty^3}{3k^*(\rho C_p)_f\left[(1-\phi) + \phi\frac{(\rho C_p)_s}{(\rho C_p)_f}\right]} + \frac{\nu_f}{2}f\theta'\\ &+\frac{\mu_f U_\infty^2 f''^2}{(T_w - T_\infty)(1-\phi)^{2.5}(\rho C_p)_f\left[(1-\phi) + \phi\frac{(\rho C_p)_s}{(\rho C_p)_f}\right]} + \frac{\nu_f x Q_0}{U_\infty(\rho C_p)_f\left[(1-\phi) + \phi\frac{(\rho C_p)_s}{(\rho C_p)_f}\right]} = 0.\end{aligned}$$

Multiplying the above equation with $\frac{(\rho C_p)_f}{k_f}$,

$$\frac{k_{nf}}{k_f\left[(1-\phi)+\phi\frac{(\rho C_p)_s}{(\rho C_p)_f}\right]}\theta''+\frac{4.4\sigma T_\infty^3}{k_f 3k^*\left[(1-\phi)+\phi\frac{(\rho C_p)_s}{(\rho C_p)_f}\right]}+\left(\frac{(\rho C_p)_f}{k_f}\right)\frac{\nu_f}{2}f\theta'$$
$$+\frac{\mu_f U_\infty^2 f''^2}{(T_w-T_\infty)k_f(1-\phi)^{2.5}\left[(1-\phi)+\phi\frac{(\rho C_p)_s}{(\rho C_p)_f}\right]}+\frac{\nu_f x Q_0}{k_f U_\infty\left[(1-\phi)+\phi\frac{(\rho C_p)_s}{(\rho C_p)_f}\right]}=0.$$

The dimensionless form of Eq. (3.3) becomes

$$m_1\theta''+\frac{4}{3N}\frac{k_f}{k_{nf}}m_1\theta''+\frac{Pr_f}{2}f\theta'+m_2Pr_fEc(f'')^2+m_3Pr_f\gamma\theta=0. \tag{3.31}$$

Now discussing the procedure for conversion of boundary conditions into dimensionless form:

$$\begin{aligned}
&u=\lambda_1\left(\frac{\partial u}{\partial y}\right)\quad \text{at}\quad y=0,\\
&U_\infty f'(\eta)=\lambda_1\frac{U_\infty^{\frac{3}{2}}}{x^{\frac{1}{2}}\nu_f^{\frac{1}{2}}}f'',\\
&f'(\eta)=\lambda_1\left(\frac{U_\infty}{x\nu_f}\right)^{\frac{1}{2}}f'',\\
&f'(\eta)=\lambda f''\quad \text{at}\quad \eta=0. \qquad (3.32)\\
&v=-v_w\quad \text{at}\quad y=0,\\
&\frac{-1}{2}\left(\frac{U_\infty\nu_f}{x}\right)^{\frac{1}{2}}f+\frac{1}{2}y\frac{U_\infty}{x}f'=-v_w,\\
&f=f_w\quad \text{at}\quad \eta=0. \qquad (3.33)\\
&T=T_w+\beta_1\left(\frac{\partial T}{\partial y}\right)\quad \text{at}\quad y=0,\\
&\theta(T_w-T_\infty)+T_\infty=T_w+\beta_1\left((T_w-T_\infty)\theta'\left(\frac{U_\infty}{x\nu_f}\right)^{\frac{1}{2}}\right),\\
&\theta=-\frac{T_\infty}{T_w-T_\infty}+\frac{T_w}{T_w-T_\infty}+\beta_1\left(\frac{U_\infty}{x\nu_f}\right)^{\frac{1}{2}}\theta'\quad\frac{(T_w-T_\infty)}{(T_w-T_\infty)},\\
&\theta=1+\beta_1\left(\frac{U_\infty}{x\nu_f}\right)^{\frac{1}{2}}\theta',\\
&\theta=1+\beta\theta'\quad \text{at}\quad \eta=0. \qquad (3.34)
\end{aligned}$$

$$
\begin{aligned}
&U_\infty f' \to U_\infty \quad \text{as} \quad y \to \infty,\\
&U_\infty f' \to U_\infty \quad \text{as} \quad y \to \infty,\\
&f' \to 1 \quad \text{as} \quad \eta \to \infty. \qquad (3.35)\\
&T \to T_\infty \quad \text{as} \quad y \to \infty,\\
&\theta(T_w - T_\infty) + T_\infty \to T_\infty,\\
&\theta(T_w - T_\infty) \to 0,\\
&\theta \to 0 \quad \text{as} \quad \eta \to \infty. \qquad (3.36)
\end{aligned}
$$

The dimensionless form of the Eqs. (3.2) , (3.3) are:

$$m_0 f''' + \frac{1}{2} f'' f = 0, \tag{3.37}$$

$$m_1\theta'' + \frac{4}{3N}\frac{k_f}{k_{nf}} m_1\theta'' + \frac{Pr_f}{2} f\theta' + m_2 Pr_f Ec (f'')^2 + m_3 Pr_f \gamma\theta = 0. \tag{3.38}$$

The corresponding boundary conditions become:

$$
\left.
\begin{aligned}
&f'(\eta) = \lambda f'', \quad f = f_w, \quad \theta = 1 + \beta\theta' \quad \text{at} \quad \eta = 0,\\
&f' \to 1, \quad \theta \to 0 \quad \text{as} \quad \eta \to \infty.
\end{aligned}
\right\} \tag{3.39}
$$

In above Eq. (3.37) to Eq. (3.39), $Ec$, $N$, $\gamma$, $\lambda$, $\beta$, $f_w$ represent Eckert number, radiation parameter, heat generation/absorption, velocity slip parameter, thermal slip parameter and prime represents derivative w.r.t $\eta$. Where, these parameter are formulated as.

$$
\begin{aligned}
&m_0 = \frac{1}{(1-\phi)^{2.5}\left[(1-\phi) + \phi\rho_s/\rho_f\right]}, \quad m_1 = \frac{k_{nf}/k_f}{(1-\phi) + \phi(\rho C_p)_s/(\rho C_p)_f}\\
&m_2 = \frac{1}{(1-\phi)^{2.5}\left[(1-\phi) + \phi(\rho C_p)_s/(\rho C_p)_f\right]}, \quad m_3 = \frac{1}{(1-\phi) + \phi(\rho C_p)_s/(\rho C_p)_f},\\
&\gamma = \frac{Q_0 x}{U_\infty(\rho C_p)_f}, \ \beta = \beta_1\left(\frac{U_\infty}{x\nu_f}\right)^{\frac{1}{2}}, \ N = \frac{k_f k^*}{4\sigma T_\infty^3},\\
&Ec = \frac{U_\infty^2}{(C_p)_f(T_w - T_\infty)}, \quad Pr_f = \frac{\nu_f}{\alpha_f}.\\
&\lambda = \lambda_1\left(\frac{U_\infty}{x\nu_f}\right)^{\frac{1}{2}}, \quad f_w = 2\left(\frac{x}{\nu_f U_\infty}\right)^{\frac{1}{2}} v_w
\end{aligned}
$$

### 3.2.2 Physical Quantities of Interest

Mathematical forms of Nusselt number and local skin-friction coefficient are.

$$C_{fx} = \frac{\tau_w}{\rho_f U_\infty^2}, \quad Nu_x = \frac{x q_w}{k_f \left(T_w - T_\infty\right)}. \tag{3.40}$$

In the above equation $\tau_w$ represents the shear stress and $q_w$ represents the heat flux, defined as:

$$\left.\begin{aligned} \tau_w &= \mu_{nf} \left(\frac{\partial u}{\partial y}\right)_{y=0}, \\ q_w &= -\left(k_{nf} + \frac{16\sigma T_\infty^3}{3k^*}\right)\left(\frac{\partial T}{\partial y}\right)_{y=0}. \end{aligned}\right\} \tag{3.41}$$

The dimensionless form of Eq. (3.41) has discussed below:

$$\begin{aligned} \tau_w &= \mu_{nf} \left(\frac{\partial u}{\partial y}\right)_{y=0}, \\ u &= (U_\infty \nu_f x)^{\frac{1}{2}} \quad \frac{\partial f}{\partial \eta} \quad \frac{\partial \eta}{\partial y}, \\ u &= (U_\infty \nu_f x)^{\frac{1}{2}} f' \left(\frac{U_\infty}{\nu_f x}\right)^{\frac{1}{2}}, \\ u &= f' U_\infty. \\ \tau_w &= \mu_{nf} \left(\frac{\partial}{\partial y}(f' U_\infty)\right) \\ \tau_w &= \mu_{nf} U_\infty f'' \left(\frac{U_\infty}{\nu_f x}\right)^{\frac{1}{2}} \end{aligned} \tag{3.42}$$

$$\begin{aligned} q_w &= -\left(k_{nf} + \frac{16\sigma T_\infty^3}{3k^*}\right)\left(\frac{\partial T}{\partial y}\right)_{y=0}, \\ T &= \theta(\eta)\left(T_w - T_\infty\right) + T_\infty, \\ \frac{\partial T}{\partial y} &= \theta' \left(\frac{U_\infty}{\nu_f x}\right)^{\frac{1}{2}} \left(T_w - T_\infty\right), \end{aligned}$$

$$q_w = -\left(k_{nf} + \frac{16\sigma T_\infty^3}{3k^*}\right)\theta' \left(\frac{U_\infty}{\nu_f x}\right)^{\frac{1}{2}} \left(T_w - T_\infty\right). \tag{3.43}$$

Using Eqs. (3.42), (3.43) in Eq. (3.40)

$$\begin{aligned}
C_{fx} &= \frac{\tau_w}{\rho_f U_\infty^2}, \\
&= \frac{\mu_{nf} U_\infty f'' U_\infty^{\frac{1}{2}}}{\rho_f U_\infty^2 (\nu_f x)^{\frac{1}{2}}}, \\
C_{fx} &= \frac{\mu_{nf}}{\rho_f} \left(\frac{1}{\nu_f x U_\infty}\right)^{\frac{1}{2}} f'' \quad \frac{\mu_f}{\mu_f}, \\
&= \frac{\nu_f \mu_{nf}}{\mu_f} \quad \frac{1}{(\nu_f x U_\infty)^{\frac{1}{2}}} f''(0) \qquad\qquad \because \nu_f = \frac{\mu_f}{\rho_f}, \\
&= \frac{\mu_{nf}}{\mu_f} \quad \frac{\nu_f^{\frac{1}{2}}}{(x U_\infty)^{\frac{1}{2}}} f''(0), \\
&= \frac{\mu_{nf}}{\mu_f} \frac{1}{(Re_x)^{\frac{1}{2}}} f''(0),
\end{aligned}$$

$$C_{fx} Re_x^{\frac{1}{2}} = \frac{\mu_{nf}}{\mu_f} f''(0). \tag{3.44}$$

$$\begin{aligned}
Nu_x &= \frac{x q_w}{k_f (T_w - T_\infty)}, \\
&= -x \left(\frac{3k_{nf}k^* + 16\sigma T_\infty^3}{3k^*}\right) \left(\frac{U_\infty}{\nu_{fx}}\right)^{\frac{1}{2}} \theta'(T_w - T_\infty)/k_f(T_w - T_\infty), \\
&= -x \frac{(3k_{nf}k^* + 16\sigma T_\infty^3) \quad U_\infty^{\frac{1}{2}} \theta'}{3k_f k^* (\nu_f x)^{\frac{1}{2}}}, \\
&= \frac{x^{\frac{1}{2}} U_\infty^{\frac{1}{2}}}{\nu_f^{\frac{1}{2}}} \quad -\frac{k_{nf}}{k_f}\theta' - \frac{4\sigma T_\infty^3}{3k_f k^*} \quad \frac{4x^{\frac{1}{2}} U_\infty^{\frac{1}{2}} \theta'}{\nu_f^{\frac{1}{2}}}, \\
&= \frac{x^{\frac{1}{2}} U_\infty^{\frac{1}{2}}}{\nu_f^{\frac{1}{2}}} \left[-\frac{k_{nf}}{k_f} - \frac{4}{3N}\right] \theta'(0), \\
&= Re_x^{\frac{1}{2}} - \left[\frac{k_{nf}}{k_f} + \frac{4}{3N}\right] \theta'(0),
\end{aligned}$$

$$Nu_x Re_x^{\frac{-1}{2}} = -\left[\frac{k_{nf}}{k_f} + \frac{4}{3N}\right] \theta'(0), \tag{3.45}$$

where Reynolds number is:

$$Re_x = \frac{U_\infty x}{\nu_f}.$$

## 3.3 Solution Methodology

In order to solve the system of ordinary differential equations (3.37) and (3.38), the shooting method has been used together with RK4 method.

$$m_0 f''' + \frac{1}{2} f'' f = 0. \tag{3.46}$$

$$m_1 \theta'' + \frac{4}{3N} \frac{k_f}{k_{nf}} m_1 \theta'' + \frac{Pr_f}{2} f\theta' + m_2 Pr_f Ec (f'')^2 + m_3 Pr_f \gamma \theta = 0. \tag{3.47}$$

subject to the boundary condition:

$$\left.\begin{aligned} &f'(\eta) = \lambda f'', \quad f = f_w, \quad \theta = 1 + \beta\theta' \quad \text{at} \quad \eta = 0, \\ &f' \to 1, \quad \theta \to 0 \quad \text{as} \quad \eta \to \infty, \end{aligned}\right\} \tag{3.48}$$

First, Eq. (3.37) is numerically solved and then calculated results for $f$, $f'$ and $f''$ are used in Eq. (3.38). By using shooting method Eq. (3.37) is solved independently as the Eq. (3.37) is independent of $\theta$. To apply shooting method, we convert the BVP into IVP by assuming the missing initial condition. In order to solve Eq. (3.37) following notation has been introduced:

$$f = y_1, \quad f' = y_2, \quad f'' = y_3. \tag{3.49}$$

Eq. (3.37) is converted into first order ODEs

$$\left.\begin{aligned} y_1' &= y_2, & y_1(0) &= 1, \\ y_2' &= y_3, & y_2(0) &= 0.5s, \\ y_3' &= -\frac{1}{2m_0} y_1 y_3, & y_3(0) &= s. \end{aligned}\right\} \tag{3.50}$$

where $s$ is the missing initial condition. RK4 method has been used to solve the above initial value problem.

As the numerical computations can not be performed on an unbounded domain, therefore the domain of the above problem has been taken as $[0, \eta_\infty]$ instead of $[0, \infty)$, where $\eta_\infty$ is an appropriate finite positive real number with chosen initial

guess $s$ such that:

$$F(s) = y_2(\eta_\infty, s) - 1 = 0. \tag{3.51}$$

To solve the above algebraic Eq. (3.51), we use the Newtons method which has the following iterative procedure:

$$s^{n+1} = s^n - \frac{(y_2(\eta_\infty, s)) - 1}{\left(\frac{\partial y_2(\eta_\infty, s)}{\partial s}\right)}. \tag{3.52}$$

We further introduce the following notations, in order to obtain the derivative $\frac{\partial y_2}{\partial s}$

$$\frac{\partial y_1}{\partial s} = y_4, \quad \frac{\partial y_2}{\partial s} = y_5, \quad \frac{\partial y_3}{\partial s} = y_6.$$

As a result of these new notations, the Newtons iterative scheme gets the form

$$s^{n+1} = s^n - \frac{(y_2(\eta_\infty)) - 1}{y_5\left(\eta_\infty\right)}.$$

Now differentiate the above system of three first order ODEs (3.50) with respect to $s$, we get three more ODEs. Writing all these six ODEs together, we have the following initial value problem (IVP).

$$\begin{aligned}
y_1' &= y_2, & y_1(0) &= 1,\\
y_2' &= y_3, & y_2(0) &= 0.5s,\\
y_3' &= -\frac{1}{2m_0} y_1 y_3, & y_3(0) &= s.\\
y_4' &= y_5', & y_4(0) &= 0,\\
y_5' &= y_6, & y_5(0) &= 0.5,\\
y_6' &= \frac{1}{2m_0}\left[y_3 y_4 + y_1 y_6\right], & y_6(0) &= 1.
\end{aligned}$$

The threshold for the shooting method is defined as follows.

$$\mid y_2\left(\eta_\infty\right) - 1 \mid < \varepsilon,$$

where $\varepsilon$ is taken as $10^{-6}$. The method has been repeated until this criteria fulfilled.

Now solving Eq. (3.38) in the same way as was done for equation Eq. (3.37) numerically along with boundary conditions (3.39). Here missing initial condition $\theta'(0)$ is denoted by $l$. Different notations have been used which are given below

$$\theta = z_1, \quad \theta' = z_2,$$

using these notations, we get a system of first order ODEs which are given below

$$\left.\begin{aligned} z_1' &= z_2, & z_1(0) &= 1 + \beta l, \\ z_2' &= -\frac{1}{m_1\left(1+\frac{4}{3N}\frac{k_f}{k_{nf}}\right)}\frac{Pr_f}{2}y_1 z_2 + m_2 Pr_f E_c (y_3)^2 & & \\ &\quad + m_3 Pr_f \gamma z_1, & z_2(0) &= l, \end{aligned}\right\} \tag{3.53}$$

The above initial value problem can be solved by using RK4 method, the missing condition is $l$ which can be defined as

$$F(l) = z_1\left(\eta_\infty, l\right) = 0, \tag{3.54}$$

The above equation can be solve by using Newton method. Newton method is given by the following iteration

$$l^{n+1} = l^n - \frac{(z_1(\eta_\infty, l)) - 0}{\left(\frac{\partial z_1(\eta_\infty, l)}{\partial l}\right)},$$

we further introduce the following notations, in order to obtain the $\frac{\partial z_1}{\partial l}$

$$\frac{\partial z_1}{\partial l} = z_3, \frac{\partial z_2}{\partial l} = z_4$$

As a result of these new notations, the Newtons iterative scheme gets the form

$$\Rightarrow l^{n+1} = l^n - \frac{(z_1(\eta_\infty, l)) - 0}{z_3\left(\eta_\infty, l\right)}. \tag{3.55}$$

Now differentiate the above system of two first order ODEs (3.53) with respect to $l$, we get another four ODEs. Writing all these four ODEs together, we have the

following initial value problem (IVP).

$$
\begin{aligned}
z_1' &= z_2, && z_1(0) = 1 + \beta l,\\
z_2' &= -\frac{1}{m_1\left(1+\frac{4}{3N}\frac{k_f}{k_{nf}}\right)}\frac{Pr_f}{2}y_1 z_2 + m_2 Pr_f Ec (y_3)^2 + m_3 Pr_f \gamma z_1, && z_2(0) = l,\\
z_3' &= z_4, && z_3(0) = \beta,\\
z_4' &= -\frac{1}{m_1\left(1+\frac{4}{3N}\frac{k_f}{k_{nf}}\right)}\frac{Pr_f}{2}y_1 z_4 + m_3 Pr_f \gamma z_3, && z_4(0) = 1.
\end{aligned}
$$

stopping criteria for the iterative process is defined as

$$| z_1(\eta_\infty) - 0 | < \varepsilon,$$

where $\varepsilon$ is taken as $10^{-6}$. The method has been repeated until this criteria would fulfilled.

## 3.4 Results and Discussion

The main objective of this section is to study the effects of different parameters on velocity profile, temperature profile, skin-friction and Nusselt number. For the conformation of the results, the present results are compared with results of Maleki et al. [52]

### 3.4.1 Skin-friction Cofficent and Nusselt Number

In Table 3.2 effects of different parameters $f_w$, $\lambda$, $\phi$ (permeability parameter, slip velocity and nanoparticle volume fraction) are shown for values of skin-friction coefficient. The value of skin-friction cofficent $\left(\frac{\mu_{nf}}{\mu_f} f''(0)\right)$ changes by changing the physical parameters. It can be noted that in case of suction and injection increasing the nanoparticle volume fraction keeping slip velocity constant, the value of skin-friction on MWCNTs increases. Also it can be seen that skin-friction shows decreasing behavior for higher values of $\lambda$.

TABLE 3.2: Variation of $C_{fx}Re_x^{\frac{1}{2}}$ under impact of various parameters

| $C_{fx}Re_x^{\frac{1}{2}}$ | | | | |
|---|---|---|---|---|
| $f_w$ | $\phi$ | $\lambda$ | **Present** | **Maleki et al.** [52] |
| 0.5 | 0 | 0.5 | 0.449282 | 0.4493 |
| 0.5 | 0.1 | 0.5 | 0.5215231 | 0.5215 |
| 0.5 | 0.2 | 0.5 | 0.6115769 | 0.6116 |
| -0.5 | 0 | 0.5 | 0.1806543 | 0.1806 |
| -0.5 | 0.1 | 0.5 | 0.2273066 | 0.2272 |
| -0.5 | 0.2 | 0.5 | 0.2904550 | 0.2898 |
| -1 | 0.5 | 0.1 | 0.0831156 | 0.0806 |
| -0.5 | 0.1 | 0.5 | 0.2273066 | 0.2272 |
| 0 | 0.1 | 0.5 | 0.3780700 | 0.3781 |
| 0.5 | 0.1 | 0.5 | 0.5215231 | 0.5215 |
| 1 | 0.1 | 0.5 | 0.6539398 | 0.6539 |
| 0.5 | 0.1 | 0 | 0.5914861 | 0.5915 |
| 0.5 | 0.1 | 0.1 | 0.5788014 | 0.5788 |
| 0.5 | 0.1 | 0.5 | 0.5215231 | 0.5215 |
| 0.5 | 0.1 | 1 | 0.4517784 | 0.4518 |

Table 3.3 is organized to demonstrate the values of $Nu_xRe_x^{\frac{-1}{2}}$ for nanofluid MWCNTs using different parameters $Ec$, $N$, $\gamma$, $\beta$, $\phi$, $\lambda$ and $f_w$.

It can be clearly seen through table that boosting the values of $N$, $\gamma$, $Ec$ and $\phi$ (radiation parameter, heat generation, Eckert number and nanoparticle volume fraction) the effect of Nusselt number for suction and impermeable plate on MWCNTs decreases, since the mechanism increases the fluid temperature near to the surface and consequently, temperature gradient at the surface shows a drop as a result of decreasing the surface heat transfer rate. Also it can be seen that by increasing the velocity slip parameter the Nusselt number will also boost for suction. While opposite behavior can be seen for injection.

TABLE 3.3: Variation of $Nu_x Re_x^{\frac{-1}{2}}$ by altering different parameters

| | | | | | | | $Nu_x Re_x^{\frac{-1}{2}}$ | |
|---|---|---|---|---|---|---|---|---|
| $f_w$ | $\phi$ | $\lambda$ | $\beta$ | $\gamma$ | $Ec$ | $N$ | **Present** | **Maleki et al.** [52] |
| -1 | 0.1 | 0.1 | 0.1 | 0.1 | 0.1 | 1 | -0.918368368 | -0.9424 |
| -0.5 | 0.1 | 0.1 | 0.1 | 0.1 | 0.1 | 1 | -0.311534129 | -0.3149 |
| 0 | 0.1 | 0.1 | 0.1 | 0.1 | 0.1 | 1 | 0.682479546 | 0.6792 |
| 0.5 | 0.1 | 0.1 | 0.1 | 0.1 | 0.1 | 1 | 1.784429627 | 1.7810 |
| 1 | 0.1 | 0.1 | 0.1 | 0.1 | 0.1 | 1 | 2.896644552 | 2.8932 |
| 0.5 | 0 | 0.1 | 0.1 | 0.2 | 0.2 | 2 | 0.910678673 | 0.9059 |
| 0.5 | 0.1 | 0.1 | 0.1 | 0.2 | 0.2 | 2 | 0.839024988 | 0.8335 |
| 0.5 | 0.2 | 0.1 | 0.1 | 0.2 | 0.2 | 2 | 0.662940088 | 0.6570 |
| 0.5 | 0 | 0.1 | 0.1 | 0.01 | 0.01 | 1 | 2.063844832 | 2.0619 |
| 0.5 | 0.1 | 0.1 | 0.1 | 0.01 | 0.01 | 1 | 2.402482301 | 2.4004 |
| 0.5 | 0.2 | 0.1 | 0.1 | 0.01 | 0.01 | 1 | 2.687888856 | 2.6858 |
| 0.5 | 0.1 | 0 | 0.1 | 0.1 | 0.1 | 1 | 1.694899974 | 1.6916 |
| 0.5 | 0.1 | 0.5 | 0.1 | 0.1 | 0.1 | 1 | 2.070046109 | 2.0662 |
| 0.5 | 0.1 | 1 | 0.1 | 0.1 | 0.1 | 1 | 2.306386995 | 2.3022 |
| 0.5 | 0.1 | 0.1 | 0 | 0.1 | 0.1 | 1 | 1.874658755 | 1.8710 |
| 0.5 | 0.1 | 0.1 | 0.5 | 0.1 | 0.1 | 1 | 1.496347124 | 1.4938 |
| 0.5 | 0.1 | 0.1 | 1 | 0.1 | 0.1 | 1 | 1.245085268 | 1.2433 |
| 0.5 | 0.1 | 0.1 | 0.1 | -0.1 | 0.1 | 1 | 2.745716672 | 2.7438 |
| 0.5 | 0.1 | 0.1 | 0.1 | -0.05 | 0.1 | 1 | 2.536867424 | 2.5347 |
| 0.5 | 0.1 | 0.1 | 0.1 | 0 | 0.1 | 1 | 2.309828002 | 2.3073 |
| 0.5 | 0.1 | 0.1 | 0.1 | 0.05 | 0.1 | 1 | 2.060741576 | 2.0579 |
| 0.5 | 0.1 | 0.1 | 0.1 | 0.1 | 0.1 | 1 | 1.784429627 | 1.7810 |
| 0.5 | 0.1 | 0.1 | 0.1 | 0.1 | 0 | 1 | 1.957331206 | 1.9545 |
| 0.5 | 0.1 | 0.1 | 0.1 | 0.1 | 0.05 | 1 | 1.870880417 | 1.8678 |
| 0.5 | 0.1 | 0.1 | 0.1 | 0.1 | 0.1 | 1 | 1.784429627 | 1.7810 |
| 0.5 | 0.1 | 0.1 | 0.1 | 0.1 | 0.1 | 0.5 | 2.027758389 | 2.0242 |
| 0.5 | 0.1 | 0.1 | 0.1 | 0.1 | 0.1 | 1 | 1.784429627 | 1.7810 |
| 0.5 | 0.1 | 0.1 | 0.1 | 0.1 | 0.1 | 2 | 1.654866003 | 1.6516 |
| 0.5 | 0.1 | 0.1 | 0.1 | 0.1 | 0.1 | 3 | 1.610295743 | 1.6071 |

### 3.4.2 Impact of Nanoparticles Volume Fraction

In Figures 3.2 to 3.4 show the behavior of velocity profiles for the nanoparticles volume fraction, for suction, injection and impermeable plate ($f_w = 1$, $f_w = -1$, $f_w = 0$). In case of suction and impermeable plate, it is noticed that by increasing the nanoparticles volume fraction, the velocity profile decreases and increases the boundary layer thickness. Reason behind this behavior is that, if we increases the nanoparticles volume fraction effective viscosity will increase which provide more resistance to fluid particles. That causes a decrease in the velocity profile, whereas an opposite behavior can be seen in case of injection. Figures 3.5 to 3.7 illustrate the influence of nanoparticles volume fraction on temperature distribution. In case of impermeable plate ($f_w = 0$) and suction ($f_w = 1$) increasing the nanoparticles volume fraction leads to an increase in the temperature distribution. By increasing nanoparticles volume fraction thermal conductivity increases therefor temperature rise,. while for injection ($f_w = -1$) opposite behavior is observed. Also, thermal boundary layer rises by boosting the $\phi$ values in all cases. Moreover, in the case of injection, due to presence of heat generation radiation and viscous dissipation fluid temperature near the wall decreases and the inverse behavior is observed.

### 3.4.3 Impact of Permeability Parameter

In Figure 3.8 represents the effect of permeability parameter on velocity profile. It can be seen that during suction ($f_w > 0$) velocity profile increases because increase in suction parameter causes increase in flow rate. So it rises the velocity of fluid and the development of boundary layer thickness reduces by absorbing fluid particle through porous wall. Near the wall the impact of suction is diminished, hence boundary layer thickness reduces and velocity seems to increase. It can also be observed that the viscosity of fluid decrease which rise the velocity. While during injection ($f_w < 0$) boundary layer region rises, which shows that injection cause more fluid diffusion and make larger the boundary layer. In suction case, wall shear stress increases, whereas in injection case shear wall stress decreases.

Figure 3.9 describes the impact of permeability on temperature distribution, it is clearly noticed that boundary layer thickness reduces by increasing the suction parameter ($f_w > 0$) which increases the heat transfer rate. Or when raising the injection parameter ($f_w < 0$) boundary layer thickness seems increase. Moreover temperature profile decreases by increasing suction, injection parameter.

### 3.4.4 Impact of Velocity Slip Parameter

Figures 3.10 to 3.12 despite the behavior of velocity profile for the slip velocity parameter. In all three cases ($f_w = 1, f_w = 0, f_w = -1$), it is observed that, velocity profile increases by increasing the slip velocity parameter. The reason behind this behavior is that if we increase $\lambda$ it offers less resistance to fluid, because viscosity of fluid decreases thus velocity increases, and boundary layer thickness reduces. In case of suction ($f_w = 1$) the effect of slip velocity parameter is more than other two cases. Figures 3.13 to 3.15 indicate the relationship for different values of slip velocity parameter on temperature distribution. It is clearly seen from figures that in all three cases ($f_w = 1, f_w = 0, f_w = -1$) rising the value of slip velocity results to decrease in temperature distribution. This is mainly due to increasing $\lambda$ kinematic viscosity decreases, so fluid particle can easily move therefore temperature decreases. It is also noticed that in case of injection boundary layer thickness accelerates.

### 3.4.5 Impact of Eckert Number

Figures 3.16 to 3.18 demonstrate the effect of Eckert number on temperature distribution. As Eckert number specify the ratio of kinetic energy and enthalpy change of flow. It is inspected through figures that by rising the value of Eckert number temperature distribution rises. Physically, the kinetic energy of the fluid particles rises as $Ec$ assumes the larger values. Hence, the temperature of the fluid increased and therefore, the associated thermal boundary layer thickness is enhanced. If we increase $Ec$ number enthalpy change of flow decreases which tends

to increase the temperature of fluid, for all three cases ($f_w = 1, f_w = 0, f_w = -1$) for different value of Eckert number.

### 3.4.6 Impact of Heat Generation/Absorption

Effect of heat generation/absorption on temperature distribution can be seen in Figure 3.19 to 3.21. It is observed that for increasing value of $\gamma$ more heat is generated, because of this temperature distribution and thermal boundary layer thickness increases, for all three cases ($f_w = 1, f_w = 0, f_w = -1$). On other hand if the value of $\gamma$ decreases, the heat will be absorbed which causes decrease in temperature and boundary layer thickness.

### 3.4.7 Impact of Radiation Parameter

Figures 3.22 to 3.24 reveal the impact of radiation parameter on temperature profile. by increasing the radiation parameter, temperature profile and boundary layer thickness decreased, in case of suction and impermeable plate ($f_w = 1$,$f_w = 0$). As in a medium the intensity of electro-magnetic radiation decreases as StefanBoltzmann constant increases so temperature decreases. In case of injection ($f_w = -1$) by increasing the radiation parameter temperature increases, because it strengthens the fact that more heat is produced due to the radiation process for which the temperature profile is increases.

### 3.4.8 Impact of Thermal Slip Parameter

Figures 3.25 to 3.27 show the effect of thermal slip parameter on temperature distribution in case of suction and impermeable plate ($f_w = 1$,$f_w = 0$) it is noticed that temperature profile decreases for increasing value of thermal slip parameter because less heat is transfered from plate to the fluid, so temperature decreases. while reversed nature can be seen in case of injection ($f_w = -1$).

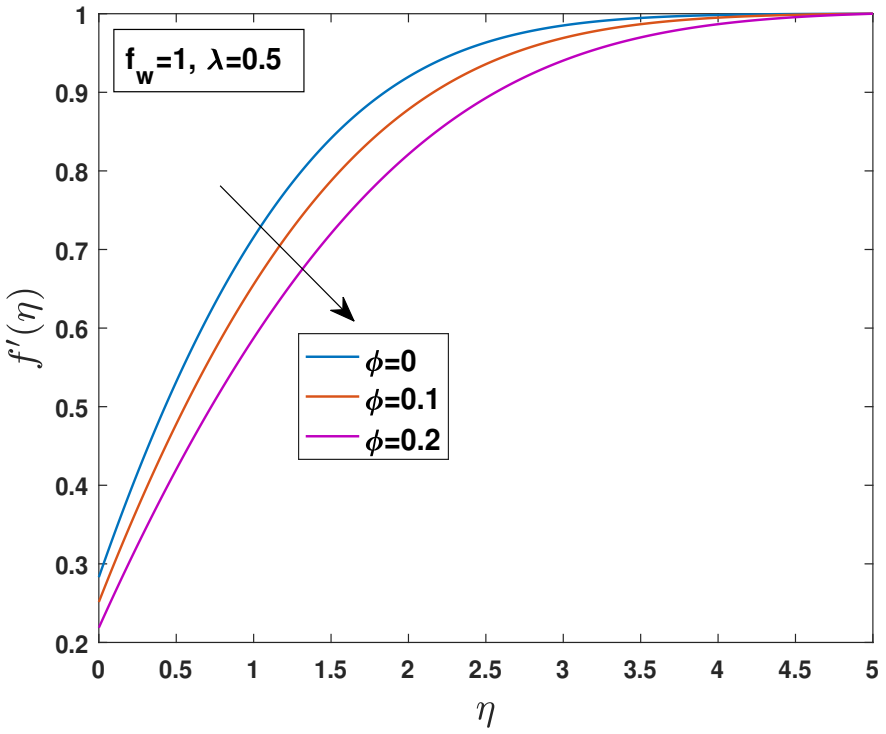


FIGURE 3.2: Effects of $\phi$ on velocity distribution for suction.

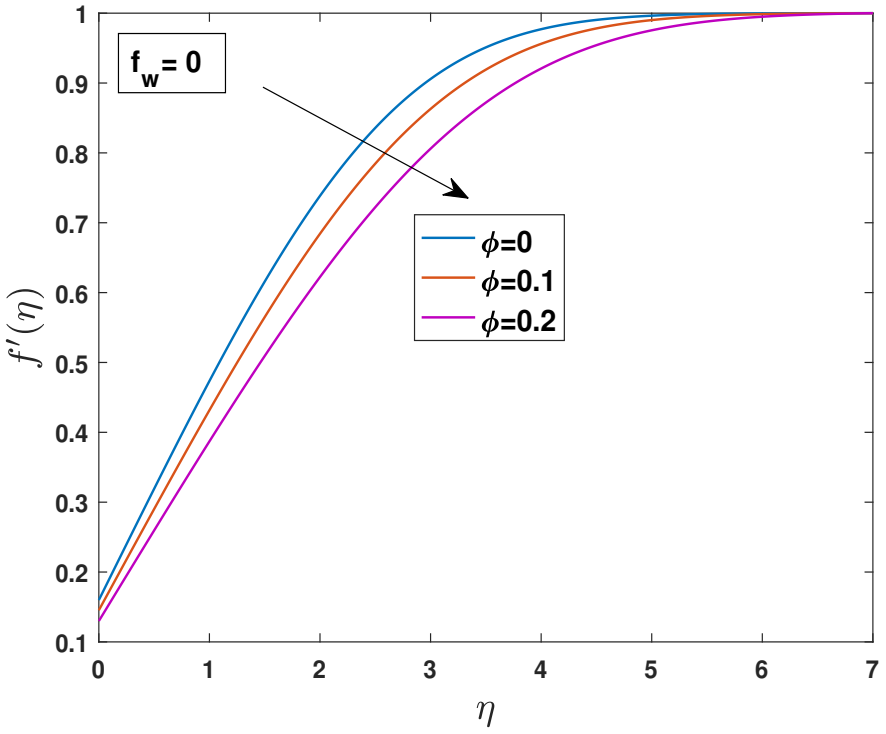


FIGURE 3.3: Effects of $\phi$ on velocity distribution for impermeable plate.

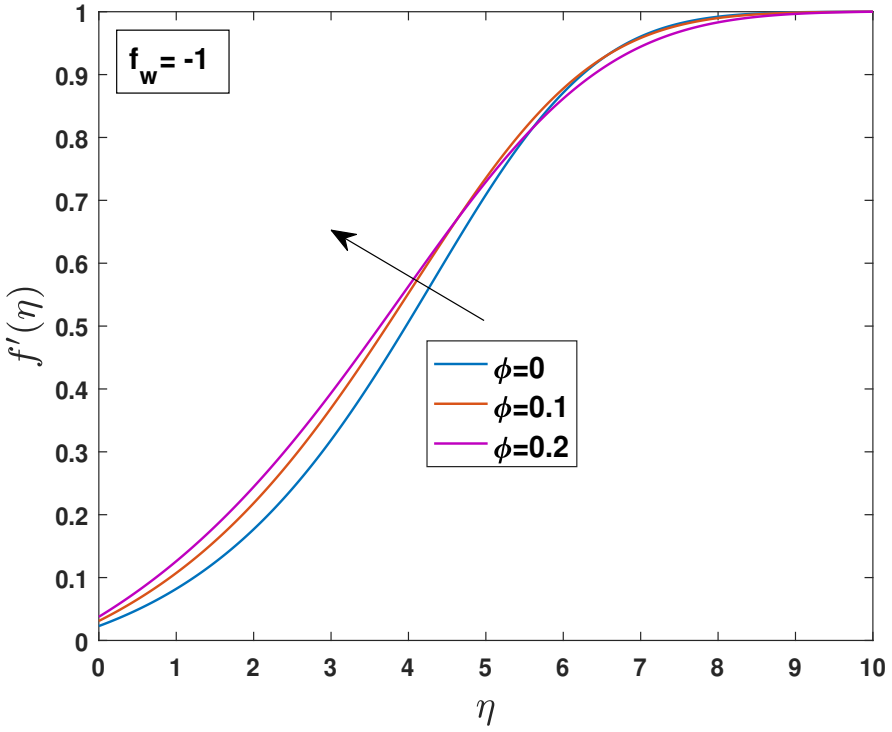


FIGURE 3.4: Effects of $\phi$ on velocity distribution for injection.

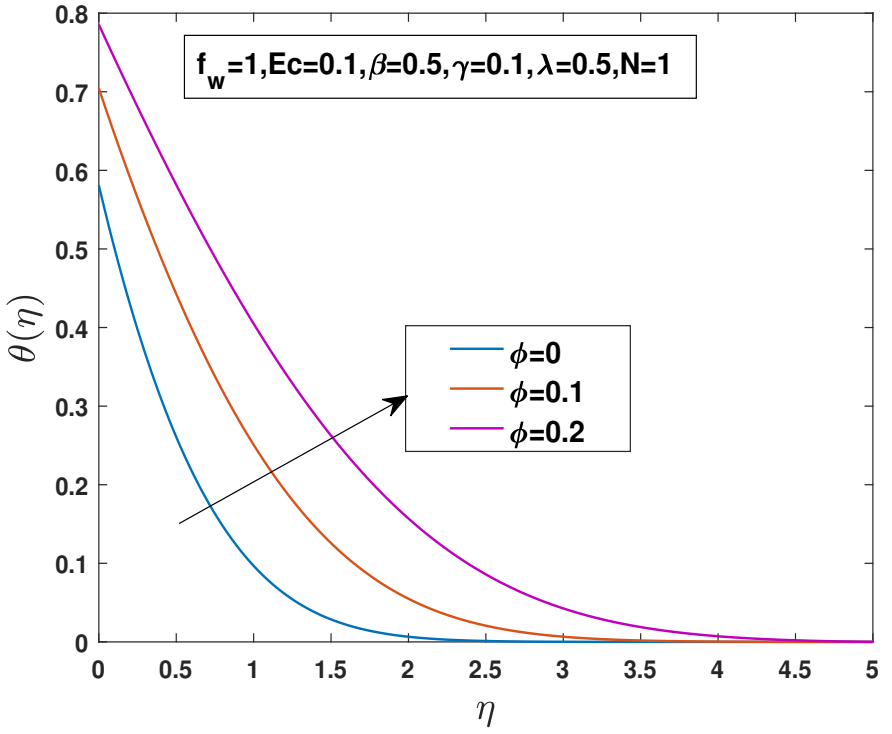


FIGURE 3.5: Effects of $\phi$ on temperature distribution for suction.

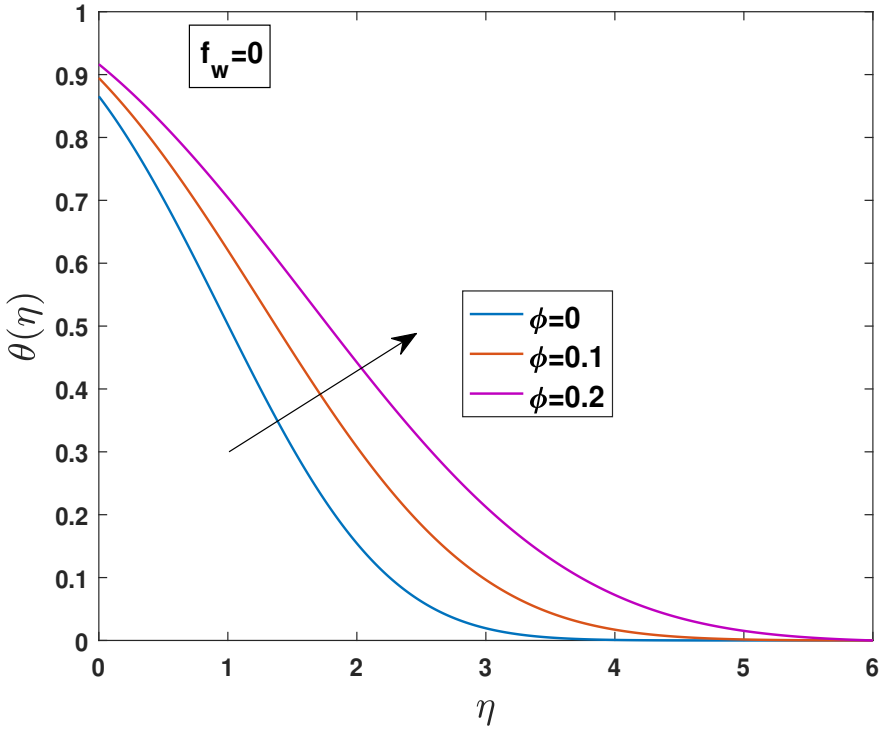


FIGURE 3.6: Effects of $\phi$ on temperature distribution for impermeable plate.

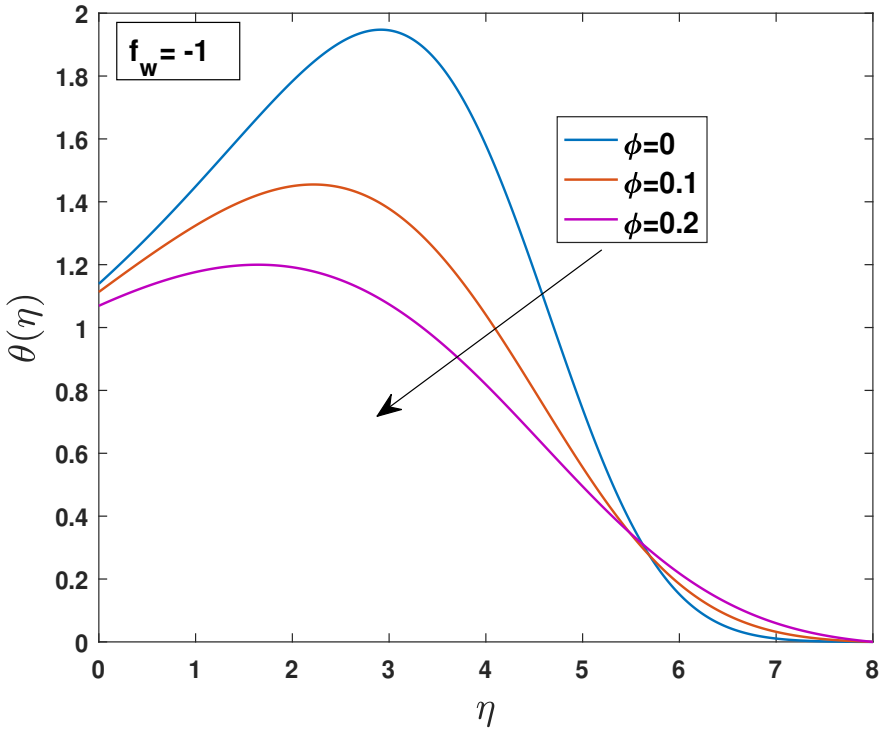


FIGURE 3.7: Effects of $\phi$ on temperature distribution for injection.

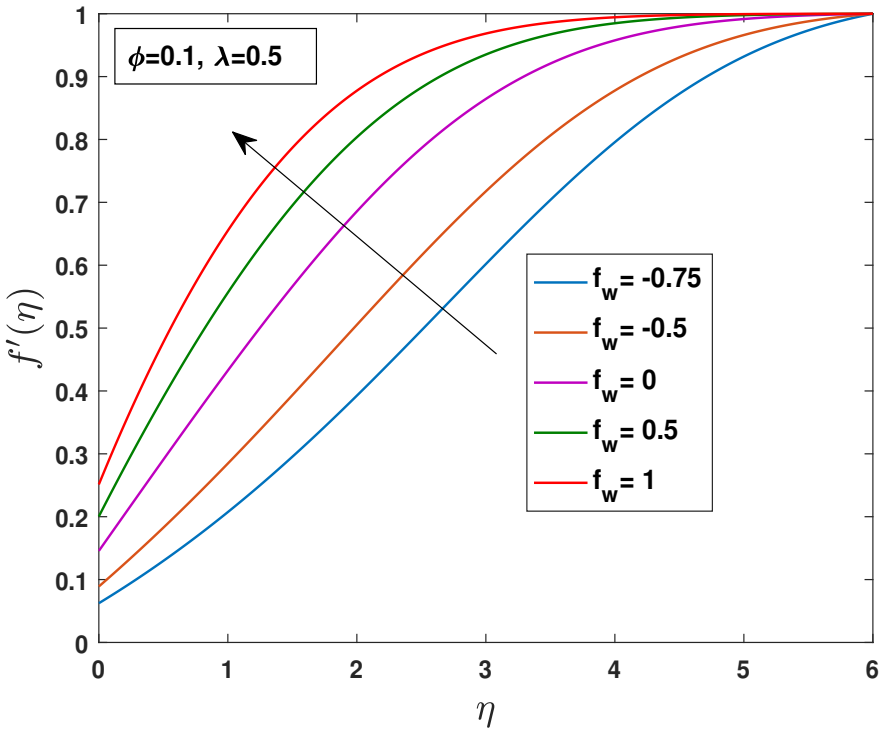


FIGURE 3.8: Effects of $f_w$ on velocity distribution.

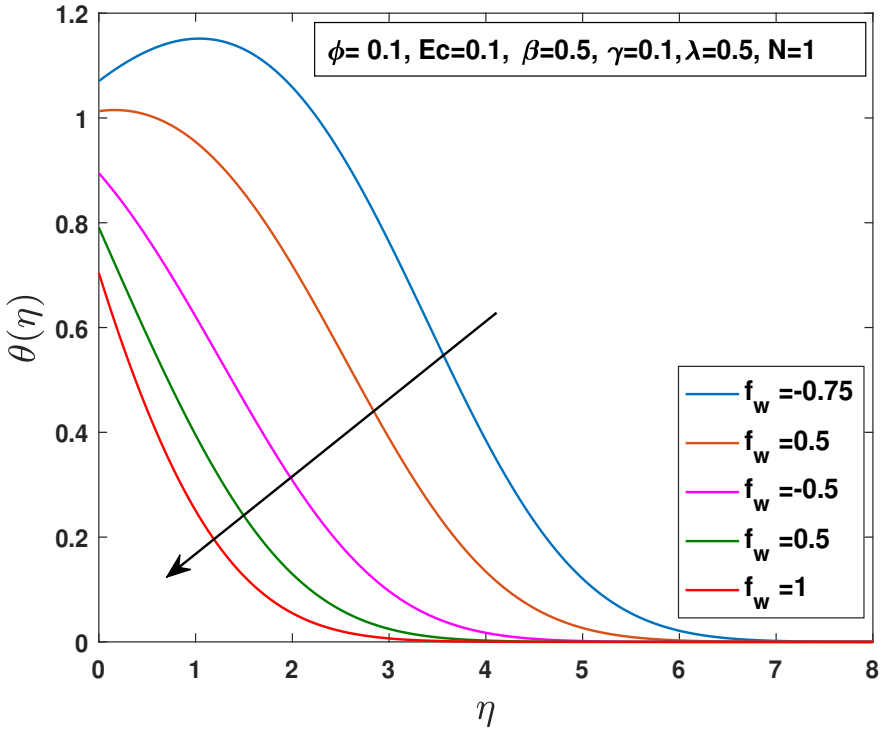


FIGURE 3.9: Effects of $f_w$ on temperature distribution.

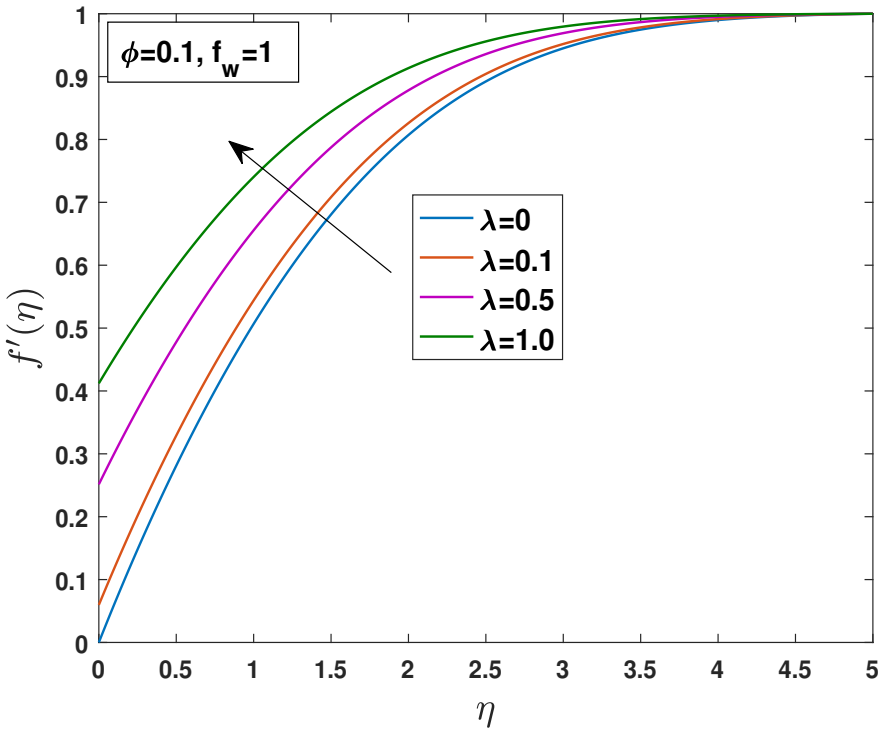


FIGURE 3.10: Effects of $\lambda$ on velocity distribution for suction.

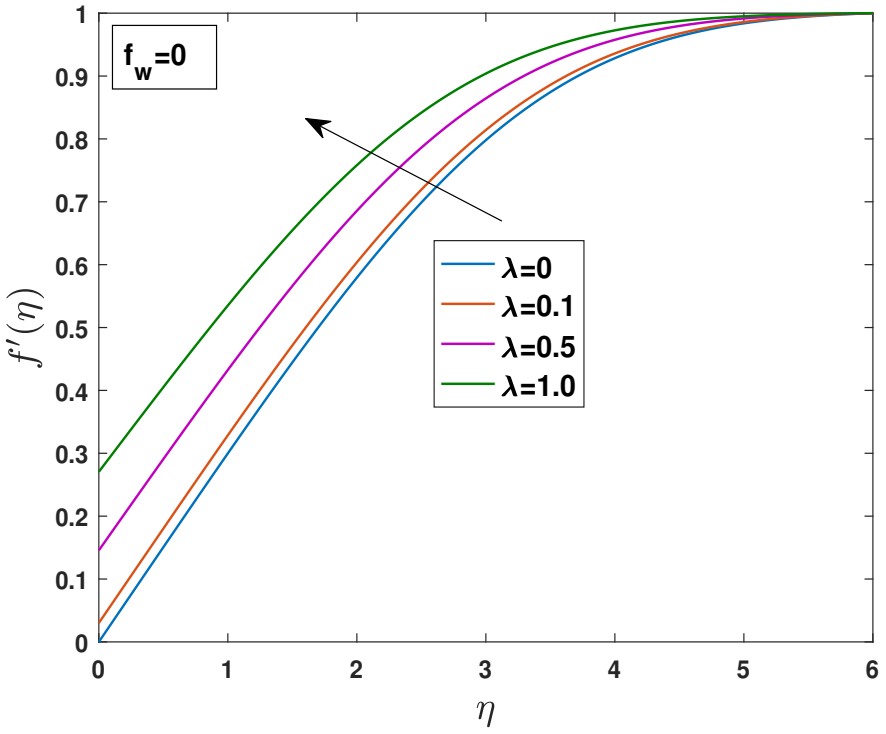


FIGURE 3.11: Effects of $\lambda$ on velocity distribution for impermeable plate.

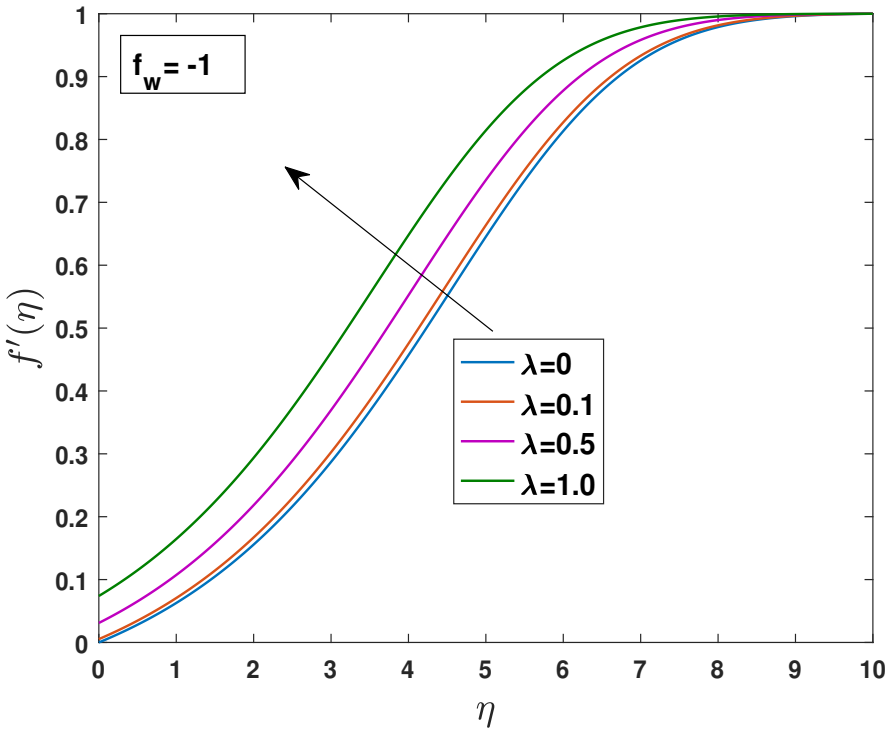


FIGURE 3.12: Effects of $\lambda$ on velocity distribution for injection.

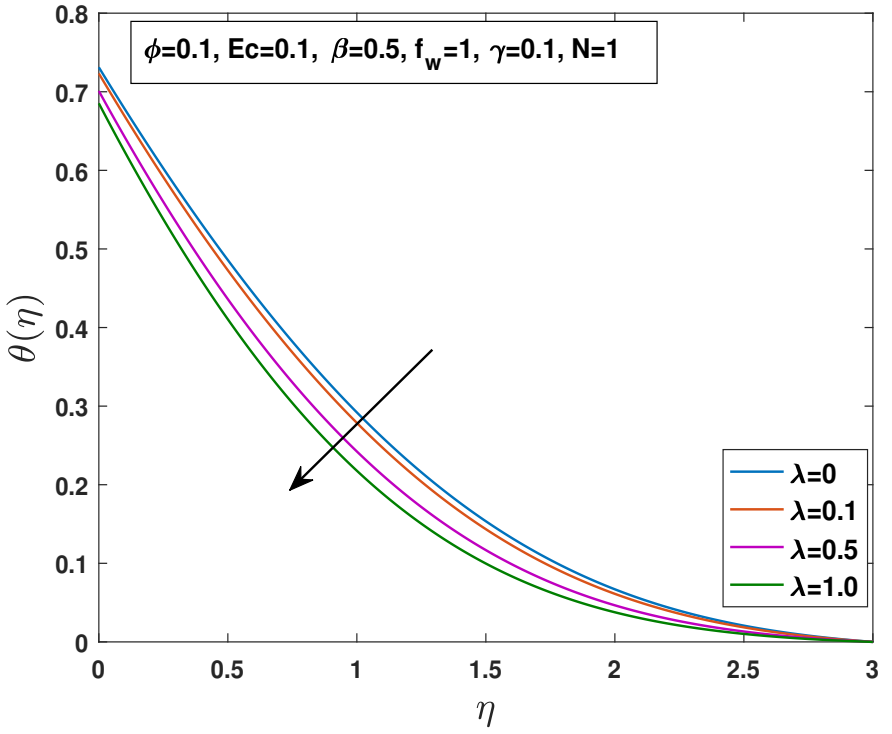


FIGURE 3.13: Effects of $\lambda$ on temperature distribution for suction.

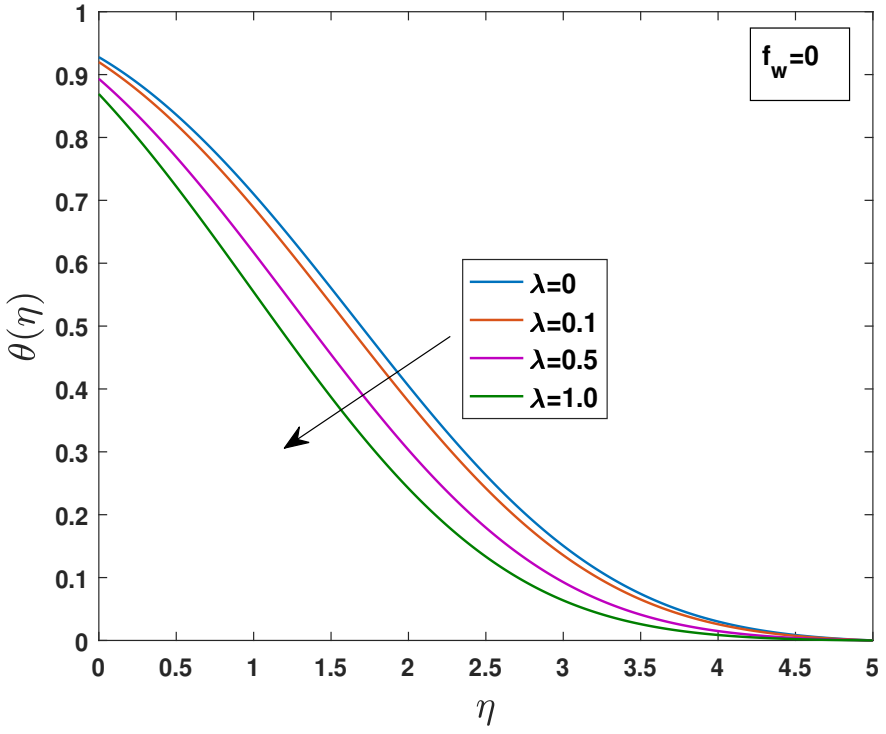


FIGURE 3.14: Effects of $\lambda$ on temperature distribution for impermeable plate.

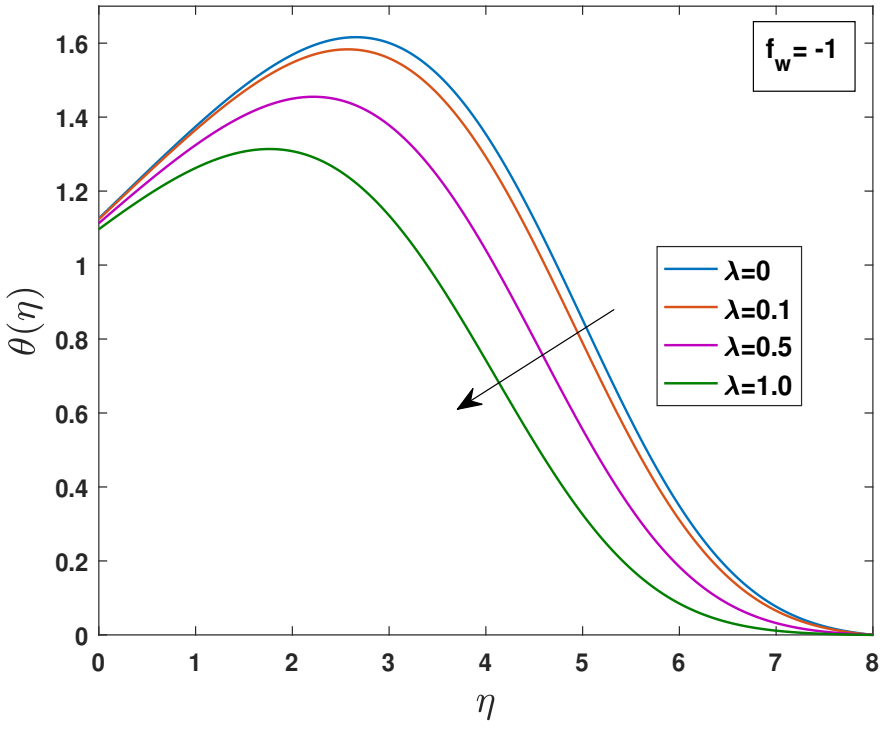


FIGURE 3.15: Effects of $\lambda$ on temperature distribution for injection.

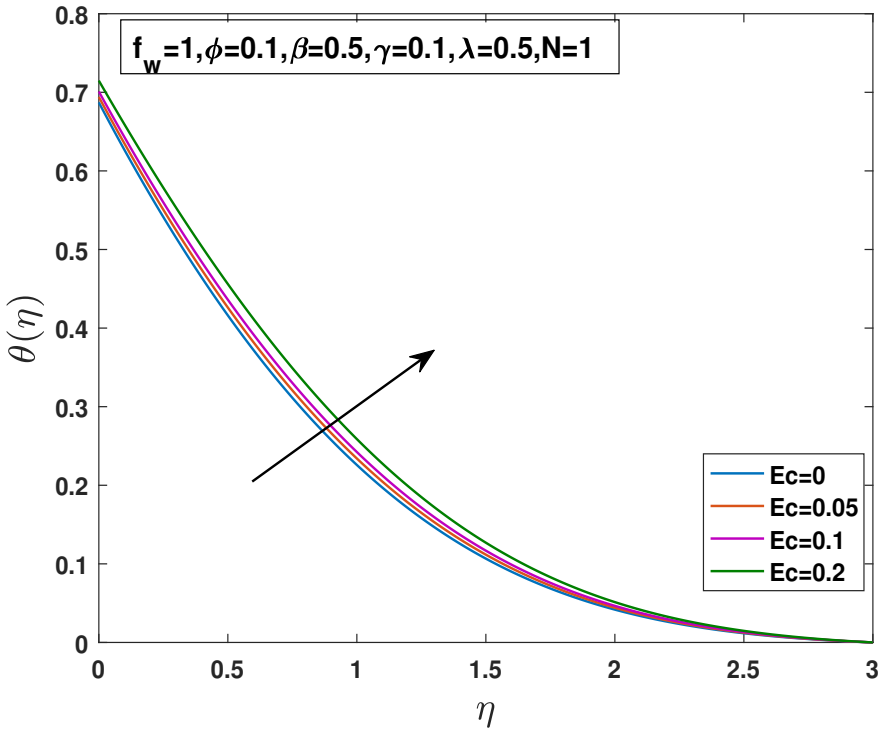


FIGURE 3.16: Effects of $Ec$ on temperature distribution for suction.

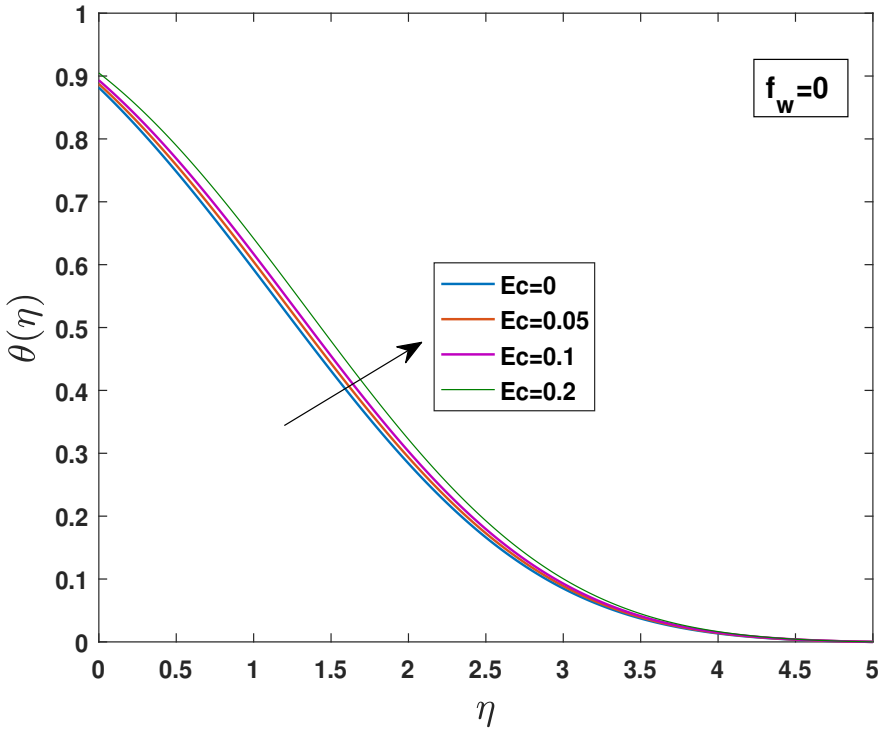


FIGURE 3.17: Effects of $Ec$ on temperature distribution for impermeable plate.

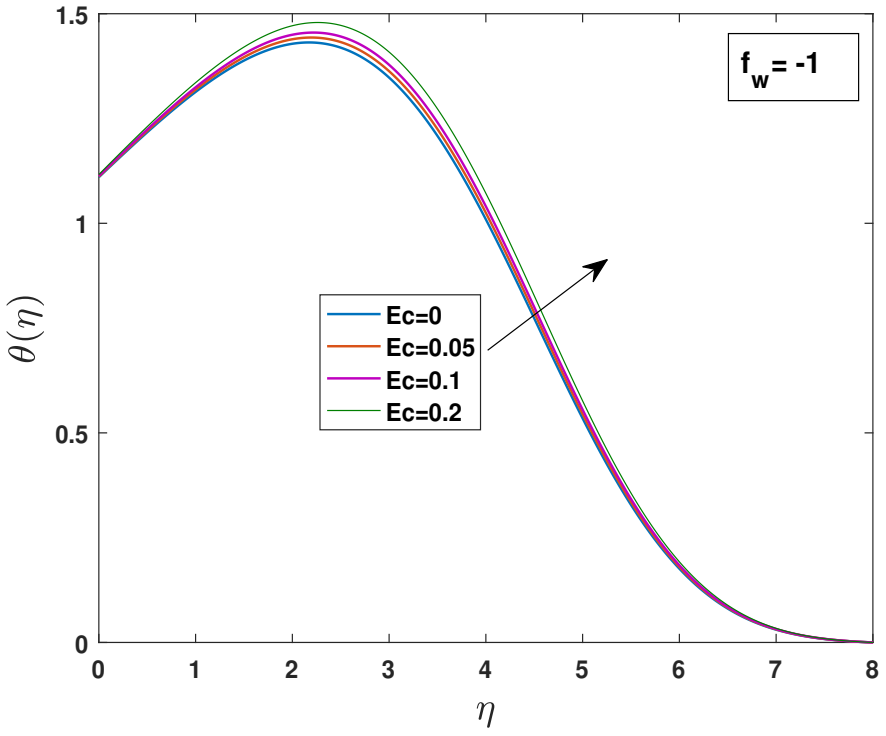


FIGURE 3.18: Effects of $Ec$ temperature distribution for injection.

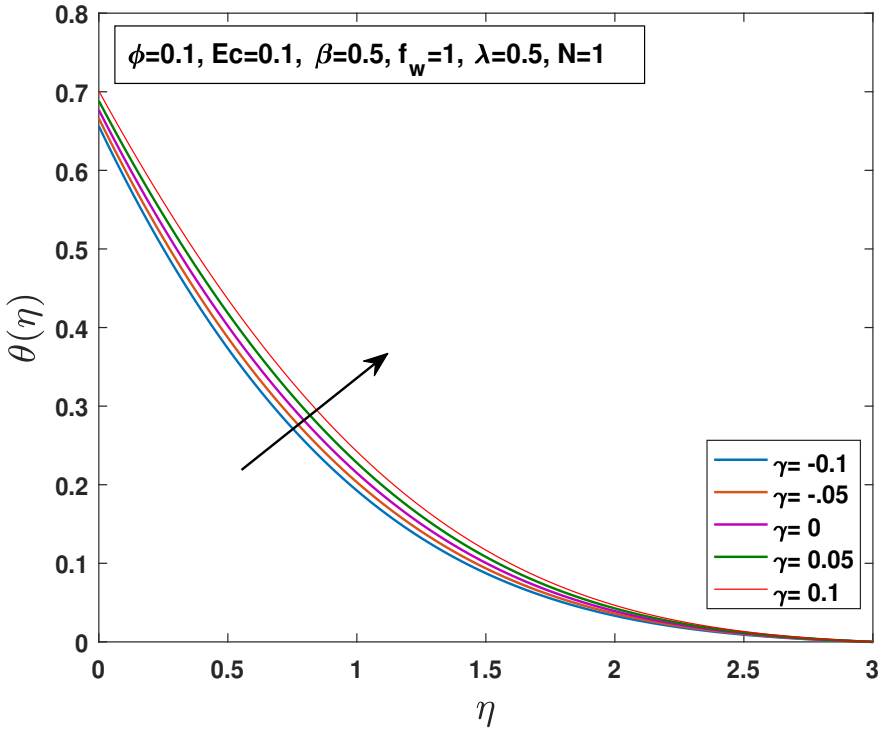


FIGURE 3.19: Effects of $\gamma$ on temperature distribution for suction.

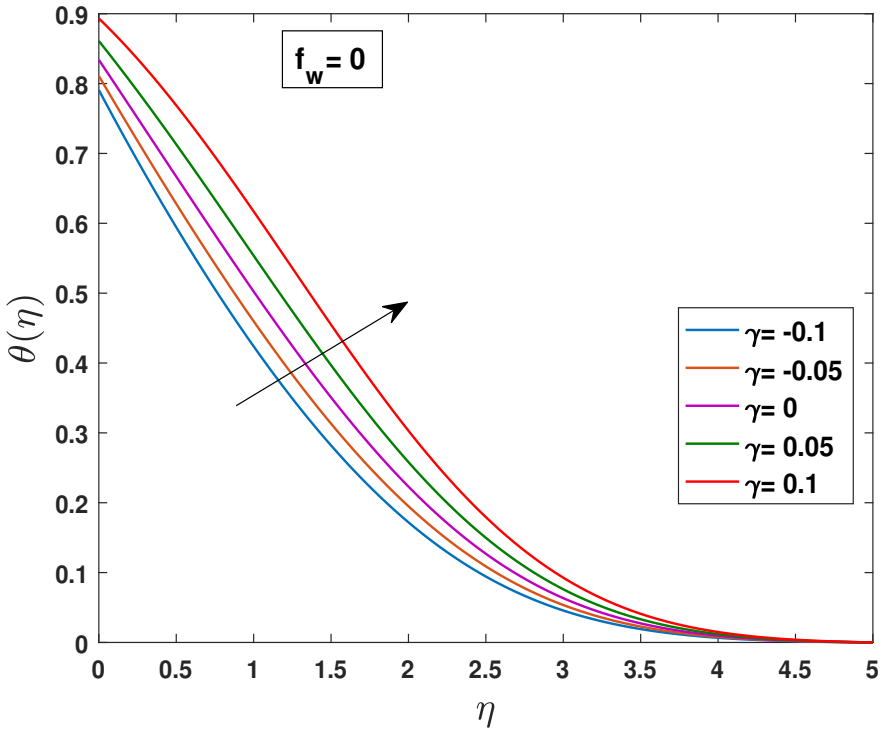


FIGURE 3.20: Effects of $\gamma$ on temperature distribution for impermeable plate.

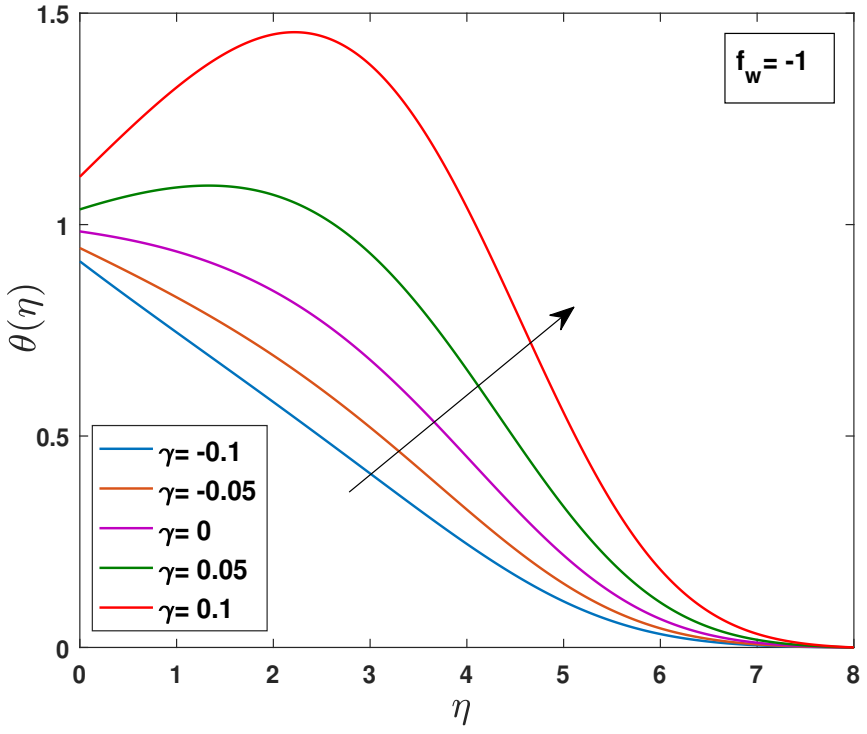


FIGURE 3.21: Effects of $\gamma$ on temperature distribution for injection.

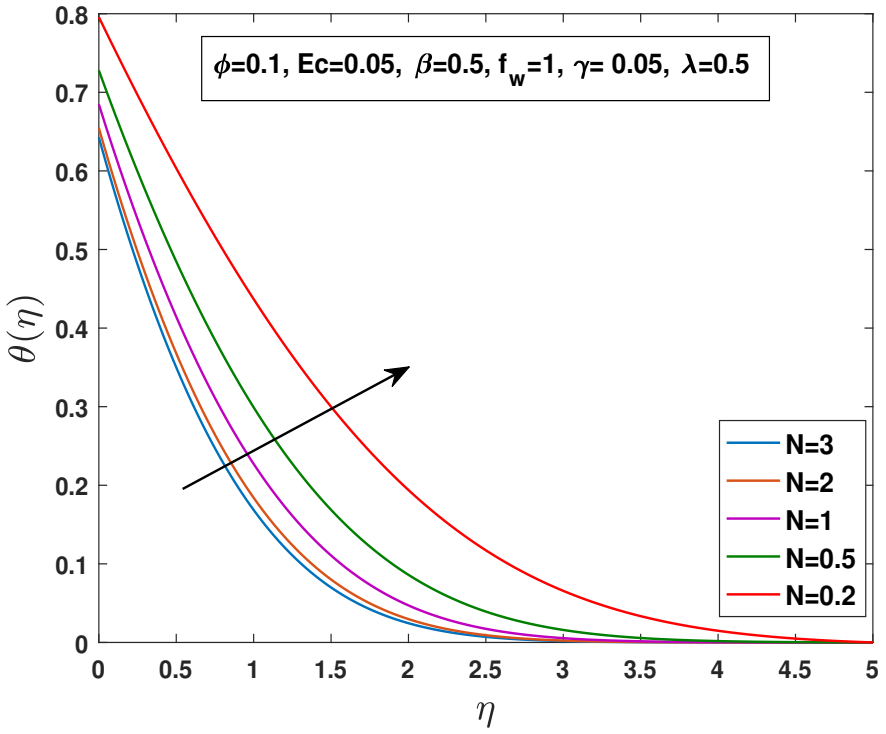


FIGURE 3.22: Effects of $N$ on temperature distribution for suction.

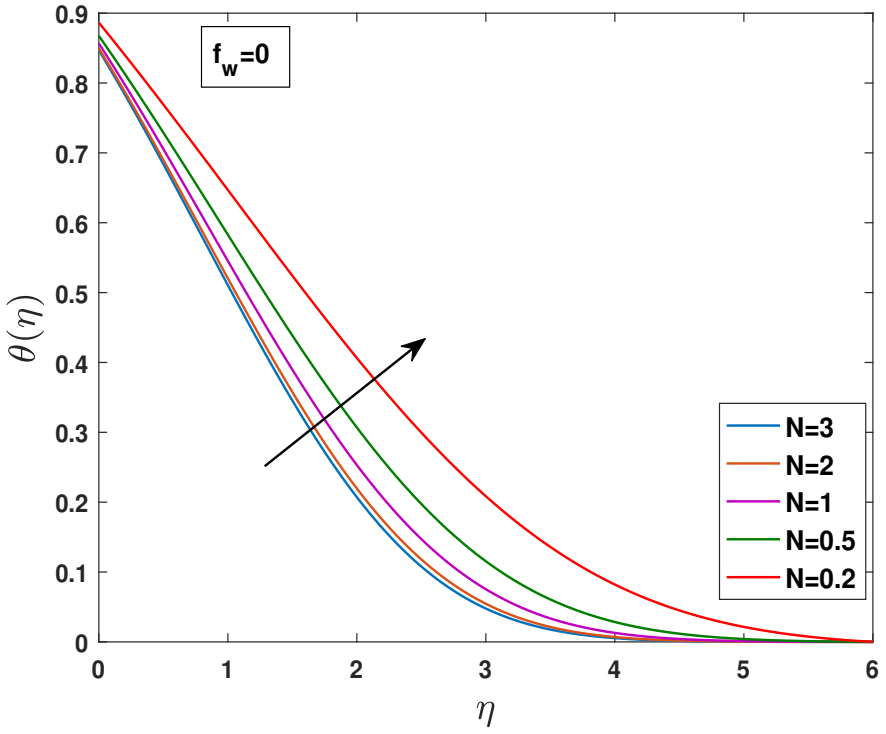


FIGURE 3.23: Effects of $N$ on temperature distribution for impermeable plate.

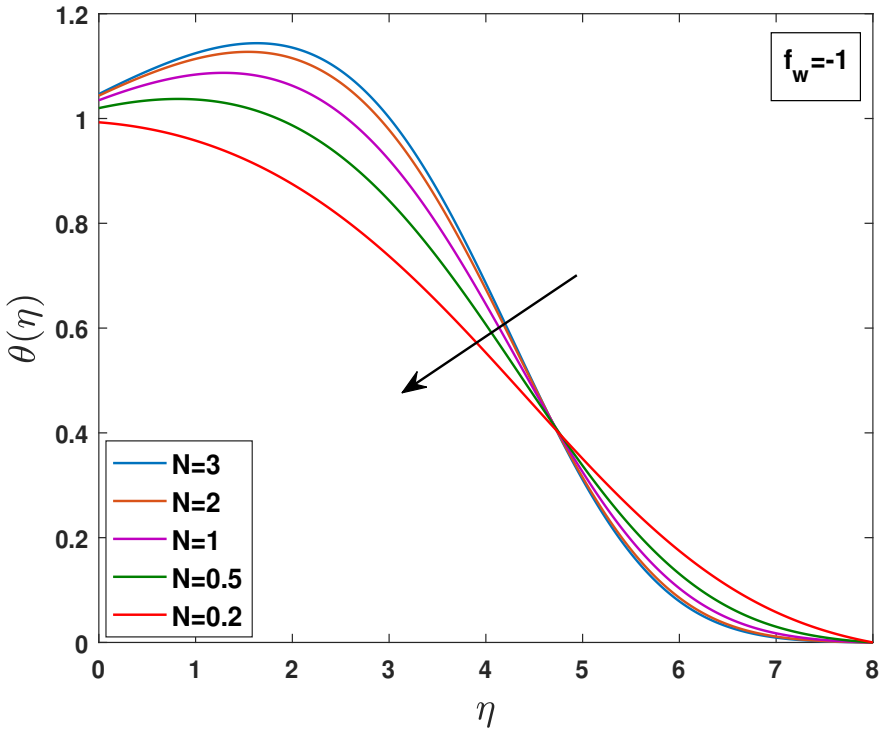


FIGURE 3.24: Effects of $N$ on temperature distribution for injection.

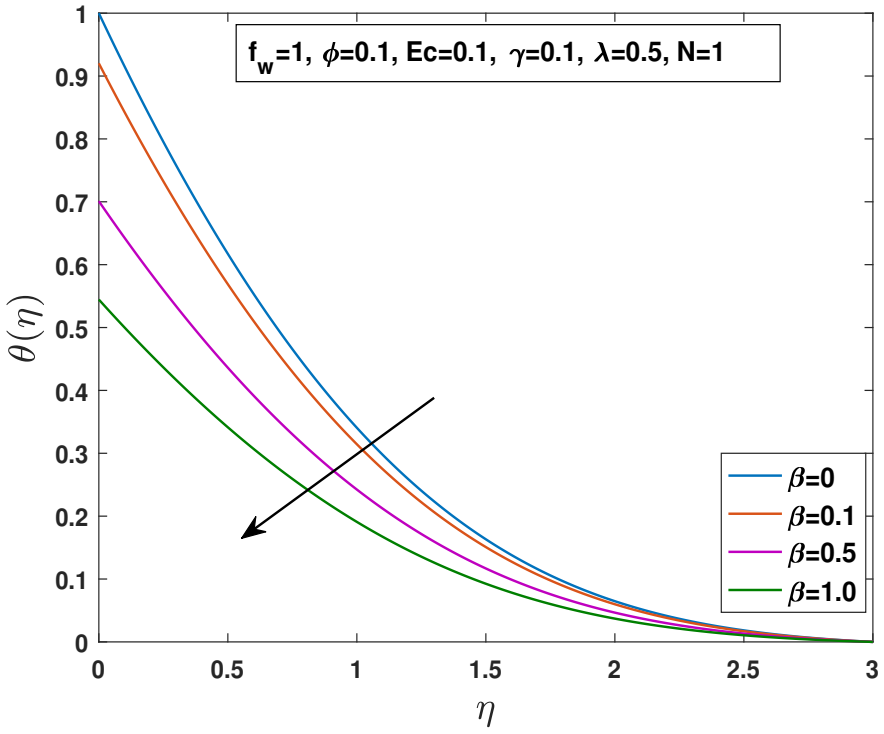


FIGURE 3.25: Effects of $\beta$ on temperature distribution for suction.

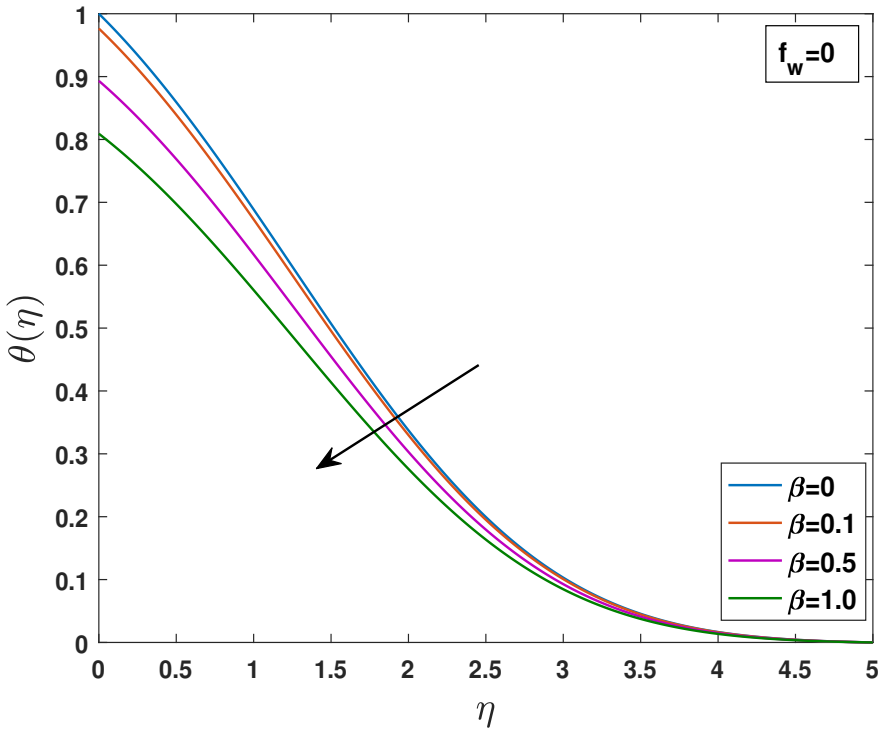


FIGURE 3.26: Effects of $\beta$ on temperature distribution for impermeable plate.

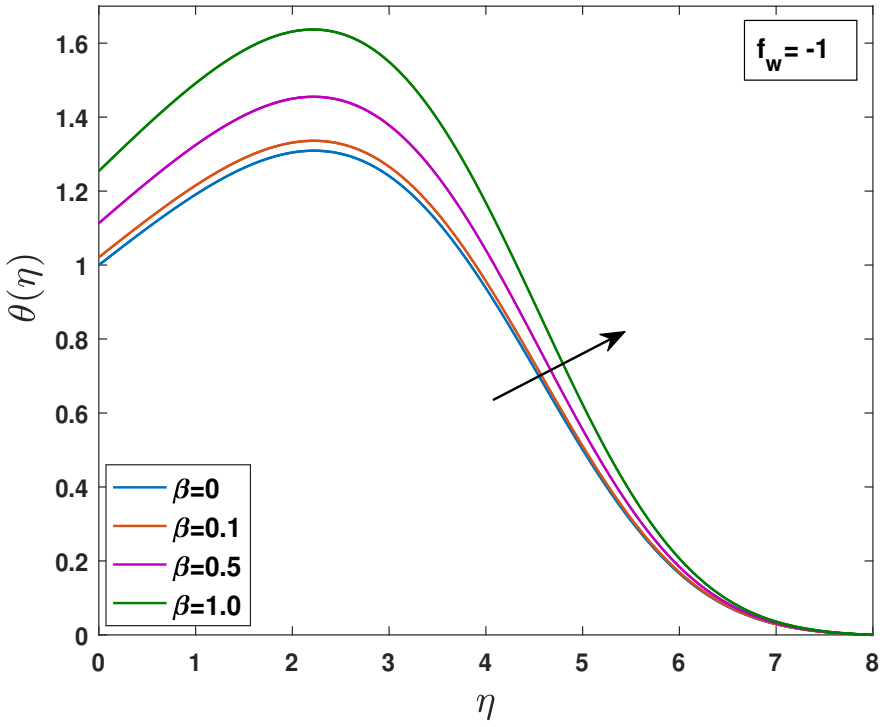


FIGURE 3.27: Effects of $\beta$ on temperature distribution for injection.

# Chapter 4

# MHD Nanofluid Flow over Porous Plate with Joule Heating Effects

The objective of this chapter is to extended the work of Maleki et al. [52] discussed in previous chapter. Flow model of Maleki et al has been extended by considering the magnetic and Joule heating effects. By using the similarity variables nonlinear PDEs of momentum and energy equations have been converted into system of ODEs. Resulting system of equations of system are solved by well know shooting method. The influence of different parameters of modeled equations on velocity and temperature profile are discussed, and results are analyzed graphically using Matlab. The work present in Chapter 3 is extended here for the nanofluid water-Multi wall carbon nanotubes.

## 4.1 Mathematical Modeling

The problem is formulated in such a way that we consider some assumptions including $2D$, incompressible, steady state and slip boundary condition of MHD over a porous plate. The coordinate system is preferred to be chosen in such a way that $x$-axis is chosen along the plate and $y$- axis is taken normal to it.

Fluid is flowing over a plate with uniform velocity when fluid strikes to the plate, after some time the velocity of fluid reach to the point where it becomes free stream velocity $U_\infty$. The slip velocity along the $x$-axis and thermal slip are given by $u = \lambda_1 \left(\frac{\partial u}{\partial x}\right)$, $T = T_w + \beta_1 \left(\frac{\partial T}{\partial y}\right)$, here $\lambda_1$ is the slip velocity parameter and $\beta_1$ is the thermal slip parameter. The magnetic field is applied normal to the plate. The induced magnetic field which is due to the motion of the fluid is neglected as compared with applied magnetic field. The free stream temperature is represented as $T_\infty$ for very large value of $y$ (i.e. $y \to \infty$).

The thermo-physical properties of fluid with nanoparticles are given in Table 3.1.

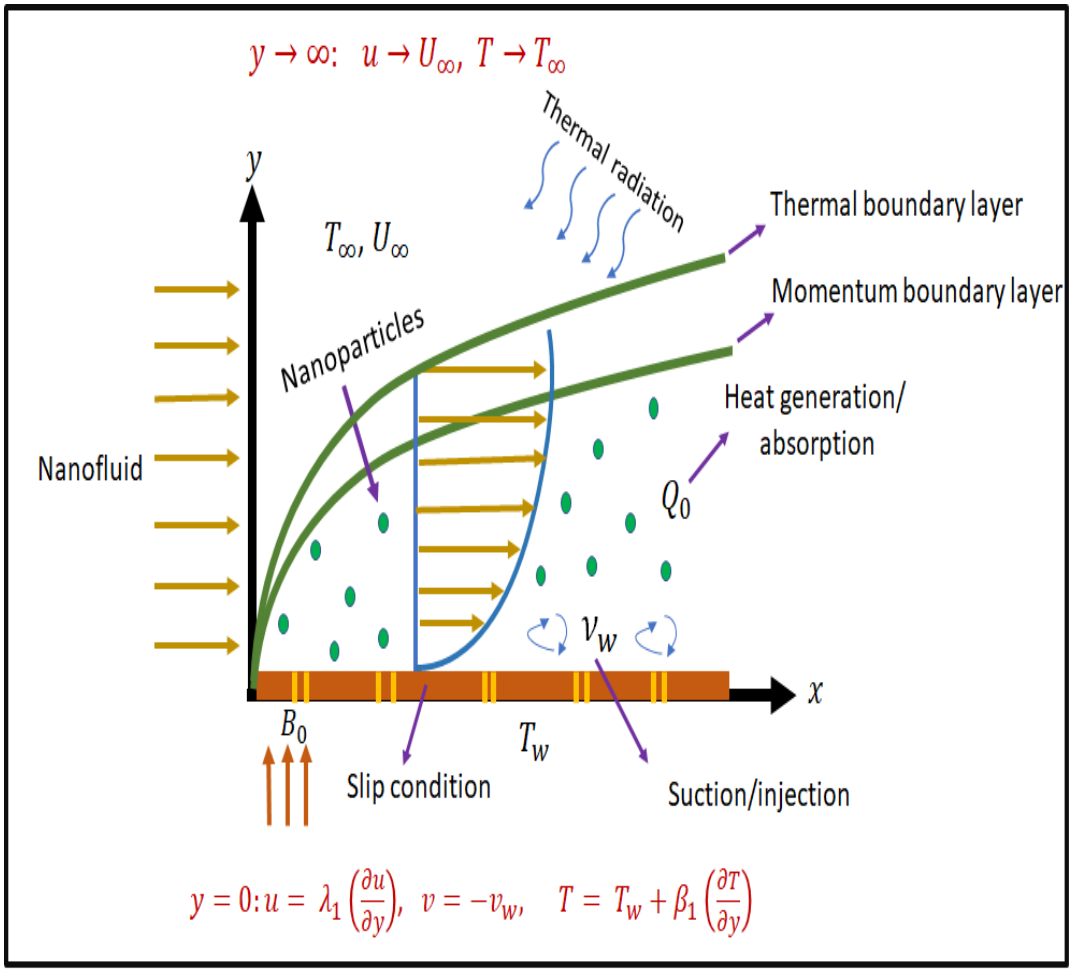


FIGURE 4.1: Geometry of physical model

.

By considering the above assumptions, the governing PDEs are:

$$\frac{\partial u}{\partial x}+\frac{\partial v}{\partial y}=0, \tag{4.1}$$

$$u\frac{\partial u}{\partial x}+v\frac{\partial u}{\partial y}=\frac{\mu_{nf}}{\rho_{nf}}\frac{\partial^2 u}{\partial y^2}-\frac{\sigma_{nf}B_0^2}{\rho_{nf}}u, \tag{4.2}$$

$$u\frac{\partial T}{\partial x}+v\frac{\partial T}{\partial y}=\alpha_{nf}\frac{\partial^2 T}{\partial y^2}+\frac{\mu_{nf}}{(\rho C_p)_{nf}}\left(\frac{\partial u}{\partial y}\right)^2+\frac{Q_0(T-T_\infty)}{(\rho C_p)_{nf}}$$
$$-\frac{1}{(\rho C_p)_{nf}}\left(\frac{\partial q_r}{\partial y}\right)+\frac{\sigma_{nf}}{(\rho C_p)_{nf}}B_0^2u^2. \tag{4.3}$$

The corresponding boundary conditions are as follow:

$$\left.\begin{aligned} &u=\lambda_1\left(\frac{\partial u}{\partial y}\right), \quad v=-v_w, \quad T=T_w+\beta_1\left(\frac{\partial T}{\partial y}\right) \quad \text{at} \quad y=0,\\ &\\ &u\to U_\infty, \quad T\to T_\infty \quad \text{as} \quad y\to\infty. \end{aligned}\right\} \tag{4.4}$$

In above equations $\beta_1$, $\lambda_1$, $\alpha_{nf}$, $\mu_{nf}$ and $\rho_{nf}$ represent the thermal slip parameter, velocity slip parameter, thermal diffusivity, dynamic viscosity and density of nanofluid, etc.

The Roseland model for radiative heat flux is calculates as:

$$q_r=-\frac{4\sigma}{3k^*}\frac{\partial T^4}{\partial y}, \tag{4.5}$$

where $T^4$, $k^*$ and $\sigma$ represent function of fluid temperature, mean absorption factor, and Stefan-Boltzmann coefficient.

### 4.1.1 Similarity Transformation

We adopt the following transformation for the conversion of partial differential equation (4.1) to (4.3) into ordinary differential equation [52].

$$\left.\eta=y\left(\frac{U_\infty}{\nu_f x}\right)^{\frac{1}{2}}, \quad \psi(\eta)=(U_\infty\nu_f x)^{\frac{1}{2}}f(\eta), \quad \theta(\eta)=\frac{T-T_\infty}{T_w-T_\infty}.\right\} \tag{4.6}$$

By using the above transformation system of PDEs (4.1) to (4.3) can be transformed into system of ODEs. As the stream function satisfies the continuity equation, the detailed procedure for the verification of the continuity Eq. (4.1) has been discussed in Chapter 3. The complete procedure of momentum and energy equation is described below. Eq. (4.2) will be converted into the dimensionless form. As the left hand side of equation Eq. (4.2) was already calculated, so it can be written as.

$$u\frac{\partial u}{\partial x} = -\frac{1}{2}y\frac{U_\infty^{\frac{5}{2}}}{\nu_f^{\frac{1}{2}}x^{\frac{3}{2}}}f''f'. \tag{4.7}$$

$$v\frac{\partial u}{\partial y} = -\frac{1}{2}\frac{U_\infty^2}{x}ff'' + \frac{1}{2}y\frac{U_\infty^{\frac{5}{2}}}{x^{\frac{3}{2}}\nu_f^{\frac{1}{2}}}f'f''. \tag{4.8}$$

Now, the right hand side of Eq. (4.2) can be calculated.

$$\begin{aligned}\frac{\partial^2 u}{\partial y^2} &= \frac{\partial}{\partial y}\left(\frac{\partial u}{\partial y}\right),\\ &= \frac{U_\infty^{\frac{3}{2}}}{x^{\frac{1}{2}}\nu_f^{\frac{1}{2}}}\left(\frac{\partial f''}{\partial \eta}\frac{\partial \eta}{\partial y}\right),\\ \frac{\partial^2 u}{\partial y^2} &= \frac{U_\infty^2}{x\nu_f}f'''.\end{aligned} \tag{4.9}$$

Utilizing Eqs. (4.7) to (4.9), we get the dimensionless form of Eq. (4.2).

$$-\frac{1}{2}y\frac{U_\infty^{\frac{5}{2}}}{\nu_f^{\frac{1}{2}}x^{\frac{3}{2}}}f''f' - \frac{1}{2}\frac{U_\infty^2}{x}ff'' + \frac{1}{2}y\frac{U_\infty^{\frac{5}{2}}}{x^{\frac{3}{2}}\nu_f^{\frac{1}{2}}}f'f'' = \frac{\mu_f}{(1-\phi)^{2.5}\left[(1-\phi)\rho_f + \phi\rho_s\right]}\left[\frac{U_\infty^2}{x\nu_f}f'''\right] - \frac{(1-\phi)\sigma_f + \phi\sigma_s}{(1-\phi)\rho_f + \phi\rho_s}B_0^2U_\infty f'(\eta),$$

$$-\frac{1}{2}\frac{U_\infty^2}{x}ff'' = \frac{\mu_f}{(1-\phi)^{2.5}\left[\rho_f[(1-\phi)+\phi\frac{\rho_s}{\rho_f}]\right]}\left[\frac{U_\infty^2}{x\nu_f}f'''\right] - \frac{\sigma_f}{\rho_f}\left[\frac{(1-\phi)+\phi\frac{\sigma_s}{\sigma_f}}{(1-\phi)+\phi\frac{\rho_s}{\rho_f}}\right]B_0^2U_\infty f'(\eta),$$

$$\frac{U_\infty^2}{x}\left[\frac{\mu_f}{\rho_f}m_0\frac{f'''}{\nu_f} + \frac{1}{2}ff'' - m_4\frac{\sigma_f}{\rho_f}B_0^2\frac{x}{U_\infty}f'(\eta)\right] = 0,$$

$$\Rightarrow m_0f''' + \frac{1}{2}ff'' - m_4\frac{\sigma_fB_0^2x}{\rho_fU_\infty}f'(\eta) = 0.$$

Final dimensionless form of Eq. (4.2) takes the form:

$$m_0 f''' + \frac{1}{2} f f'' - m_4 M f'(\eta) = 0. \tag{4.10}$$

Presently, we incorporate the below strategy for the transformation of Eq. (4.3) into the dimensionless form:

$$\frac{\partial T}{\partial x} = (T_w - T_\infty)\theta' - \frac{1}{2} y \left(\frac{U_\infty}{\nu_f}\right)^{\frac{1}{2}} x^{\frac{-3}{2}}.$$

$$u\frac{\partial T}{\partial x} = -\frac{1}{2} y \frac{U_\infty^{\frac{3}{2}}}{\nu_f^{\frac{1}{2}}} x^{\frac{-3}{2}} (T_w - T_\infty) f'\theta'. \tag{4.11}$$

$$v\frac{\partial T}{\partial y} = -\frac{1}{2}(T_w - T_\infty)\frac{U_\infty}{x} f\theta' + \frac{1}{2} y \frac{U_\infty^{\frac{3}{2}}(T_w - T_\infty)}{x^{\frac{3}{2}} \nu_f^{\frac{1}{2}}} \theta' f'. \tag{4.12}$$

Using Eq. (4.11) to Eq. (4.12) the left hand side of Eq. (4.3) can be written as:

$$u\frac{\partial T}{\partial x} + v\frac{\partial T}{\partial y} = \frac{-1}{2}(T_w - T_\infty)\frac{U_\infty}{x} f\theta'. \tag{4.13}$$

Similarly, the right hand side terms of Eq. (4.3) can be written as

$$\frac{\partial^2 T}{\partial y^2} = (T_w - T_\infty)\left(\frac{U_\infty}{x\nu_f}\right)\theta''. \tag{4.14}$$

$$\left(\frac{\partial u}{\partial y}\right)^2 = \frac{U_\infty^3}{x\nu_f} f''^2. \tag{4.15}$$

$$\frac{\partial q_r}{\partial y} = -\frac{16\sigma T_\infty^3 (T_w - T_\infty)}{3k^*}\left(\frac{U_\infty}{x\nu_f}\right)\theta''. \tag{4.16}$$

Using Eq. (4.13) to Eq. (4.16) in Eq. (4.3), we get

$$-\frac{1}{2}(T_w - T_\infty)\frac{U_\infty}{x} f\theta' = \alpha_{nf}(T_w - T_\infty)\frac{U_\infty}{x\nu_f}\theta'' + \frac{\mu_{nf}}{(\rho C_p)_{nf}}\left(\frac{U_\infty^3}{x\nu_f} f''^2\right) + \frac{Q_0\theta(T_w - T_\infty)}{\rho C_p)_{nf}} + \frac{16\sigma T_\infty^3 (T_w - T_\infty)}{3(\rho C_p)_{nf} k^*}\frac{U_\infty}{x\nu_f}\theta'' + \frac{\sigma_{nf}}{(\rho C_p)_{nf}} B_o^2 u^2.$$

Multiplying above equation with $\frac{x\nu_f}{U_\infty(T_w - T_\infty)}$,

$$\frac{\nu_f}{2}f\theta' + \alpha_{nf}\theta'' + \frac{16\sigma T_\infty^3}{3k^*(\rho C_p)_{nf}}\theta'' + \frac{\mu_{nf}U_\infty^2}{(\rho C_p)_{nf}(T_w - T_\infty)}f''^2 + \frac{xQ_0\theta\nu_f}{U_\infty(\rho C_p)_{nf}} + \frac{\sigma_f\left[(1-\phi) + \phi\frac{\sigma_s}{\sigma_f}\right]}{(\rho C_p)_f\left[(1-\phi) + \phi\frac{(\rho C_p)_s}{(\rho C_p)_f}\right]} \times \frac{x\nu_f}{U_\infty(T_w - T_\infty)}B_0^2U_\infty^2f'^2 = 0.$$

Putting values of $\alpha_{nf}$, $\mu_{nf}$ and $(\rho C_p)_{nf}$, (3.8) to (3.11), we get

$$\frac{k_{nf}}{(\rho C_p)_f\left[(1-\phi) + \phi\frac{(\rho C_p)_s}{(\rho C_p)_f}\right]}\theta'' + \frac{16\sigma T_\infty^3}{3k^*(\rho C_p)_f\left[(1-\phi) + \phi\frac{(\rho C_p)_s}{(\rho C_p)_f}\right]} + \frac{\nu_f}{2}f\theta' + \frac{\mu_f U_\infty^2 f''^2}{(T_w - T_\infty)(1-\phi)^{2.5}(\rho C_p)_f\left[(1-\phi) + \phi\frac{(\rho C_p)_s}{(\rho C_p)_f}\right]} + \frac{\nu_f xQ_0}{U_\infty(\rho C_p)_f\left[(1-\phi) + \phi\frac{(\rho C_p)_s}{(\rho C_p)_f}\right]} + \frac{\sigma_f\left[(1-\phi) + \phi\frac{\sigma_s}{\sigma_f}\right]}{(\rho C_p)_f\left[(1-\phi) + \phi\frac{(\rho C_p)_s}{(\rho C_p)_f}\right]} \times \frac{x\nu_f}{U_\infty(T_w - T_\infty)}B_0^2U_\infty^2f'^2 = 0.$$

Multiplying above equation with $\frac{(\rho C_p)_f}{k_f}$,

$$\frac{k_{nf}}{k_f\left[(1-\phi) + \phi\frac{(\rho C_p)_s}{(\rho C_p)_f}\right]}\theta'' + \frac{4.4\sigma T_\infty^3}{k_f 3k^*\left[(1-\phi) + \phi\frac{(\rho C_p)_s}{(\rho C_p)_f}\right]} + \left(\frac{(\rho C_p)_f}{k_f}\right)\frac{\nu_f}{2}f\theta' + \frac{\mu_f U_\infty^2 f''^2}{(T_w - T_\infty)k_f(1-\phi)^{2.5}\left[(1-\phi) + \phi\frac{(\rho C_p)_s}{(\rho C_p)_f}\right]} + \frac{\nu_f xQ_0}{k_f U_\infty\left[(1-\phi) + \phi\frac{(\rho C_p)_s}{(\rho C_p)_f}\right]} + \frac{\sigma_f\left[(1-\phi) + \phi\frac{\sigma_s}{\sigma_f}\right]}{(\rho C_p)_f\left[(1-\phi) + \phi\frac{(\rho C_p)_s}{(\rho C_p)_f}\right]}B_0^2U_\infty^2f'^2 \times \frac{x\nu_f}{U_\infty(T_w - T_\infty)}\left(\frac{(\rho C_p)_f}{k_f}\right) = 0.$$

The dimensionless form of Eq. (4.3) is becomes

$$m_1\theta'' + \frac{4}{3N}\frac{k_f}{k_{nf}}m_1\theta'' + \frac{Pr_f}{2}f\theta' + m_2Pr_fEc(f'')^2 + m_3Pr_f\gamma\theta + m_5MPr_fEcf'^2 = 0 \tag{4.17}$$

Final dimensionless form of Eq. (4.2) to Eq.(4.3) become

$$m_0f''' + \frac{1}{2}ff'' - m_4Mf'(\eta) = 0 \tag{4.18}$$

$$m_1\theta'' + \frac{4}{3N}\frac{k_f}{k_{nf}}m_1\theta'' + \frac{Pr_f}{2}f\theta' + m_2 Pr_f Ec(f'')^2 + m_3 Pr_f\gamma\theta + m_5 M Pr_f Ec f'^2 = 0 \tag{4.19}$$

The related boundary conditions take the form:

$$\left.\begin{aligned} &f'(\eta) = \lambda f'', \quad f = f_w, \quad \theta = 1 + \beta\theta' \quad \text{at} \quad \eta = 0, \\ &f' \to 1, \quad \theta \to 0 \quad \text{as} \quad \eta \to \infty. \end{aligned}\right\} \tag{4.20}$$

These different parameters used in above equations have the following formulations:

$$m_0 = \frac{1}{(1-\phi)^{2.5}\left[(1-\phi) + \phi\rho_s/\rho_f\right]}, \quad m_1 = \frac{k_{nf}/k_f}{(1-\phi) + \phi(\rho C_p)_s/(\rho C_p)_f}$$
$$m_2 = \frac{1}{(1-\phi)^{2.5}\left[(1-\phi) + \phi(\rho C_p)_s/(\rho C_p)_f\right]}, \quad m_3 = \frac{1}{(1-\phi) + \phi(\phi C_p)_s/(\rho C_p)_f},$$
$$m_4 = \left[\frac{(1-\phi) + \phi\frac{\sigma_s}{\sigma_f}}{(1-\phi) + \phi\frac{\rho_s}{\rho_f}}\right], \quad m_5 = \left[\frac{(1-\phi) + \phi\frac{\sigma_s}{\sigma_f}}{(1-\phi) + \phi\frac{(\rho C_p)_s}{(\rho C_p)_s}}\right]$$
$$\gamma = \frac{Q_0 x}{U_\infty(\rho C_p)_f}, \quad \beta = \beta_1\left(\frac{U_\infty}{x\nu_f}\right)^{\frac{1}{2}},$$
$$Ec = \frac{U_\infty^2}{(C_p)_f(T_w - T_\infty)}, \quad Pr_f = \frac{\nu_f}{\alpha_f}, \quad .$$
$$\lambda = \lambda_1\left(\frac{U_\infty}{x\nu_f}\right)^{\frac{1}{2}}, \quad f_w = 2\left(\frac{x}{\nu_f U_\infty}\right)^{\frac{1}{2}} v_w$$
$$N = \frac{k_f k^*}{4\sigma T_\infty^3}, \quad M = \frac{\sigma_f B_0^2 x}{\rho_f U_\infty}$$

## 4.2 Numerical Treatment

To apply shooting method , we convert the BVP into IVP by assuming the missing initial condition. with the help of shooting technique we solve Eq. (4.18) to Eq. (4.19) using the boundary condition (4.20) firstly, Eq. (4.18) is numerically solved, and then the obtained results of $f$, $f'$ and $f''$ are used in Eq. (4.19). For this following notations has been introduced

$$f = y_1, \quad f' = y_2, \quad f'' = y_3. \tag{4.21}$$

Eq. (4.18) is converted into first order ODEs,

$$\left.\begin{aligned} y_1' &= y_2, & y_1(0) &= 1, \\ y_2' &= y_3, & y_2(0) &= 0.5p, \\ y_3' &= -\frac{1}{2m_0} y_1 y_3 + \frac{m_4}{m_0} M y_2, & y_3(0) &= p, \end{aligned}\right\} \tag{4.22}$$

where $p$ is the missing initial condition. RK4 method has been used to solve the above initial value problem. As the numerical computations can not be performed on an unbounded domain, therefore the domain of the above problem has been taken as $[0, \eta_\infty]$ instead of $[0, \infty)$, where $\eta_\infty$ is an appropriate finite positive real number with chosen initial guess $p$ such that:

$$y_2(\eta_\infty, p) - 1 = 0. \tag{4.23}$$

To solve the above algebraic Eq. (4.23), we use the Newtons method which has the following iterative procedure:

$$p^{n+1} = p^n - \frac{(y_2(\eta_\infty, p)) - 1}{\left(\frac{\partial y_2(\eta_\infty, p)}{\partial p}\right)}. \tag{4.24}$$

We further introduce the following notations, in order to obtain the derivative $\frac{\partial y_2}{\partial p}$

$$\begin{aligned} \frac{\partial y_1}{\partial p} &= y_4, \\ \frac{\partial y_2}{\partial p} &= y_5, \\ \frac{\partial y_3}{\partial p} &= y_6. \end{aligned}$$

As a result of these new notations, the Newtons iterative scheme gets the form

$$p^{n+1} = p^n - \frac{(y_2(\eta_\infty)) - 1}{y_5(\eta_\infty)}.$$

Now differentiate the above system of three first order ODEs with respect to $p$ (4.22) we get three more ODEs. Writing all these six ODEs together, we have the

following initial value problem (IVP).

$$\begin{aligned}
y_1' &= y_2, & y_1(0) &= 1,\\
y_2' &= y_3, & y_2(0) &= 0.5p,\\
y_3' &= -\frac{1}{2m_0} y_1 y_3 + \frac{m_4}{m_0} M y_2, & y_3(0) &= p.\\
y_4' &= y_5', & y_4(0) &= 0,\\
y_5' &= y_6, & y_5(0) &= 0.5,\\
y_6' &= -\frac{1}{2m_0}\left[y_3 y_4 + y_1 y_6\right] + \frac{m_4}{m_0} M(y_5), & y_6(0) &= 1.
\end{aligned}$$

The threshold for the shooting method is defined as follows:

$$\mid y_2\left(\eta_\infty\right) - 1 \mid < \varepsilon, \tag{4.25}$$

where $\varepsilon$ is taken as $10^{-6}$, the iterative procedure has been repeated until this criteria is fulfilled.

Now solving Eq. (4.19) in the same way as was done for equation Eq. (4.18) numerically along with boundary conditions (4.20). Here missing initial condition $\theta'(0)$ is denoted by $q$. Different notations have been used which are given below

$$\theta = z_1, \quad \theta' = z_2,$$

Using these notations, we get a system of first order ODEs which are given below

$$\left.\begin{aligned}
z_1' &= z_2, & z_1(0) &= 1 + \beta q,\\
z_2' &= -\frac{1}{m_1\left(1 + \frac{4}{3N}\frac{k_f}{k_{nf}}\right)} \frac{Pr_f}{2} y_1 z_2 + m_2 Pr_f Ec (y_3)^2 & & \\
&\quad + m_3 Pr_f \gamma z_1 + m_5 M Pr_f Ec (y_2)^2, & z_2(0) &= q,
\end{aligned}\right\} \tag{4.26}$$

where $q$ is the missing initial condition. Above initial value problem (4.26) can be solve by using RK4 method, the missing condition is $q$ which can be defined as

$$z_1\left(\eta_\infty, q\right) = 0, \tag{4.27}$$

Above algebraic equation (4.27) can be solve by using Newton method. Newton method is given by the following iteration

$$q^{n+1} = q^n - \frac{(z_1(\eta_\infty, q)) - 0}{\left(\frac{\partial z_1(\eta_\infty, q)}{\partial q}\right)}.$$

We further introduce the following notations, in order to obtain the $\frac{\partial z_1}{\partial q}$

$$\frac{\partial z_1}{\partial q} = z_3,$$

$$\frac{\partial z_2}{\partial q} = z_4.$$

As a result of these new notations, the Newtons iterative scheme gets the form

$$\Rightarrow q^{n+1} = q^n - \frac{(z_1(\eta_\infty, q)) - 0}{z_3\left(\eta_\infty, q\right)}. \tag{4.28}$$

Now differentiate the above system of two first order ODEs (4.26) with respect to q we get another system of two ODEs. Writing all these four ODEs together, we have the following initial value problem (IVP).

$$\begin{aligned}
z_1' &= z_2, && z_1(0) = 1 + \beta q,\\
z_2' &= -\frac{1}{m_1\left(1 + \frac{4}{3N}\frac{k_f}{k_{nf}}\right)}\frac{Pr_f}{2} y_1 z_2 + m_2 Pr_f Ec (y_3)^2 \\
&\quad + m_3 Pr_f \gamma z_1 + m_5 M Pr_f Ec (y_2)^2, && z_2(0) = q,\\
z_3' &= z_4, && z_3(0) = \beta,\\
z_4' &= -\frac{1}{m_1\left(1 + \frac{4}{3N}\frac{k_f}{k_{nf}}\right)}\frac{Pr_f}{2} y_1 z_4 + m_3 Pr_f \gamma z_3, && z_4(0) = 1.
\end{aligned}$$

stopping criteria for the iterative process is defined as:

$$\mid z_1\left(\eta_\infty\right) - 0 \mid < \varepsilon,$$

where $\varepsilon$ is taken as $10^{-6}$. The method has been repeated until this criteria is fulfilled.

## 4.3 Results and Discussion

The main purpose of this section is to analyze the numerical results of temperature and velocity profile with the help of graphs by using different parameters.

### 4.3.1 Impact of Magnetic Parameter $M$

Figures 4.2 to 4.4 present the impact of magnetic parameter on velocity and temperature profiles for all three cases, suction, injection and impermeable plate ($f_w = 1$, $f_w = -1$ and $f_w = 0$). The higher value of $M$ shows decreasing behavior of velocity profile. As $M$ specify as ratio of Lorentz forces to the viscous forces, so with an increment in $M$ Lorentz force becomes dominant and it reduces the velocity of fluid. Figures. 4.5 to 4.7 show the effect of $M$ on temperature profile. The temperature profile rises by increasing the value of $M$. Joule heating effects are responsible for rising in temperature of the nanofluid when strong magnetic field is applied. Moreover, a resistive force is generated in the flow direction of the fluid which becomes the cause in the enhancement of temperature, for suction, injection and impermeable plate. If we take $M = 0$, then the results of chapter 3 are obtained.

### 4.3.2 Impact of Nanoparticles Volume Fraction

Figures 4.8 to 4.10 demonstrate the impact of nanoparticles volume fraction on velocity profile. In case of suction and impermeable plate ($f_w = 0$,$f_w = 1$), it is noticed that by increasing nanoparticles volume fraction, the velocity profile decreases and increases the boundary layer thickness. Reason behind this behavior is that, if we increase the nanoparticles volume fraction effective viscosity will increase which provide more resistance to fluid particles. That causes a decrease in the velocity profile, whereas an opposite behavior can be seen in case of injection ($f_w = -1$). Figures 4.11 to 4.13 depict the effect of nanoparticles volume fraction on dimensionless temperature. In case of impermeable plate ($f_w = 0$) and suction

($f_w = 1$) increasing the nanoparticles volume fraction leads to a increase in the temperature distribution. By increasing nanoparticle volume fraction thermal conductivity increases therefor temperature increases, while for injection ($f_w = -1$) opposite behavior is observed. Also, thermal boundary layer rises by boosting the $\phi$ values in all cases. Moreover, in the case of injection due to presence of heat generation radiation and viscous dissipation fluid temperature near the wall decreases and the inverse behavior is observed.

### 4.3.3 Impact of Velocity Slip Parameter

Figures 4.14 to 4.16 illustrate the behavior of velocity profile for slip velocity parameter. In all three cases ($f_w = 1, f_w = 0, f_w = -1$), it is observed that, velocity parameter increases by increasing the slip velocity parameter. The reason behind this behavior is that if we increase $\lambda$ it offers less resistance to fluid, because viscosity of fluid decreases, thus the velocity increases, and the boundary layer thickness reduces. In case of suction ($f_w = 1$) the effect of slip velocity parameter is more than other two cases. Figures 4.17 to 4.19 indicate the relationship for different values of slip velocity parameter on temperature distribution. It is clearly seen from figures that in all three cases ($f_w = 1, f_w = 0, f_w = -1$) rising the value of slip velocity results to decrease in temperature distribution. This is mainly due to increasing $\lambda$ kinematic viscosity decreases, so fluid particle can easily move therefore temperature decreases. It is also noticed that in case of injection boundary layer thickness accelerates.

### 4.3.4 Impact of Permeability Parameter

Figure 4.20 represents the effect of permeability parameter on velocity profile. It can be seen that during suction ($f_w > 0$) velocity profile increases because increase in suction parameter causes increase in flow rate. So it rises the velocity of fluid and the development of boundary layer thickness reduces by absorbing fluid particle through porous wall. Near the wall the impact of suction is diminished,

hence boundary layer thickness reduces and velocity seems to increase. It can also be observed that the viscosity of fluid decrease which rise the velocity. While during injection ($f_w < 0$) boundary layer region rises, which shows that injection cause more fluid diffusion and make larger the boundary layer. In suction case, wall shear stress increases, whereas in injection case shear wall stress decreases. Figure 4.21 describes the impact of permeability on temperature distribution, it is clearly noticed that boundary layer thickness reduces by increasing the suction parameter ($f_w > 0$) which increases the heat transfer rate. Or when raising the injection parameter ($f_w < 0$) boundary layer thickness seems increase. Moreover temperature profile decreases by increasing suction, injection parameter.

### 4.3.5 Impact of Eckert Number

Figures 4.22 to 4.24 show the effect of Eckert number on temperature distribution. As Eckert number specify the ratio of kinetic energy and enthalpy change of flow, it is inspected through figures that by rising the value of Eckert number temperature profile increases. Physically, the kinetic energy of the fluid particles rises as $Ec$ assumes the larger values. Hence, the temperature of the fluid increased and therefore, the associated thermal boundary layer thickness is enhanced. If we increases $Ec$ number enthalpy change of flow would decrease, which tends to increase in the temperature of fluid in all three cases ($f_w = 1, f_w = 0, f_w = -1$) for different value of Eckert number.

### 4.3.6 Impact of Heat Generation/Absorption

Figures 4.25 to 4.27 show the effect of heat generation/absorption on temperature distribution. It is observed that for increasing value of $\gamma$, which generated more heat, because of this temperature distribution and thermal boundary layer thickness increases, for all three cases ($f_w = 1, f_w = 0, f_w = -1$). On other hand if the value of $\gamma$ decreases, the heat will be absorbed which causes a decreases in temperature and boundary layer thickness.

### 4.3.7 Impact of Radiation Parameter

Figures 4.28 to 4.30 reveal the impact of radiation parameter on temperature profile. by increasing the radiation parameter, temperature profile and boundary layer thickness decreased, in case of suction and impermeable plate ($f_w = 1$,$f_w = 0$). As in a medium the intensity of electro-magnetic radiation decreases as StefanBoltzmann constant increases so temperature decreases. In case of injection ($f_w = -1$) temperature increases, because it strengthens the fact that more heat is produced due to the radiation process for which the temperature profile is increased.

### 4.3.8 Impact of Thermal Slip Parameter

Figures 4.31 to 4.33 show the effect of thermal slip parameter on temperature distribution. In case of suction and impermeable plate ($f_w = 1$ or $f_w = 0$) it is noticed that temperature profile decreases for increasing value of thermal slip parameter because less heat is transfered from plate to the fluid, so temperature decreases. while reversed nature can be seen in case of injection ($f_w = -1$). Moreover the effect of thermal slip parameter is greater on surface temperature, in case of suction ($f_w = 1$) or impermeable plate ($f_w = 0$).

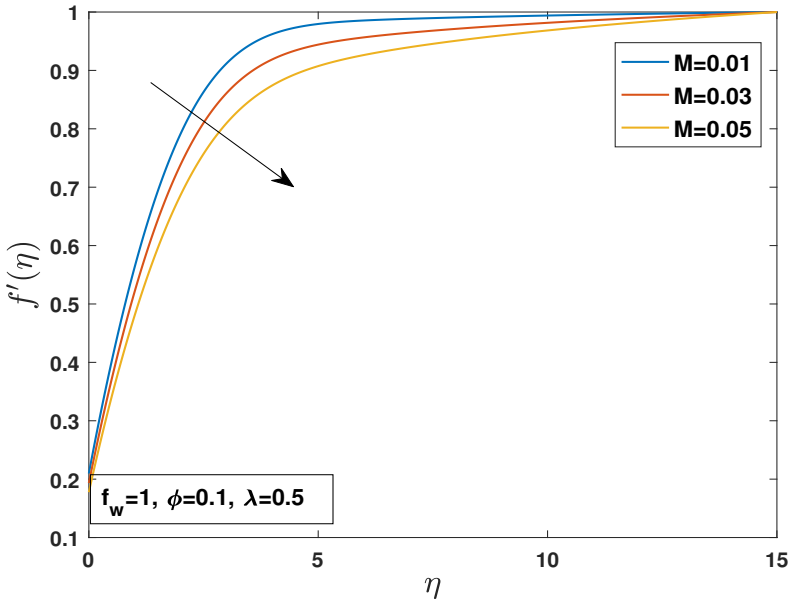


FIGURE 4.2: Effects of $M$ on velocity distribution for suction.

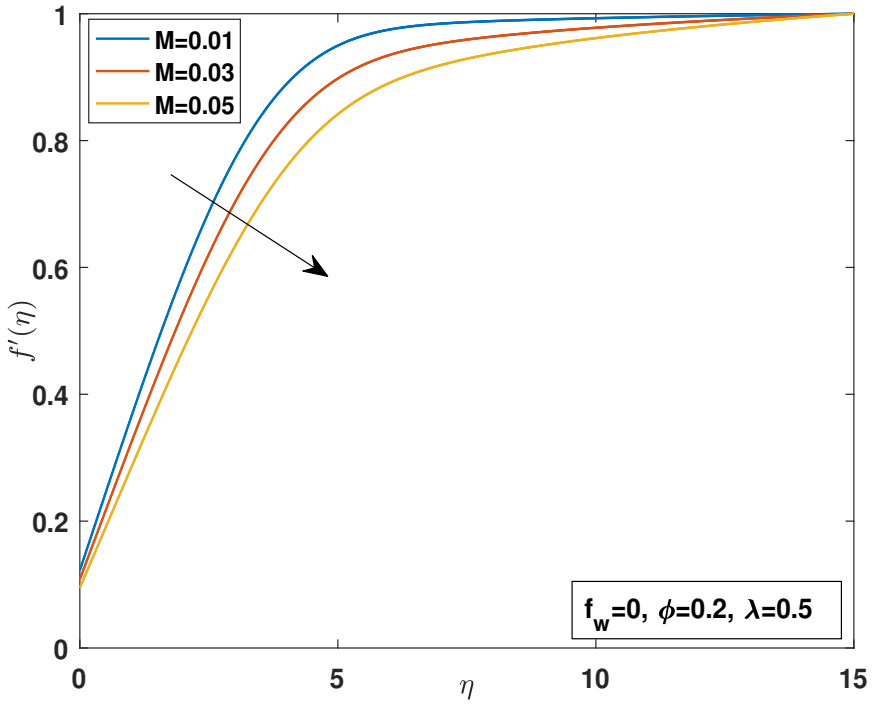


FIGURE 4.3: Effects of $M$ on velocity distribution for impermeable plate.

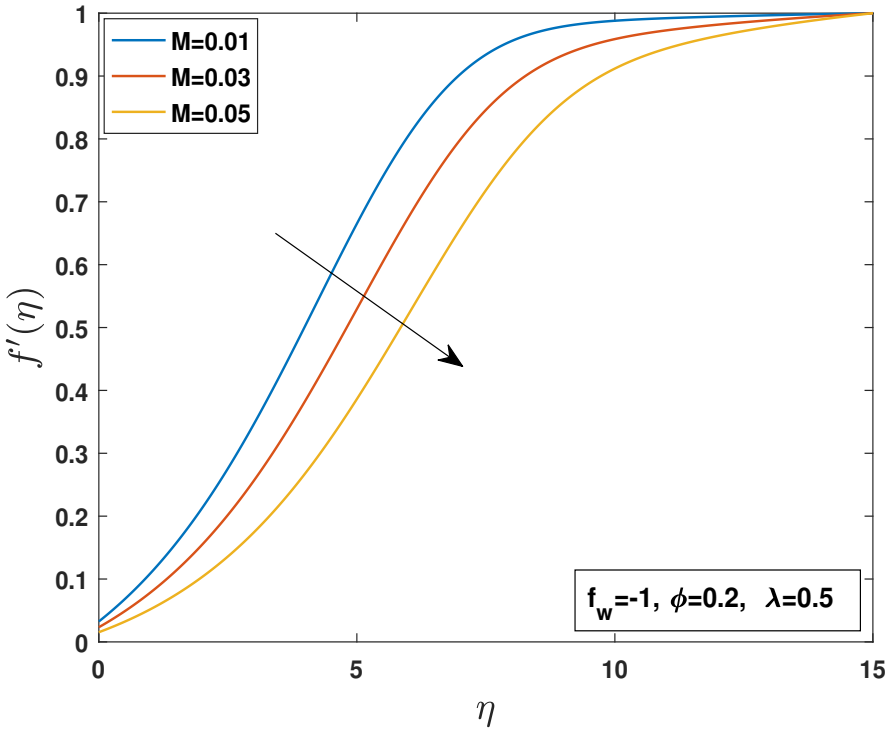


FIGURE 4.4: Effects of $M$ on velocity distribution for injection.

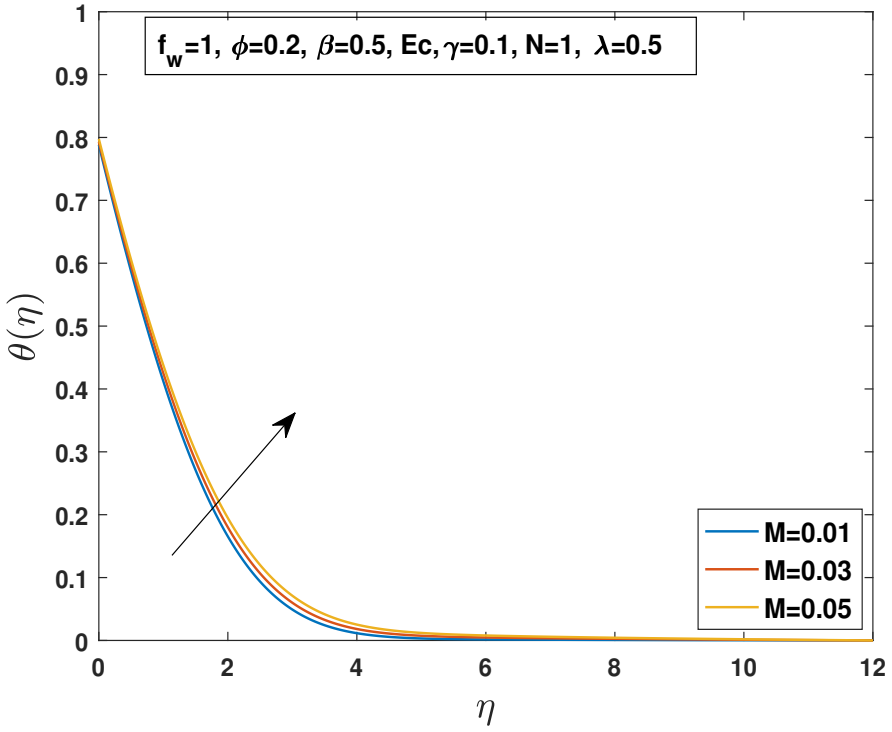


FIGURE 4.5: Effects of $M$ on temperature distribution for suction

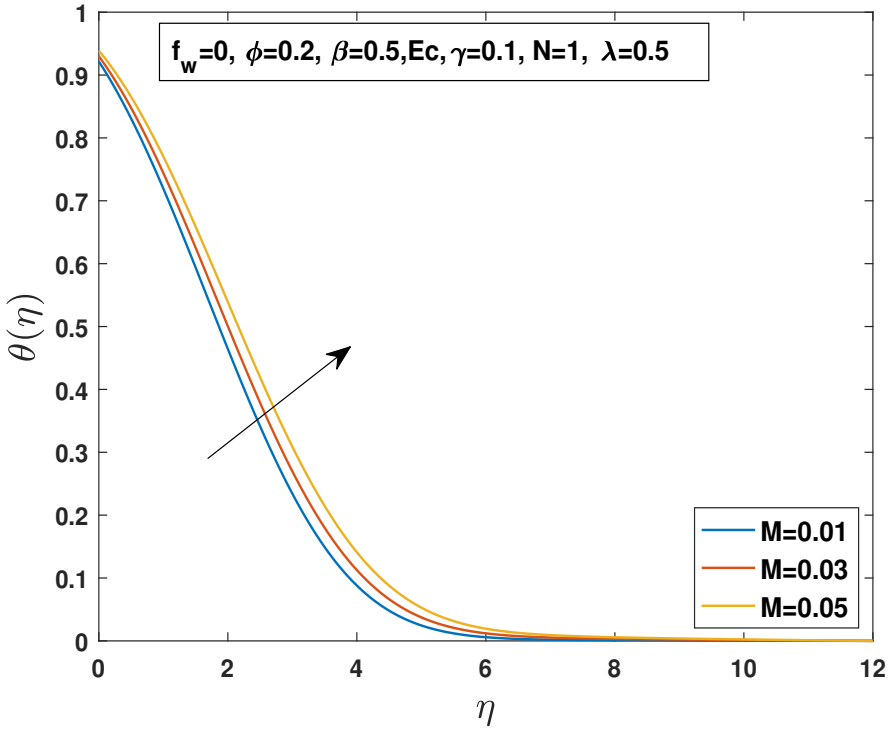


FIGURE 4.6: Effects of $M$ on temperature distribution for impermeable plate.

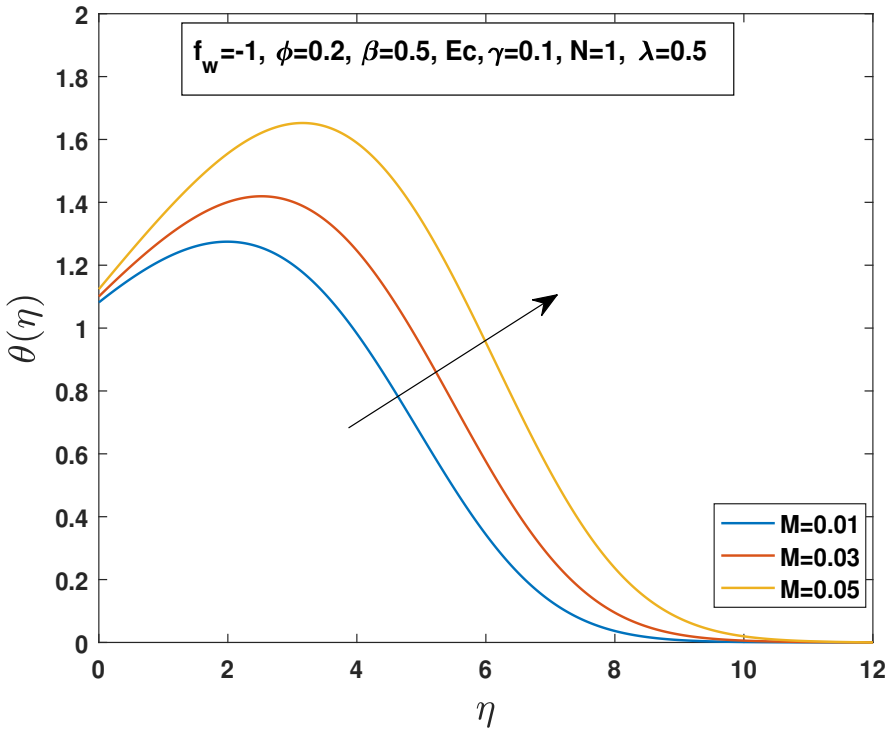


FIGURE 4.7: Effects of $M$ on temperature distribution for injection.

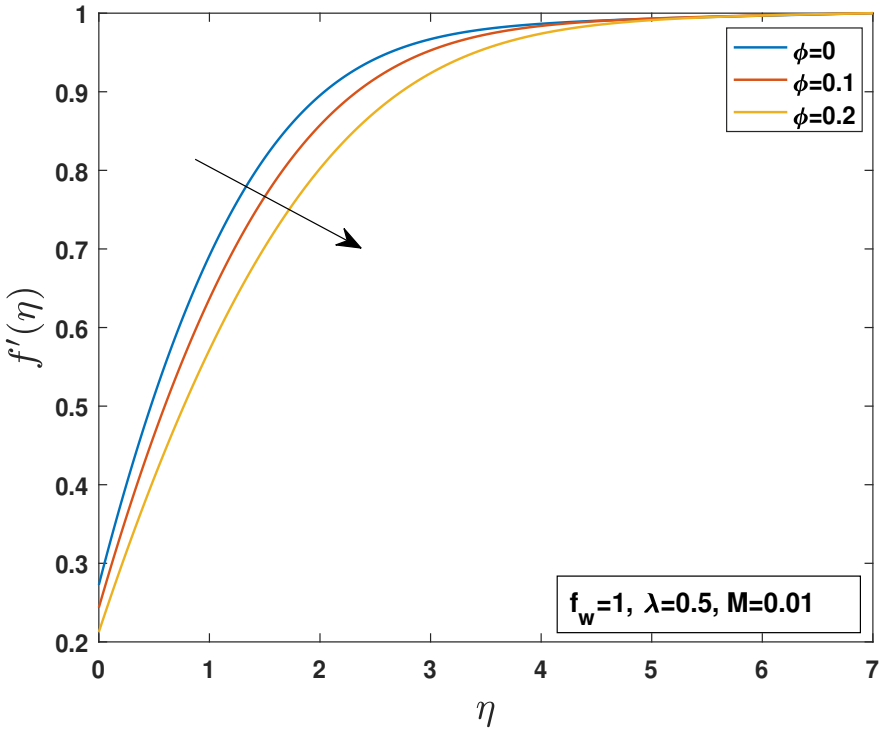


FIGURE 4.8: Effects of $\phi$ on velocity distribution for suction.

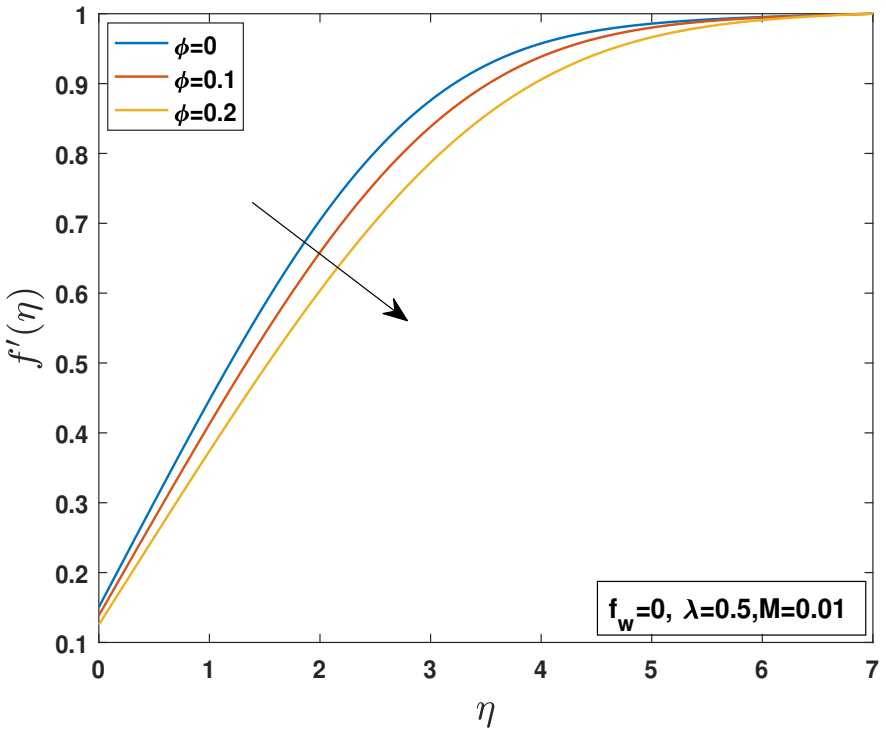


FIGURE 4.9: Effects of $\phi$ on velocity distribution for impermeable plate.

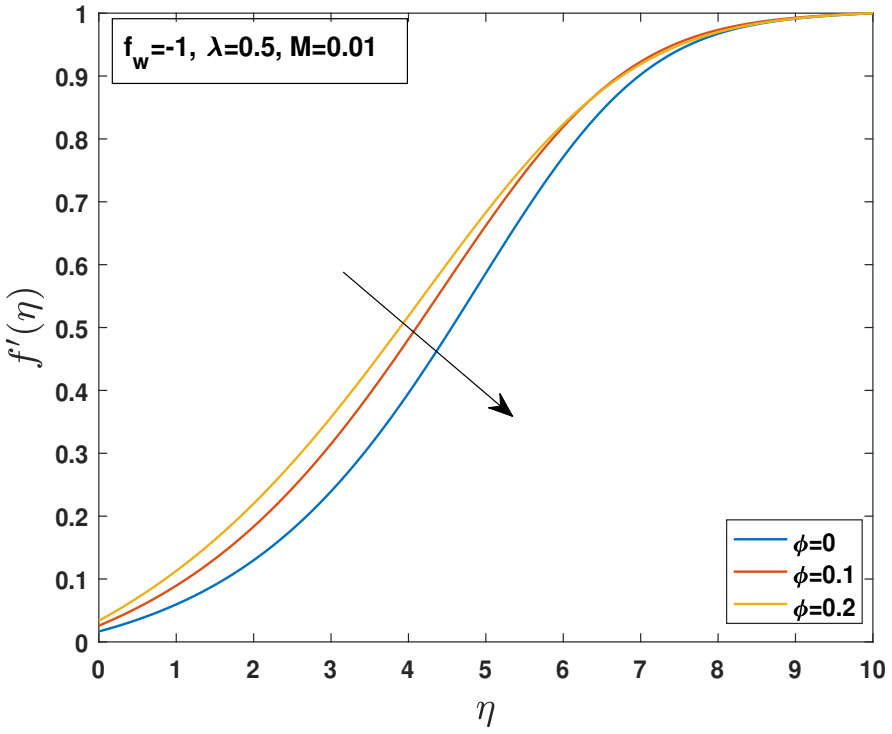


FIGURE 4.10: Effects of $\phi$ on velocity distribution for injection.

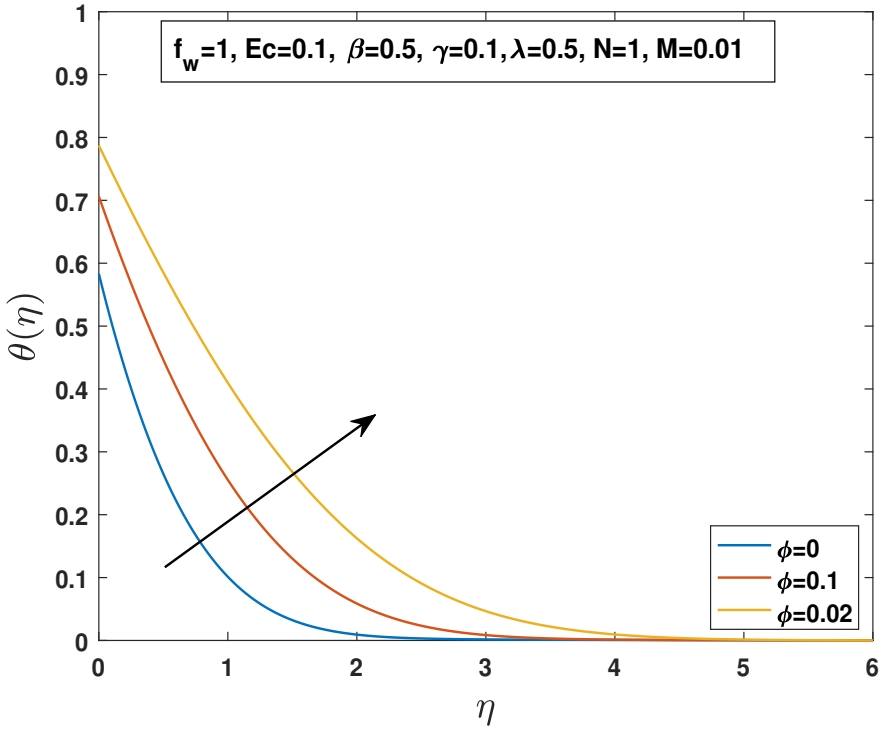


FIGURE 4.11: Effects of $\phi$ on temperature distribution for suction.

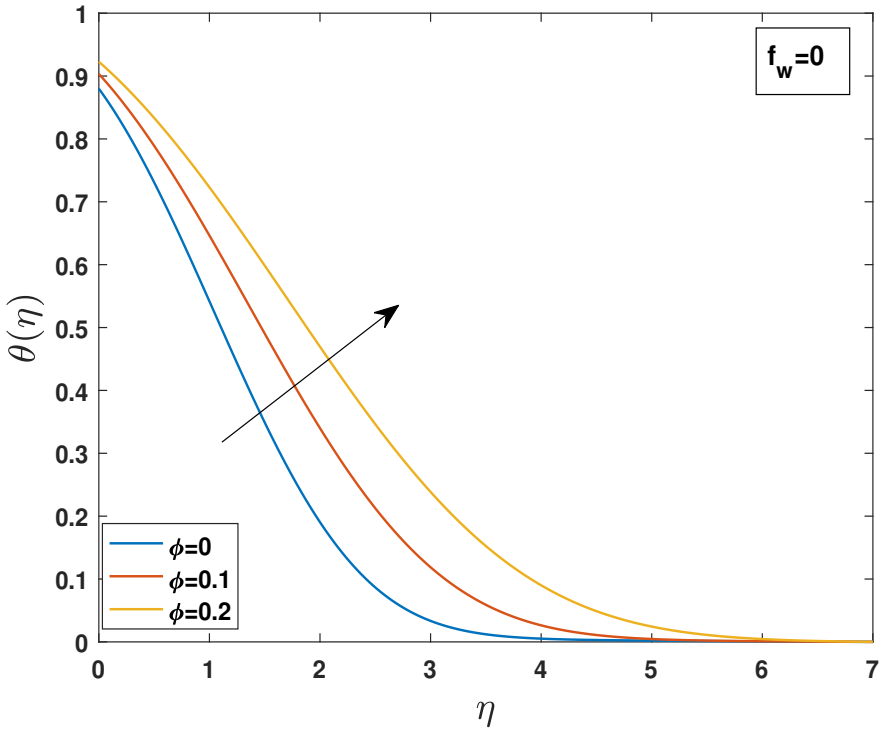


FIGURE 4.12: Effects of $\phi$ on temperature distribution for impermeable plate.

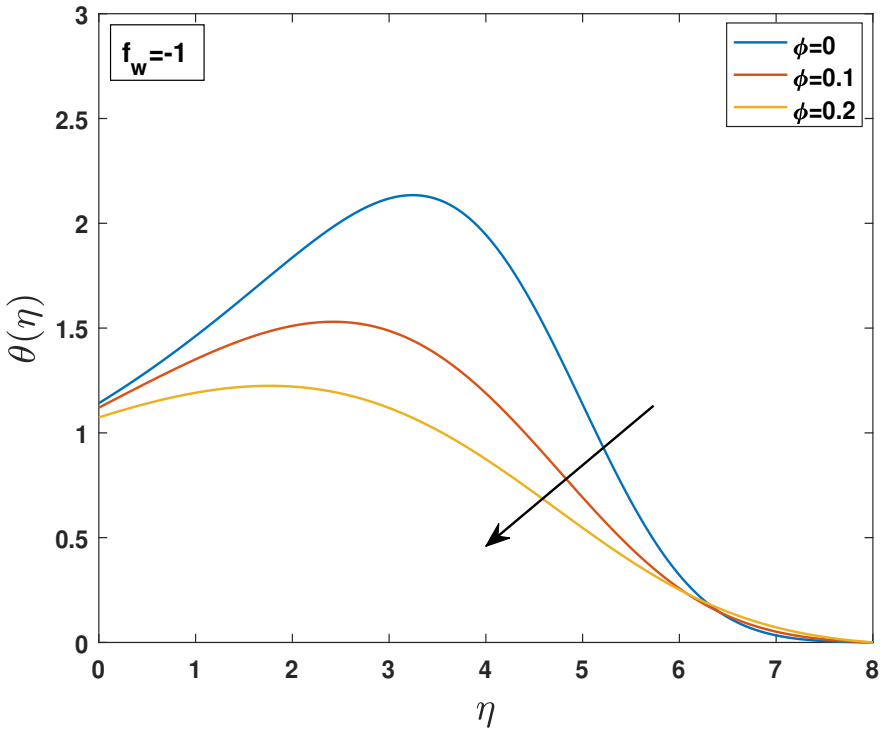


FIGURE 4.13: Effects of $\phi$ on temperature distribution for injection.

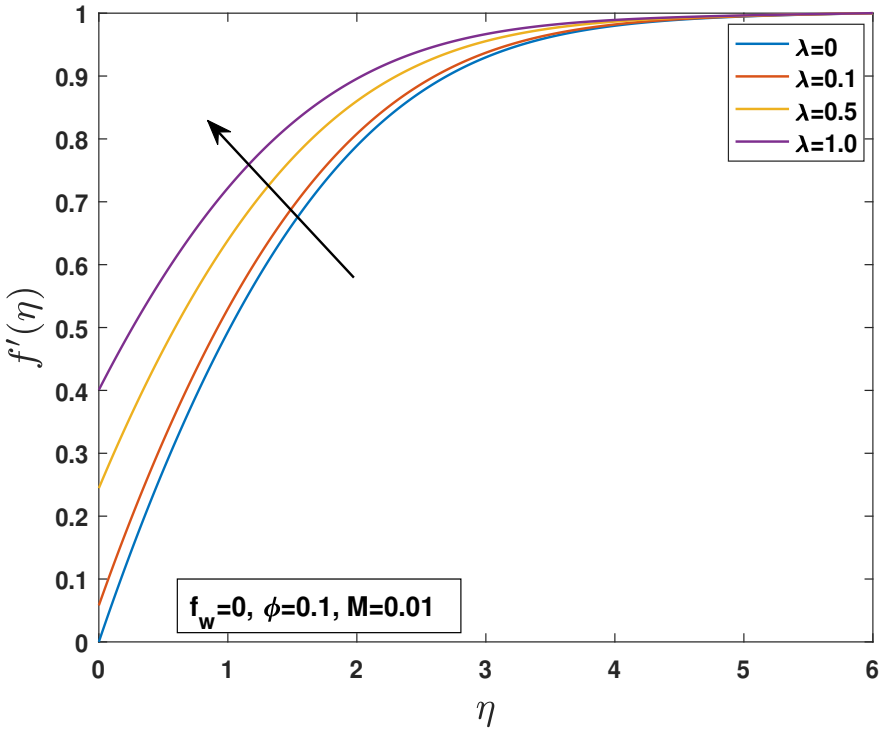


FIGURE 4.14: Effects of $\lambda$ on velocity distribution for suction.

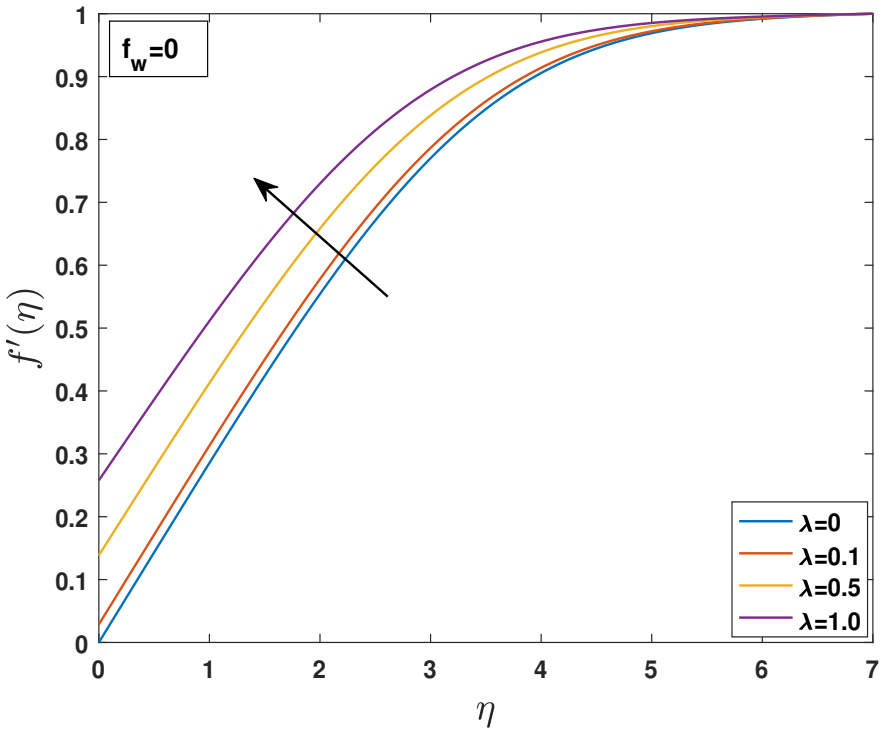


FIGURE 4.15: Effects of $\lambda$ on velocity distribution for impermeable plate.

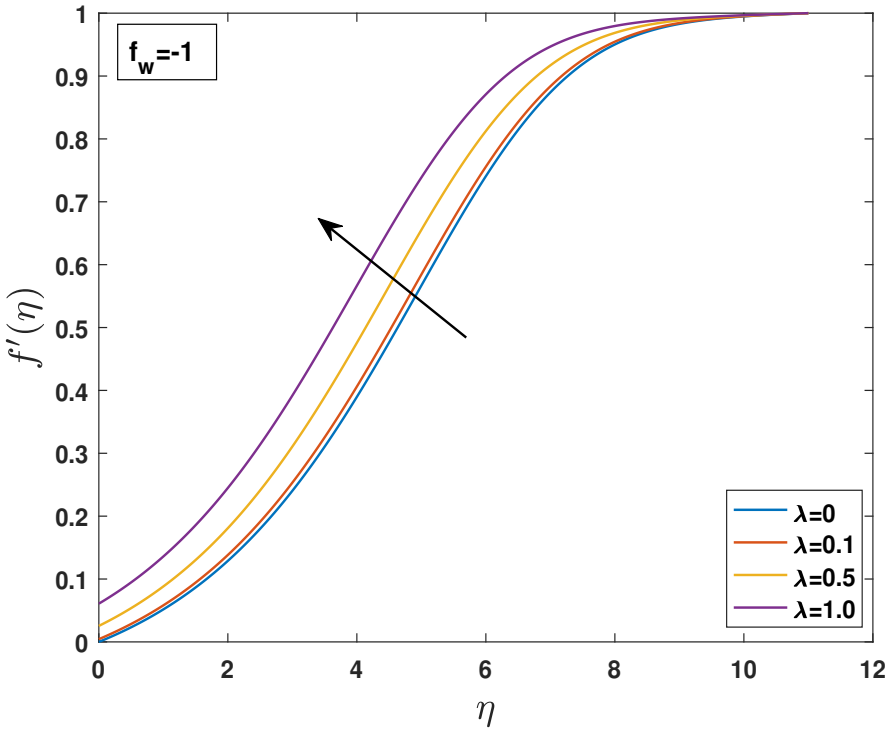


FIGURE 4.16: Effects of $\lambda$ on velocity distribution for injection.

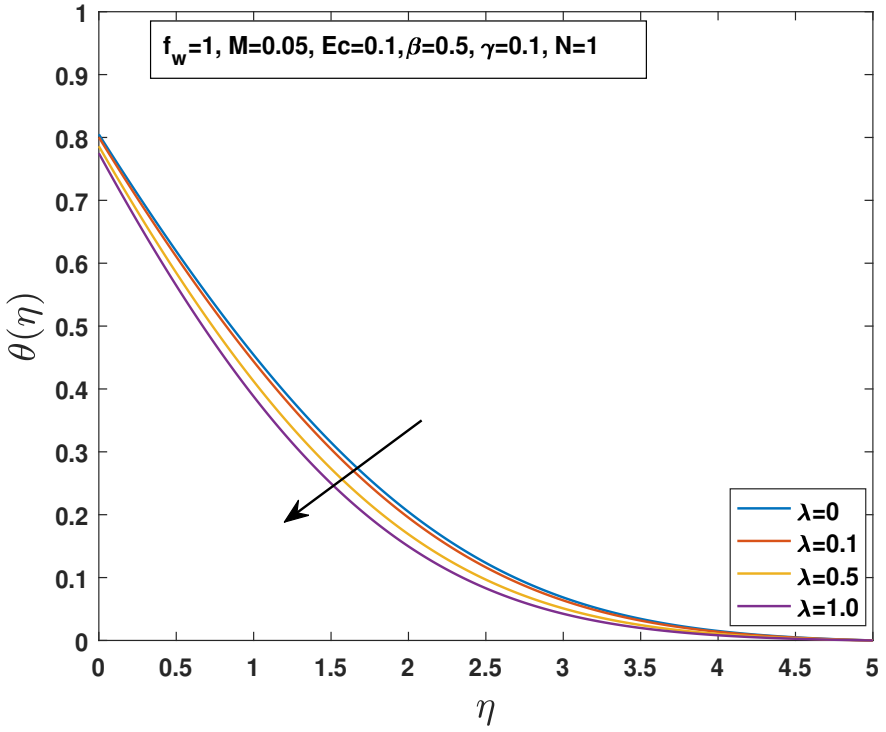


FIGURE 4.17: Effects of $\lambda$ on temperature distribution for suction.

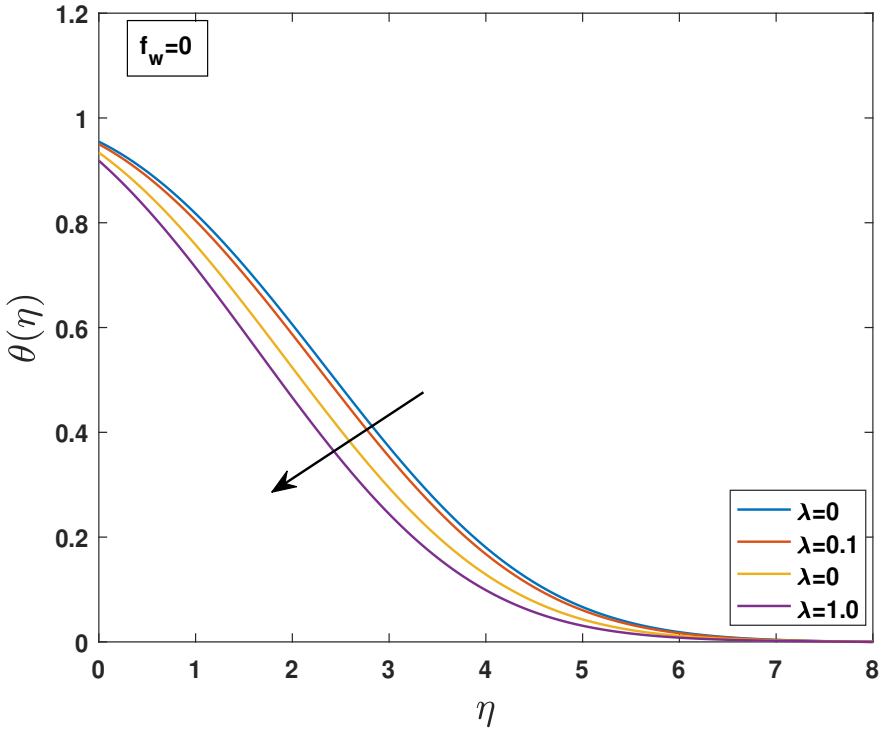


FIGURE 4.18: Effects of $\lambda$ on temperature distribution for impermeable plate.

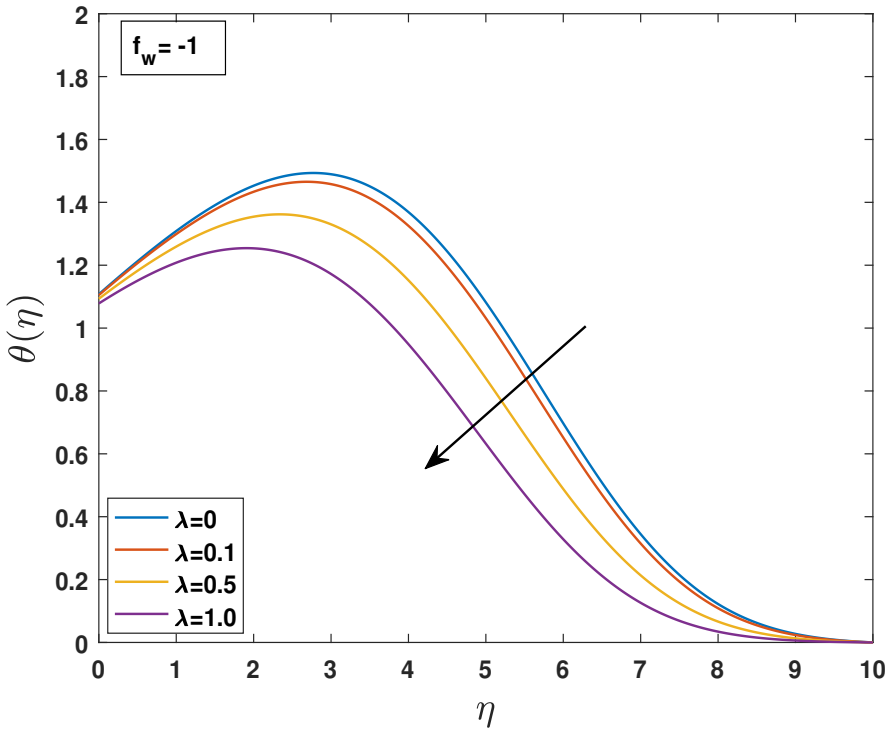


FIGURE 4.19: Effects of $\lambda$ on temperature distribution for injection.

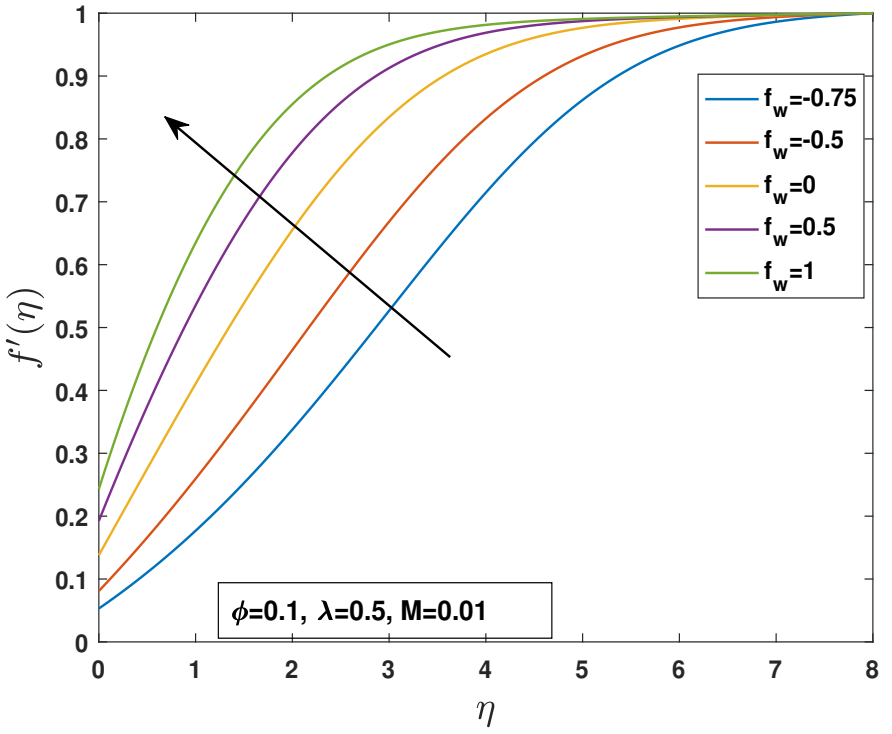


FIGURE 4.20: Effects of permeability parameter on velocity distribution.

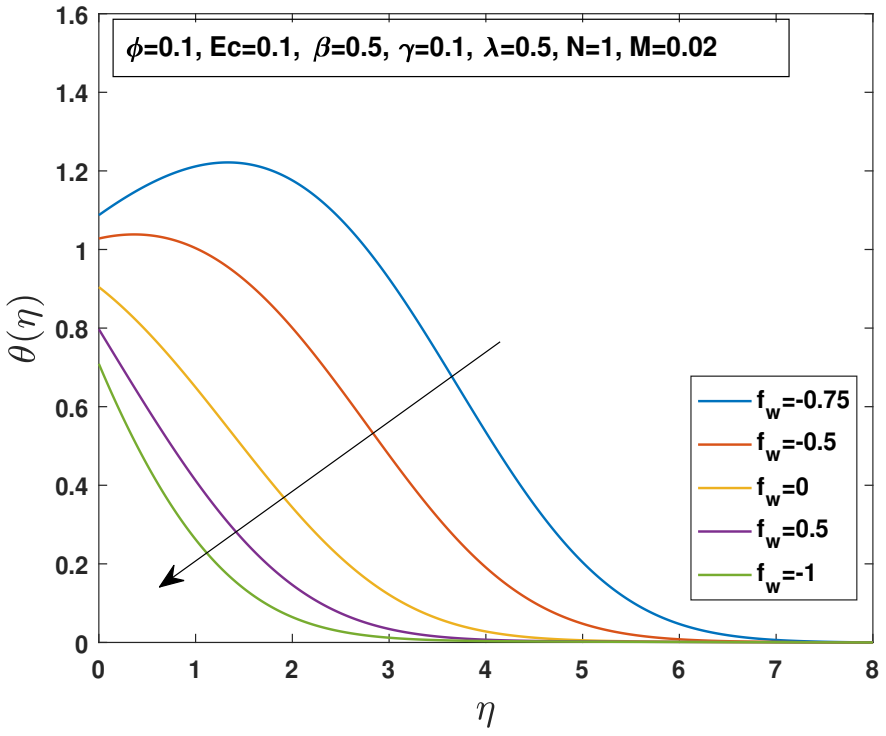


FIGURE 4.21: Effects of permeability parameter on temperature distribution.

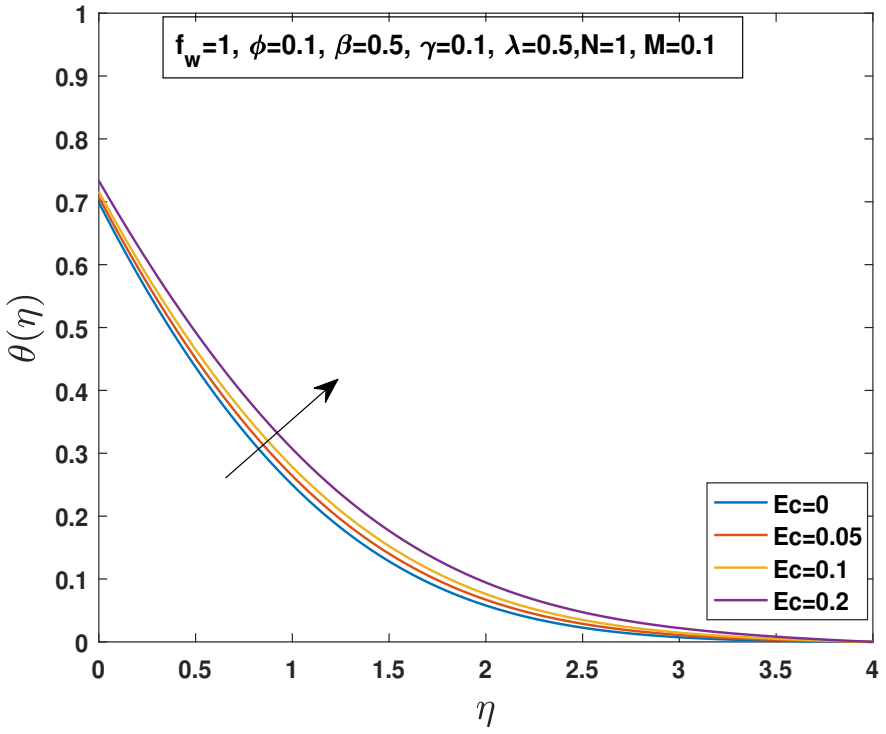


FIGURE 4.22: Effects of $Ec$ on temperature distribution for suction.

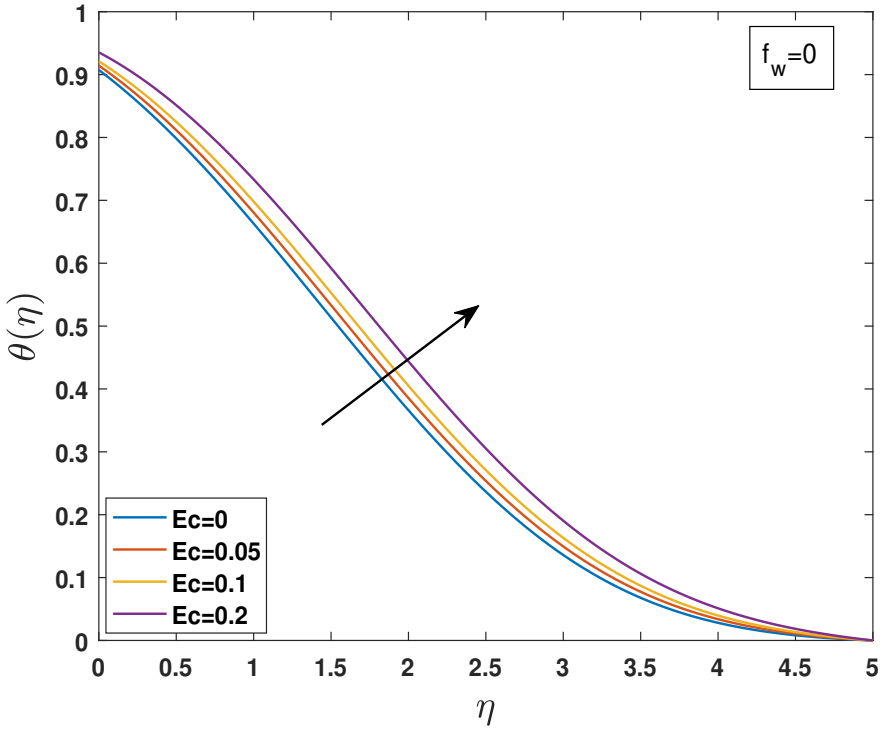


FIGURE 4.23: Effects of $Ec$ on temperature distribution for impermeable plate.

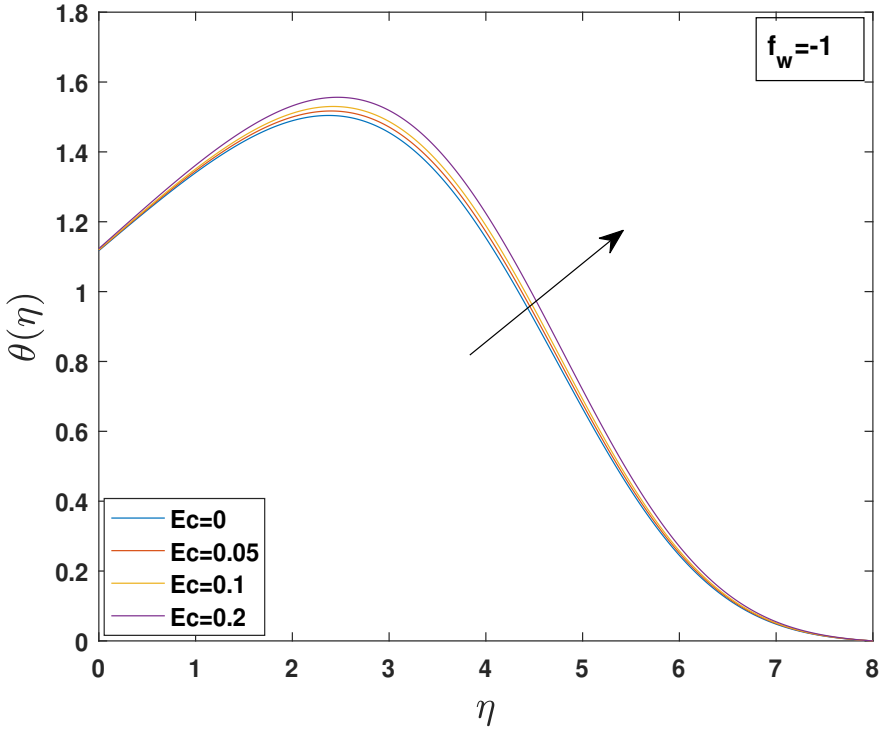


FIGURE 4.24: Effects of $Ec$ on temperature distribution for injection.

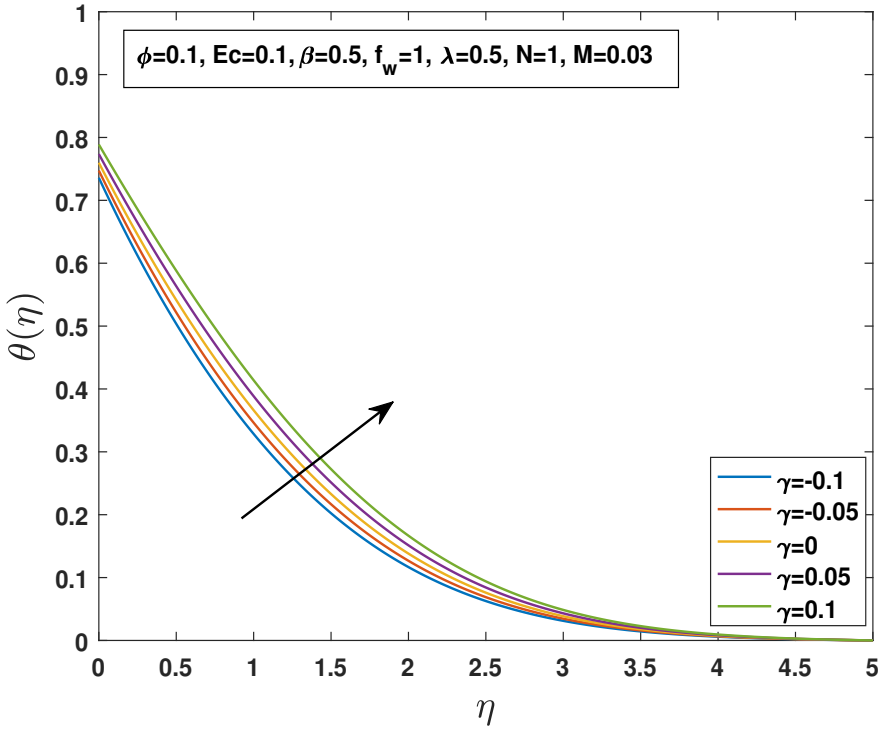


FIGURE 4.25: Effects of $\gamma$ on temperature distribution for suction.

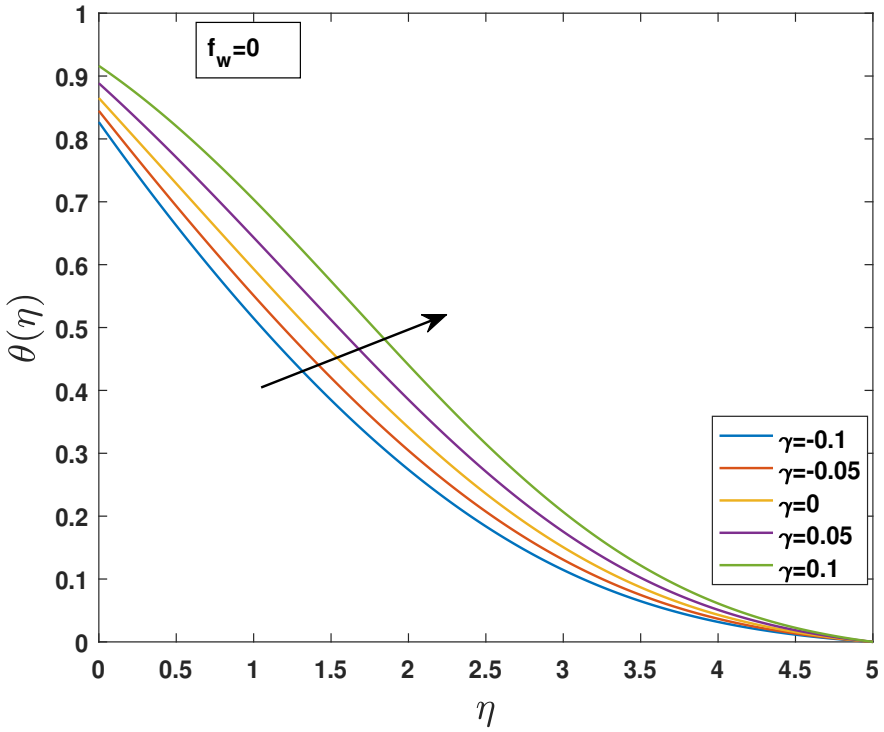


FIGURE 4.26: Effects of $\gamma$ on temperature distribution for impermeable plate.

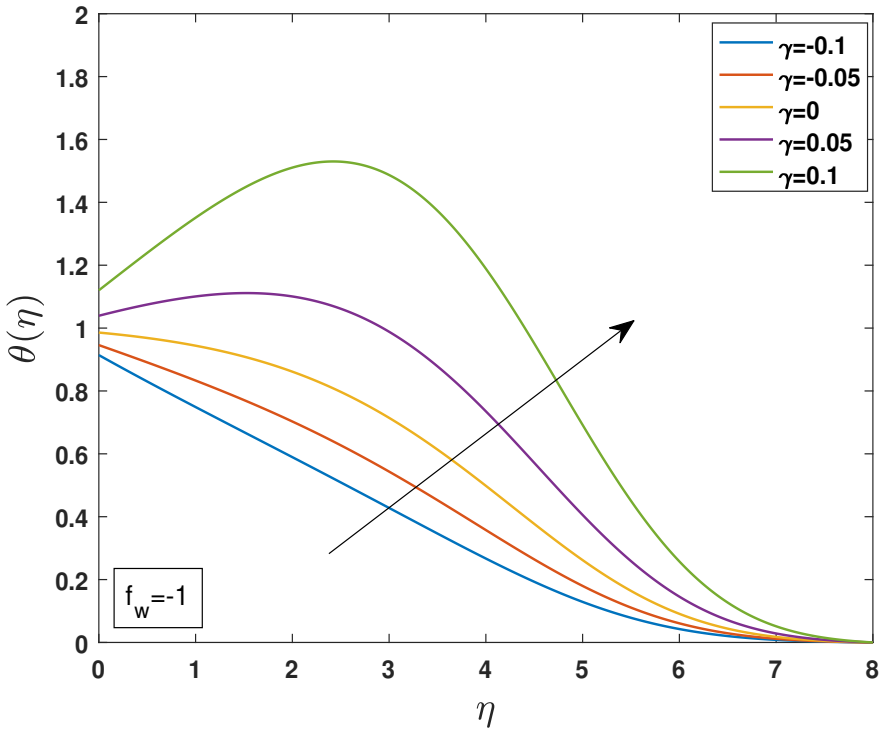


FIGURE 4.27: Effects of $\gamma$ on temperature distribution for injection.

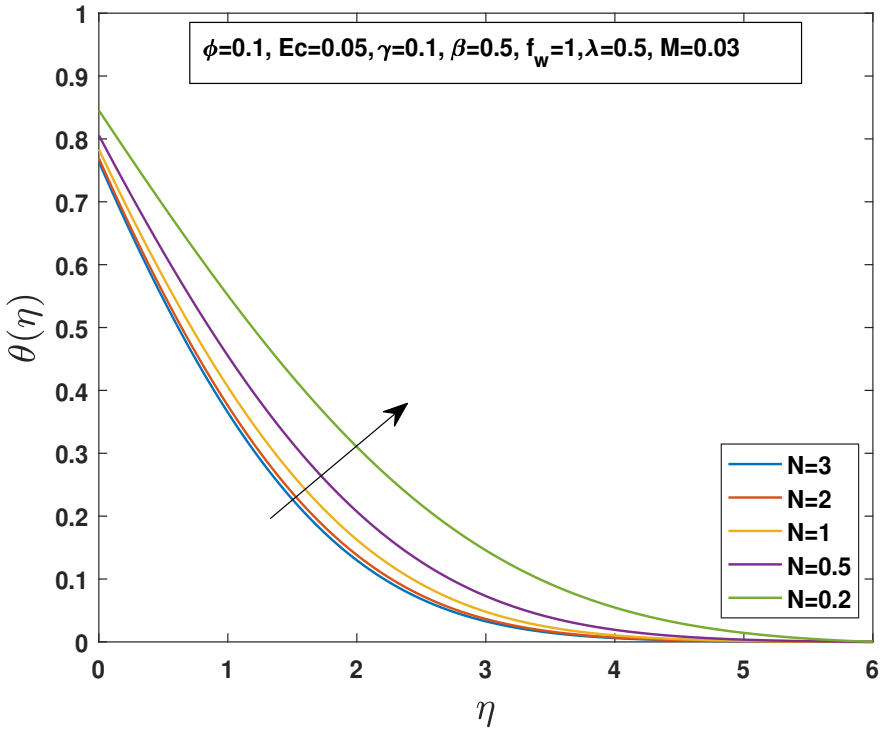


FIGURE 4.28: Effects of $N$ on temperature distribution for suction.

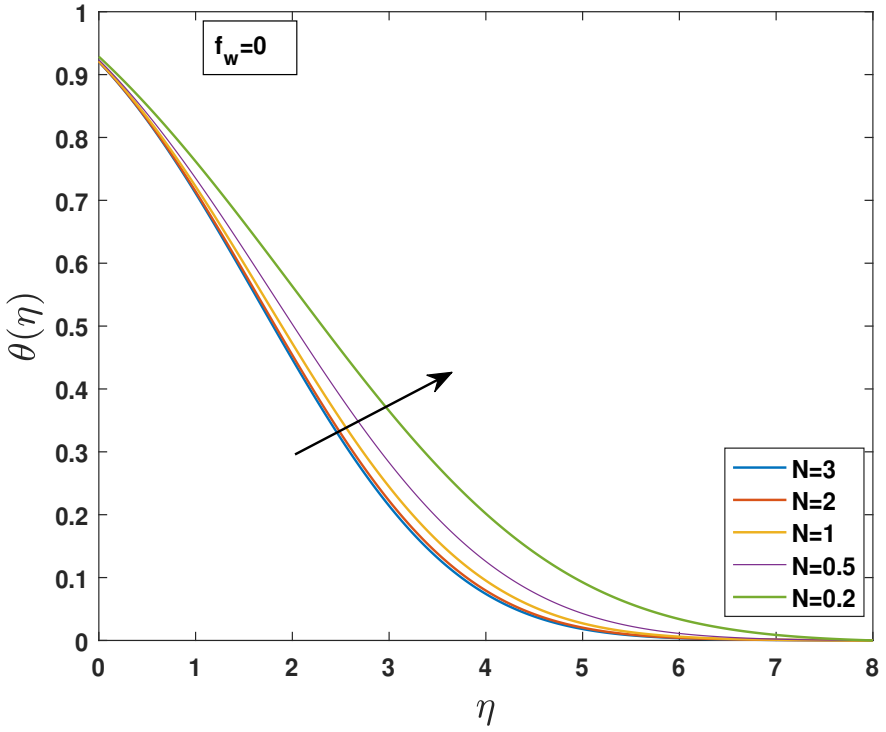


FIGURE 4.29: Effects of $N$ on temperature distribution for impermeable.

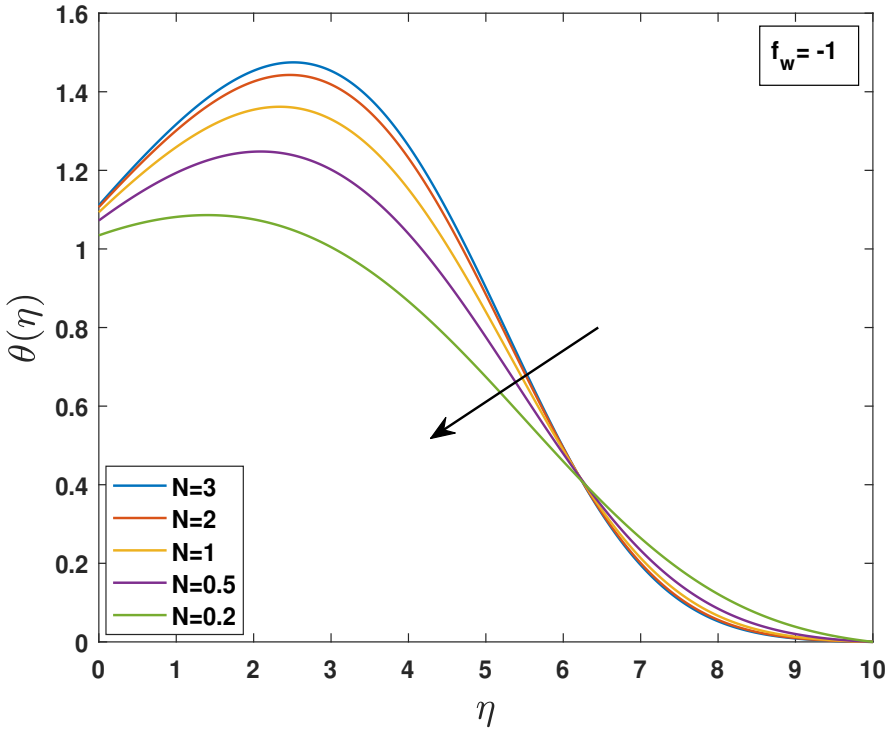


FIGURE 4.30: Effects of $N$ on temperature distribution for injection.

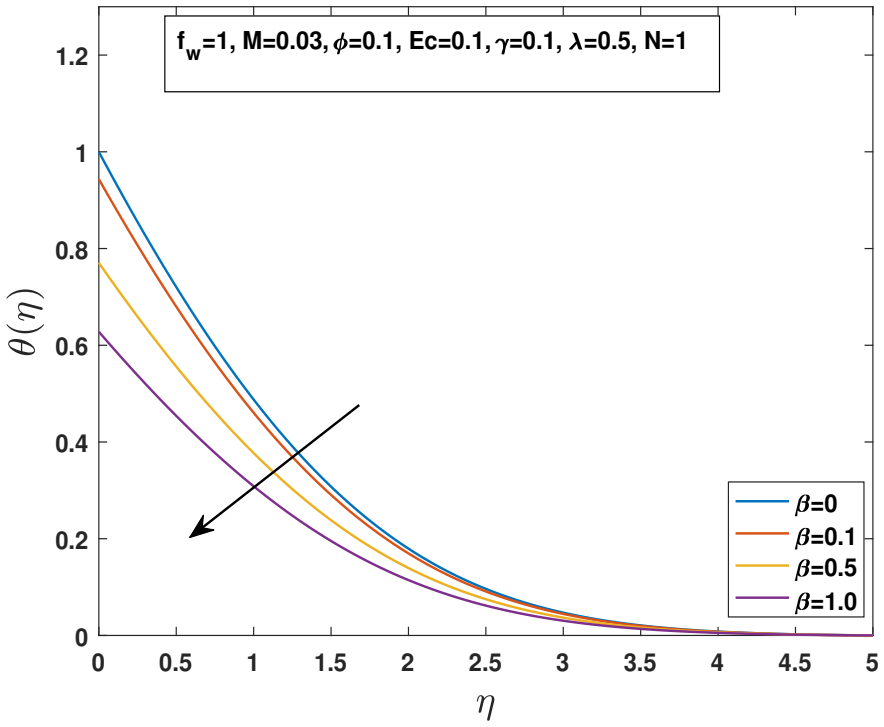


FIGURE 4.31: Effects of $\beta$ on temperature distribution for suction.

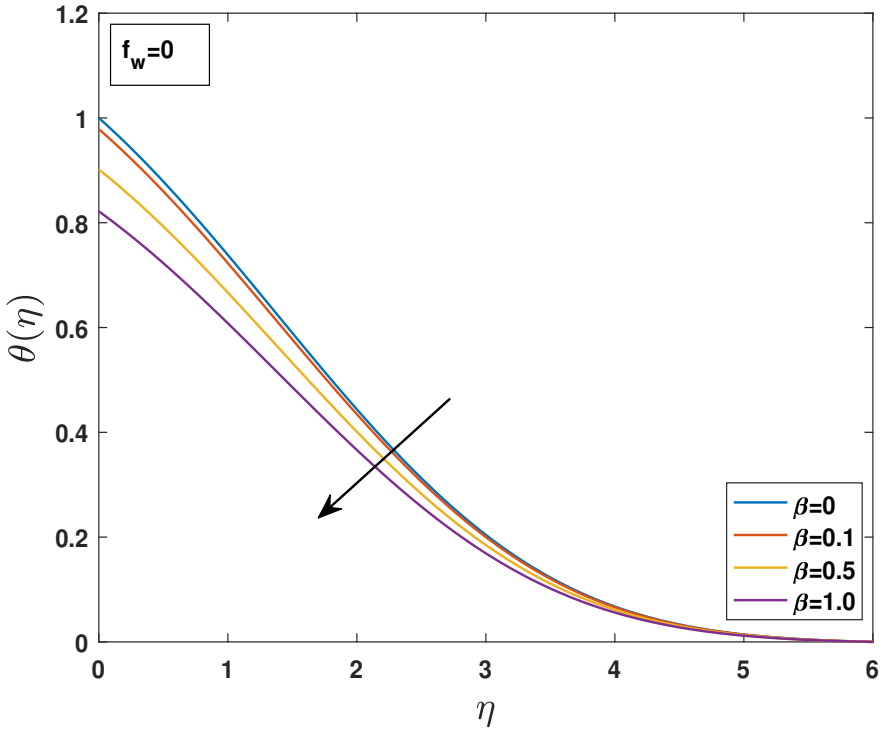


FIGURE 4.32: Effects of $\beta$ on temperature distribution for impermeable plate.

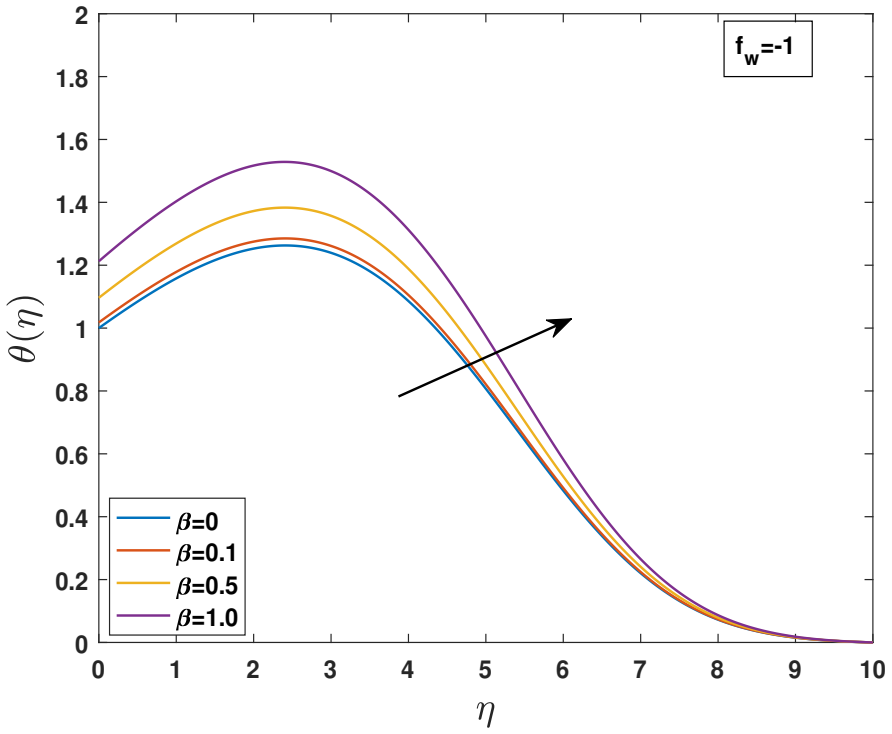


FIGURE 4.33: Effects of $\beta$ on temperature distribution for injection.

# Chapter 5

# Conclusion

In this thesis, we examined the numerical investigation of the MHD heat transfer and boundary layer flow of nanofluid over a porous plate by considering the effect of various parameter including thermal radiation, viscous dissipation, heat generation/absorption and Joule heating effects. Moreover, slip boundary condition at the boundary is also considered. By using similarity transformation we convert the governing PDEs into system of ODEs. The shooting technique has been used for the calculation of numerical results along with RK4. Impact of different parameter such as Magenetic parametr $M$, Eckert number $Ec$, nanoparticle volume fraction $\phi$, heat generation/absorption $\gamma$, Radiation parameter $N$, permeability parameter $f_w$ velocity slip parameter $\lambda$ and thermal slip parameter $\beta$ on the velocity and temperature profile is discussed graphically. The investigation showed a different results in some cases with the outcomes of other researchers.

Results obtained in this thesis are summarized below:

- Nanoparticles volume fraction tends to decrease the velocity for the case of suction and impermeable plate, whereas opposite trend has been observed for injection.
- With an increase in the nanoparticles volume fraction, the temperature of the fluid also increases for suction and impermeable plate. while for injection

boosting the nanoparticles volume fraction has potential to decrease the heat transfer rate.

- Rise in magnetic number exhibit decreases the velocity of nanofluid.
- The temperature profile increases by rising the magnetic number.
- The velocity profile increases by increasing the slip velocity parameter but opposite trend is observed for temperature profile.
- Increasing the value of radiation parameter, Eckert number and heat generation/absorption results in an increases in the temperature profile.
- In case of suction and impermeable plate local skin-friction rises by rising the nanaoparticles volume fraction.
- Local skin-fricition decreases by increases the slip velocity and injection parameter. However, for suction parameter it is increases.
- Boosting the value of nanoparticles volume fraction, Eckert number and radiation parameter, the local Nusselt number is decreased.

# Bibliography


[1] F. M. White, *Fluid Mechanics Seventh Edition.* MC-Graw Hill Brasil, 1962.

[2] D. W. Vasco and A. Datta-Gupta, *Subsurface Fluid Flow and Imaging: With Applications for Hydrology, Reservoir Engineering, and Geophysics.* Cambridge University Press, 2016.

[3] E. J. Finnemore and J. B. Franzini, *Fluid mechanics with engineering applications.* McGraw-Hill New York, 2002, vol. 10.

[4] J.-F. Gerbeau, M. Vidrascu, and P. Frey, "Fluid–structure interaction in blood flows on geometries based on medical imaging," *Computers & Structures*, vol. 83, no. 2-3, pp. 155–165, 2005.

[5] S. U. Choi and J. A. Eastman, "Enhancing thermal conductivity of fluids with nanoparticles," Argonne National Lab., IL (United States), Tech. Rep., 1995.

[6] J. Buongiorno, "Convective transport in nanofluids," *Journal of heat transfer*, vol. 128, no. 3, pp. 240–250, 2006.

[7] R. Pal, "A novel method to determine the thermal conductivity of interfacial layers surrounding the nanoparticles of a nanofluid," *Nanomaterials*, vol. 4, no. 4, pp. 844–855, 2014.

[8] M. H. Bahmani, G. Sheikhzadeh, M. Zarringhalam, O. A. Akbari, A. A. Alrashed, G. A. S. Shabani, and M. Goodarzi, "Investigation of turbulent heat transfer and nanofluid flow in a double pipe heat exchanger," *Advanced Powder Technology*, vol. 29, no. 2, pp. 273–282, 2018.

[9] M. Bahiraei, M. Jamshidmofid, and M. Goodarzi, "Efficacy of a hybrid nanofluid in a new microchannel heat sink equipped with both secondary channels and ribs," *Journal of Molecular Liquids*, vol. 273, pp. 88–98, 2019.

[10] M. Mahmoodi and S. Kandelousi, "Kerosene-Alumina nanofluid flow and heat transfer for cooling application," *Journal of Central South University*, vol. 23, no. 4, pp. 983–990, 2016.

[11] A. Kasaeian, R. Daneshazarian, O. Mahian, L. Kolsi, A. J. Chamkha, S. Wongwises, and I. Pop, "Nanofluid flow and heat transfer in porous media: a review of the latest developments," *International Journal of Heat and Mass Transfer*, vol. 107, pp. 778–791, 2017.

[12] N. V. Ganesh, A. A. Hakeem, and B. Ganga, "Darcy-Forchheimer flow of hydromagnetic nanofluid over a stretching/shrinking sheet in a thermally stratified porous medium with second order slip, viscous and Ohmic dissipations effects," *Ain Shams Engineering Journal*, vol. 9, no. 4, pp. 939–951, 2018.

[13] A. Zeeshan, N. Shehzad, T. Abbas, and R. Ellahi, "Effects of radiative electromagnetohydrodynamics diminishing internal energy of pressure-driven flow of titanium dioxide-water nanofluid due to entropy generation," *Entropy*, vol. 21, no. 3, p. 236, 2019.

[14] S. Ghadikolaei, K. Hosseinzadeh, D. Ganji, and B. Jafari, "Nonlinear thermal radiation effect on magneto Casson nanofluid flow with Joule heating effect over an inclined porous stretching sheet," *Case Studies in Thermal Engineering*, vol. 12, pp. 176–187, 2018.

[15] Y. Xuan and Q. Li, "Investigation on convective heat transfer and flow features of nanofluids," *J. Heat transfer*, vol. 125, no. 1, pp. 151–155, 2003.

[16] Y. Hwang, Y. Ahn, H. Shin, C. Lee, G. Kim, H. Park, and J. Lee, "Investigation on characteristics of thermal conductivity enhancement of nanofluids," *Current Applied Physics*, vol. 6, no. 6, pp. 1068–1071, 2006.

[17] Y. Hwang, H. Park, J. Lee, and W. Jung, "Thermal conductivity and lubrication characteristics of nanofluids," *Current Applied Physics*, vol. 6, pp. e67–e71, 2006.

[18] M. Sabiha, R. Mostafizur, R. Saidur, and S. Mekhilef, "Experimental investigation on thermophysical properties of single walled carbon nanotube nanofluids," *International Journal of Heat and Mass Transfer*, vol. 93, pp. 862–871, 2016.

[19] M. Hajmohammadi, H. Maleki, G. Lorenzini, and S. Nourazar, "Effects of $Cu$ and $Ag$ nanoparticles on flow and heat transfer from permeable surfaces," *Advanced Powder Technology*, vol. 26, no. 1, pp. 193–199, 2015.

[20] B. Xia and D.-W. Sun, "Applications of computational fluid dynamics (CFD) in the food industry: a review," *Computers and electronics in agriculture*, vol. 34, no. 1-3, pp. 5–24, 2002.

[21] Z. Zhai, "Application of computational fluid dynamics in building design: aspects and trends," *Indoor and built environment*, vol. 15, no. 4, pp. 305–313, 2006.

[22] C. Zhang, M. Saadat, P. Y. Li, and T. W. Simon, "Heat transfer in a long, thin tube section of an air compressor: An empirical correlation from CFD and a thermodynamic modeling," in *ASME International Mechanical Engineering Congress and Exposition*, vol. 45233. American Society of Mechanical Engineers, 2012, pp. 1601–1607.

[23] O. Mahian, A. Kianifar, S. A. Kalogirou, I. Pop, and S. Wongwises, "A review of the applications of nanofluids in solar energy," *International Journal of Heat and Mass Transfer*, vol. 57, no. 2, pp. 582–594, 2013.

[24] W. Liu, P. Liu, J. Wang, N. Zheng, and Z. Liu, "Energy destruction minimization: A principle to convective heat transfer enhancement," *International Journal of Heat and Mass Transfer*, vol. 122, pp. 11–21, 2018.

[25] S. Sadri and M. Babaelahi, "Analysis of a laminar boundary layer flow over a flat plate with injection or suction," *Journal of Applied Mechanics and Technical Physics*, vol. 54, no. 1, pp. 59–67, 2013.

[26] S. Iijima, "Helical microtubules of graphitic carbon," *Nature*, vol. 354, no. 6348, pp. 56–58, 1991.

[27] R. U. Haq, S. Nadeem, Z. H. Khan, and N. F. M. Noor, "Convective heat transfer in MHD slip flow over a stretching surface in the presence of carbon nanotubes," *Physica B: condensed matter*, vol. 457, pp. 40–47, 2015.

[28] M. M. Nandeppanavar, R. S. Reddy Gorla, and S. Shakunthala, "Magneto-hydrodynamic Blasius flow and heat transfer from a flat plate in the presence of suspended carbon nanofluids," *Proceedings of the Institution of Mechanical Engineers, Part N: Journal of Nanomaterials, Nanoengineering and Nanosystems*, vol. 232, no. 1, pp. 31–40, 2018.

[29] H. Xie, H. Lee, W. Youn, and M. Choi, "Nanofluids containing multiwalled carbon nanotubes and their enhanced thermal conductivities," *Journal of Applied physics*, vol. 94, no. 8, pp. 4967–4971, 2003.

[30] B. C. Sakiadis, "Boundary-layer behavior on continuous solid surfaces: I. boundary-layer equations for two-dimensional and axisymmetric flow," *AIChE Journal*, vol. 7, no. 1, pp. 26–28, 1961.

[31] H. Blasius, *Grenzschichten in Flüssigkeiten mit kleiner Reibung.* Druck von BG Teubner, 1907.

[32] L. Howarth, "On the solution of the laminar boundary layer equations," *Proceedings of the Royal Society of London. Series A, Mathematical and Physical Sciences*, pp. 547–579, 1938.

[33] E. G. Fisher, "Extrusion of plastics," 1976.

[34] L. J. Crane, "Flow past a stretching plate," *Zeitschrift für angewandte Mathematik und Physik ZAMP*, vol. 21, no. 4, pp. 645–647, 1970.

[35] C. Wang, "Stagnation flow towards a shrinking sheet," *International Journal of Non-Linear Mechanics*, vol. 43, no. 5, pp. 377–382, 2008.

[36] K. Das, T. Chakraborty, and P. Kumar Kundu, "Slip effects on nanofluid flow over a nonlinear permeable stretching surface with chemical reaction," *Proceedings of the Institution of Mechanical Engineers, Part C: Journal of Mechanical Engineering Science*, vol. 230, no. 14, pp. 2473–2482, 2016.

[37] N. S. Akbar, S. Nadeem, R. U. Haq, and Z. Khan, "Radiation effects on MHD stagnation point flow of nano fluid towards a stretching surface with convective boundary condition," *Chinese Journal of Aeronautics*, vol. 26, no. 6, pp. 1389–1397, 2013.

[38] I. Sumirat, Y. Ando, and S. Shimamura, "Theoretical consideration of the effect of porosity on thermal conductivity of porous materials," *Journal of Porous Materials*, vol. 13, no. 3-4, pp. 439–443, 2006.

[39] R. A. Mahdi, H. Mohammed, K. Munisamy, and N. Saeid, "Review of convection heat transfer and fluid flow in porous media with nanofluid," *Renewable and Sustainable Energy Reviews*, vol. 41, pp. 715–734, 2015.

[40] K. M. Khanafer and A. J. Chamkha, "Mixed convection flow in a lid-driven enclosure filled with a fluid-saturated porous medium," *International Journal of Heat and Mass Transfer*, vol. 42, no. 13, pp. 2465–2481, 1999.

[41] G. R. Machireddy and V. R. Kattamreddy, "Impact of velocity slip and Joule heating on MHD peristaltic flow through a porous medium with chemical reaction," *Journal of the Nigerian Mathematical society*, vol. 35, no. 1, pp. 227–244, 2016.

[42] J. Misra, G. Shit, and H. J. Rath, "Flow and heat transfer of a mhd viscoelastic fluid in a channel with stretching walls: Some applications to haemodynamics," *Computers & Fluids*, vol. 37, no. 1, pp. 1–11, 2008.

[43] N. Bondarenko, E. Gak, and M. Gak, "Application of mhd effects in electrolytes for modeling vortex processes in natural phenomena and in solving

engineering-physical problems," *Journal of engineering physics and thermophysics*, vol. 75, no. 5, pp. 1234–1247, 2002.

[44] H. M. Shawky, N. T. Eldabe, K. A. Kamel, and E. A. Abd-Aziz, "MHD flow with heat and mass transfer of Williamson nanofluid over stretching sheet through porous medium," *Microsystem Technologies*, vol. 25, no. 4, pp. 1155–1169, 2019.

[45] H. Alfvén, "Existence of electromagnetic-hydrodynamic waves," *Nature*, vol. 150, no. 3805, pp. 405–406, 1942.

[46] R. Chodhury and B. Dey, "Flow features of a conducting visco-elastic fluid past a vertical permeable plate," *Global Journal of Pure and Applied Mathematics*, vol. 13, no. 9, pp. 5687–5702, 2017.

[47] M. H. M. Yasin, A. Ishak, and I. Pop, "MHD heat and mass transfer flow over a permeable stretching/shrinking sheet with radiation effect," *Journal of Magnetism and Magnetic Materials*, vol. 407, pp. 235–240, 2016.

[48] T. Hayat, M. Waqas, M. I. Khan, and A. Alsaedi, "Impacts of constructive and destructive chemical reactions in magnetohydrodynamic (MHD) flow of Jeffrey liquid due to nonlinear radially stretched surface," *Journal of Molecular Liquids*, vol. 225, pp. 302–310, 2017.

[49] A. Muhammad and O. D. Makinde, "Thermodynamics analysis of unsteady MHD mixed convection with slip and thermal radiation over a permeable surface," in *Defect and Diffusion Forum*, vol. 374. Trans Tech Publ, 2017, pp. 29–46.

[50] F. Aman, A. Ishak, and I. Pop, "Magnetohydrodynamic stagnation-point flow towards a stretching/shrinking sheet with slip effects," *International Communications in Heat and Mass Transfer*, vol. 47, pp. 68–72, 2013.

[51] K. H. Kabir, M. A. Alim, and L. S. Andallah, "Effects of viscous dissipation on MHD natural convection flow along a vertical wavy surface," *Journal of Theoretical and Applied Physics*, vol. 7, no. 1, p. 31, 2013.

[52] H. Maleki, J. Alsarraf, A. Moghanizadeh, H. Hajabdollahi, and M. R. Safaei, "Heat transfer and nanofluid flow over a porous plate with radiation and slip boundary conditions," *Journal of Central South University*, vol. 26, no. 5, pp. 1099–1115, 2019.

[53] Y. Cengel and J. M. Cimbala, "Fluid mechanics, 2006."

[54] S. S. Molokov, R. Moreau, and H. K. Moffatt, *Magnetohydrodynamics: Historical evolution and trends*. Springer Science & Business Media, 2007, vol. 80.

[55] S. K. Das, S. U. Choi, W. Yu, and T. Pradeep, *Nanofluids: science and technology*. John Wiley & Sons, 2007.

[56] D. F. Young, B. R. Munson, T. H. Okiishi, and W. W. Huebsch, *A brief introduction to fluid mechanics*. John Wiley & Sons, 2010.

[57] Y. A. Cengel, *Fluid mechanics*. Tata McGraw-Hill Education, 2010.

[58] H. Chanson, *Applied hydrodynamics: an introduction to ideal and real fluid flows*. CRC press, 2009.

[59] F. Irgens, "Generalized Newtonian fluids," in *Rheology and Non-Newtonian Fluids*. Springer, 2014, pp. 113–124.

[60] H. Schlichting and K. Gersten, *Boundary-layer theory*. Springer, 2016.

[61] C. Kothandaraman, *Fundamentals of heat and mass transfer*. New Age International, 2006.

[62] W. M. Rohsenow, J. P. Hartnett, Y. I. Cho *et al.*, *Handbook of heat transfer*. McGraw-Hill New York, 1998, vol. 3.

[63] J. N. Reddy and D. K. Gartling, *The finite element method in heat transfer and fluid dynamics*. CRC press, 2010.

[64] J. Kunes, *Dimensionless physical quantities in science and engineering*. Elsevier, 2012.

[65] T.Y.Na, *Computational methods in engineering boundary value problems*. Academic Press, 1979.